

Pharmacological and Physicochemical Properties Optimization for Dual-Target Dopamine D₃ (D₃R) and μ -Opioid (MOR) Receptors Ligands as Potentially Safer Analgesics

Alessandro Bonifazi,^{†*} Elizabeth Saab,^{†°} Julie Sanchez,^{‡,||} Antonina L. Nazarova,[⊥] Saheem A. Zaidi,[⊥] Khorshada Jahan,[†] Vsevolod Katritch,[⊥] Meritxell Canals,^{‡,||} J. Robert Lane,^{‡,||} Amy Hauck Newman^{†*}

[†]*Medicinal Chemistry Section, Molecular Targets and Medications Discovery Branch, National Institute on Drug Abuse – Intramural Research Program, National Institutes of Health, 333 Cassell Drive, Baltimore, Maryland 21224, United States*

[‡]*Division of Physiology, Pharmacology and Neuroscience, School of Life Sciences, Queen's Medical Centre, University of Nottingham, Nottingham NG7 2UH, United Kingdom*

^{||}*Centre of Membrane Protein and Receptors, Universities of Birmingham and Nottingham, Midlands NG2 7AG, United Kingdom*

[⊥]*Department of Quantitative and Computational Biology, Department of Chemistry, Dornsife Center for New Technologies in Drug Discovery and Development, Bridge Institute, Michelson Center for Convergent Biosciences, University of Southern California, Los Angeles, California 90089, United States*

[°]These authors equally contributed

*Corresponding authors:

Amy Hauck Newman:

Phone: (443)-740-2887. Fax: (443)-740-2111.

E-mail: anewman@intra.nida.nih.gov

ORCID: 0000-0001-9065-4072

Alessandro Bonifazi:

Phone: (443)-740-2897. Fax: (443)-740-2111

Email: alessandro.bonifazi2@nih.gov

ORCID: 0000-0002-7306-0114

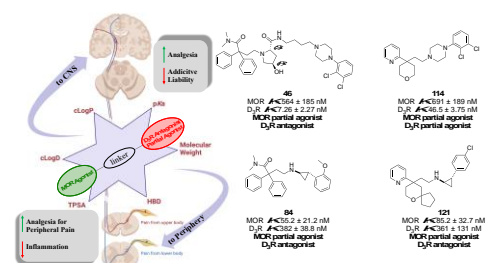
KEYWORDS

Dopamine D₃R Receptors, μ -Opioid Receptors, Bivalent Ligands, Analgesia, Opioid Use Disorders, Addictive Liability, Dual-Target Drug Design, Central Nervous System Multiparameter Optimization Score, Blood Brain Barrier

ABSTRACT

A new generation of dual-target mu opioid receptor (MOR) agonist/dopamine D₃ receptor (D₃R) antagonist/partial agonists with optimized physicochemical properties was designed and synthesized. Combining *in vitro* cell-based on-target/off-target affinity screening, *in silico* computer-aided drug design, and BRET functional assays, we identified new structural scaffolds that achieved high affinity and agonist/antagonist potencies for MOR and D₃R, respectively, improving the dopamine receptor subtype selectivity (e.g., D₃R over D₂R) and significantly enhancing Central Nervous System Multiparameter Optimization (CNS-MPO) scores for predicted blood brain barrier (BBB) permeability. We identified the substituted *trans*-(2*S*,4*R*)-pyrrolidine and *trans*-phenylcyclopropyl amine as key dopaminergic moieties and tethered these to different opioid scaffolds, derived from the MOR agonists **TRV130** (**3**) or **Loperamide** (**6**). The lead compounds **46**, **84**, **114** and **121** have the potential of producing analgesic effects through MOR partial agonism with reduced opioid-misuse liability via D₃R antagonism. Moreover, the peripherally limited derivatives could have therapeutic indications for inflammation and neuropathic pain.

Table of Contents (TOC)



INTRODUCTION

The on-going opioid epidemic remains a serious public health crisis affecting social and economic welfare globally. The COVID-19 pandemic has sadly increased opioid-related overdose with no end in sight.⁵ Although there are medications to treat both opioid use disorders (OUD) (e.g., buprenorphine and methadone) and overdose (e.g., naloxone), these have proven inadequate to reverse the surge of opioid-related deaths in the past decade. Moreover, prevention of dependence on opioids prescribed for pain management, such as oxycodone, has not been addressed pharmacologically. Indeed, dependence on prescription opioids remains a major contributor to the current opioid crisis in the U.S.,¹⁻⁶ although recently the easy and cheap access to synthetic opioids such as fentanyl, have become the major driver in opioid overdose.⁷ Alongside social and public health programs, the National Institutes of Health (NIH) has supported improvement in access to treatment and recovery, campaigns to promote safe opioid prescription practices and overdose prevention, and movements to combat the stigma associated with OUD. The development of innovative medications for OUD and safe, effective, non-addictive strategies to manage pain, while minimizing risk of relapse, is the focus of a highly translational NIH scientific effort, culminating with the launch of the HEAL initiative (Helping to End Addiction Long-term).

In 2019, the National Institute on Drug Abuse (NIDA) published a list of the ten most wanted medication development and therapeutic priorities, targeting pharmacological mechanisms to prevent and treat OUD and opioid overdose.⁸ One of the main priorities was the development of dopamine D₃ receptors (D₃R) antagonists and partial agonists.

The D₃R belongs to the D₂-like receptor family and is activated by the endogenous neurotransmitter dopamine (DA). This dopamine receptor subtype is predominantly expressed in

Formatted: Highlight

the mesolimbic DA region of the brain, which controls behaviors associated with drug-related cues, reinforcement, motivation, and reward.⁹ Numerous labs have pioneered drug design and pre-clinical development of highly selective D₃R partial agonists and antagonists as pharmacotherapeutics for the treatment of psychostimulant use disorders (PSUD) and OUD.¹⁰ For example, recent drug candidates (**±**)-1 and (**R**)-2 (**Figure 1**), two highly selective D₃R antagonists, both decrease oxycodone drug-seeking and self-administration without decreasing anti-nociception,¹¹ and importantly, without affecting peripheral biometric [cardiovascular](#) parameters when administered alone or in the presence of **oxycodone**¹² or **cocaine**. Also, (**±**)-1 decreases dose escalation of opioid self-administration in both male and female rats and reduces the acquisition of drug seeking behavior.¹²⁻¹⁴ These data have supported the preclinical development of these and other related compounds for not only the treatment of OUD, but potential prevention of opioid dependence, if administered with a prescription opioid for pain management.^{13, 15, 16} These observations have supported drug development campaigns toward combination treatments with opioid analgesics, or potentially with methadone or buprenorphine, to improve their efficacy in preventing relapse and minimizing the possibility of cardiovascular or other opioid-driven side effects. Furthermore, achieving D₃R subtype selectivity over D₂R may limit extrapyramidal side effects, locomotor impairments, and metabolic disorders, associated with D₂R antagonism,¹⁷⁻²⁰ improving their tolerability and compliance in this patient population.

Despite significant efforts toward developing analgesics that are non-opioids, the primary target for pain medications continues to be the μ -opioid receptors (MOR); the most effective opioid painkillers act as agonists at MOR. MOR, within the central nervous system (CNS), are expressed in brain regions associated with reward and aversion and in areas controlling pain sensation and respiratory processes that have high concentrations of GABA neurons. MOR activation efficiently

reduces severe pain, especially acute or perioperative pain, but the concomitant reward, tolerance and respiratory depression effects pose a significant threat and risk for OUD and overdose.

Recently, efforts ~~have been~~ directed towards generating safer opioid analgesics,²¹ ~~with~~ ~~have~~ ~~focused~~ on developing biased agonists, ~~compounds that able to~~ preferentially activate the G-protein dependent signaling cascade associated with MOR, ~~and consequent analgesia, with~~ ~~while~~ ~~limiting~~ β -arrestin recruitment. Observations made in β -arrestin2 knockout mice ~~suggested that β -arrestin2 MOR signaling may mediate side effects such as constipation and respiratory depression~~ showed reduced respiratory depression in response to morphine, suggesting that G-protein signaling might mediate analgesia but that β -arrestin2 MOR signaling may mediate ~~side effects such as constipation and respiratory depression.~~²² However, ~~more~~ recent ~~conflicting~~ evidence ~~suggests~~ ~~shows~~ that β -arrestin2 does not mediate ~~the development of~~ opioid-induced respiratory depression.²³⁻²⁷ ~~and~~ ~~indeed,~~ some such biased agonists still appear to induce ~~risk of respiratory depression and~~ self-administration in experimental animals, ~~despite initial evidence supporting the *in vivo* advantageous profiles of selective G-protein mediated mechanisms.~~²¹ ~~Nevertheless, some of the compounds identified as biased appear to show improved separation between their anti-nociceptive and respiratory depressive doses.~~²⁸ Recent studies have suggested that the low intrinsic efficacy (weak partial agonism) of these compounds may ~~underlie~~ cause their improved ~~separation between anti-nociceptive and respiratory depressive doses and their~~ safety profile.^{24, 29-33} It is evident that parsing out mechanisms underlying pharmacologically desired versus unwanted effects, and differentiating these at a cellular signaling level is still difficult when exclusively targeting the MOR.

TRV130 (3) and PMZM21 (4) (Figure 1)³⁴⁻³⁶ are among some of the most recently studied MOR agonists. The former, was initially reported to exclusively activate the $G_{i/o}$ signaling

pathway, without β -arrestin recruitment, with a rapid analgesic profile and limited side effects. However, despite ongoing investigations ~~on~~ [into](#) its application for post-surgery pain, preclinical studies report abuse potential and constipation. Similar findings have been observed for the biased agonist **4**³⁷ ~~which~~ ~~:- initially reported as a highly selective G-protein biased agonist with prolonged induced analgesia and limited side effects (constipation, respiratory depression, locomotion, and reward),~~ it was recently shown to induce respiratory depression comparable to morphine.³⁸ ~~More recently,~~ **TRV734 (5; Figure 1)**, a [more recent](#) structural analog of **3** with a significantly improved oral bioavailability,³⁹ is being evaluated in translational studies for its safety, pharmacodynamic profile, and pharmacokinetic parameters.⁴⁰

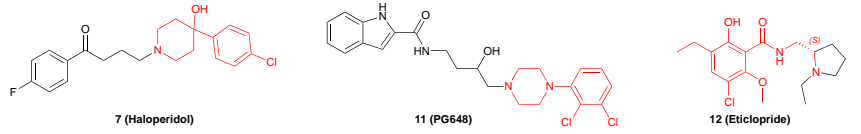
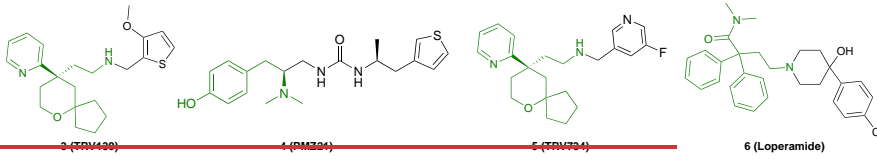
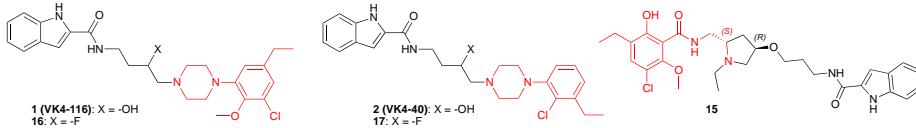
Opioid-based pain medications can swiftly induce tolerance, dose-escalation, and opioid induced hyperalgesia (OIH),⁴¹ a paradoxical effect of increased peripheral nerve hypersensitivity. Proposed biased agonists, **3** and **4**, have also been found to induce OIH and hyperalgesic priming in an animal model for transition to chronic pain.⁴²

In an effort to control pain at a peripheral level and limit addictive liability, the development of peripherally limited MOR agonists that induce antinociception by targeting the peripheral opioid receptors located in sensory neurons has been pursued. In particular, peripheral opioid agonists can attenuate inflammation-induced excitability of primary afferent neurons and reduce the release of proinflammatory neuropeptides from peripheral terminals. In injured tissues, this can lead to analgesia and anti-inflammatory effects.⁴³

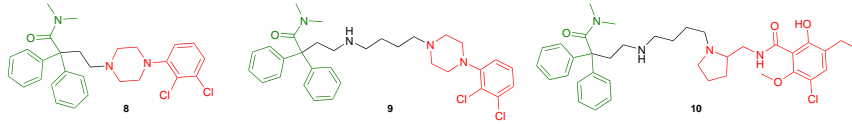
Loperamide (**6; Figure 1**; an over-the-counter anti-diarrheal medication) is a peripherally restricted MOR agonist, due to its high affinity as a P-glycoprotein (P-gp) transporter substrate, which limits its ability to be retained in the CNS. Loperamide (**6**) was the first commercially available peripherally limited MOR agonist to show anti-hyperalgesic properties on its own,

particularly in reducing heat and mechanical hyperalgesia in nerve injured rats,^{21, 44} mediated at the peripheral terminals of the afferent fibers.^{45, 46} It has also been found to produce a synergistic peripherally mediated analgesia in a mouse inflammatory pain model, when administered in combination with the δ -opioid receptor agonist oxymorphone.⁴⁴

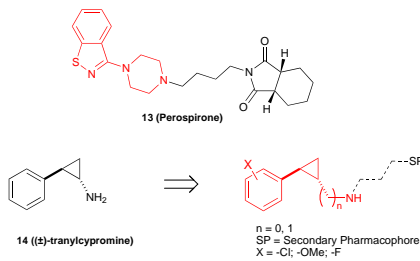
Reference MOR agonists and D₂R antagonists/partial agonists



Dual-Target MOR-D₂R



Alternative Synthons as D₂R PP



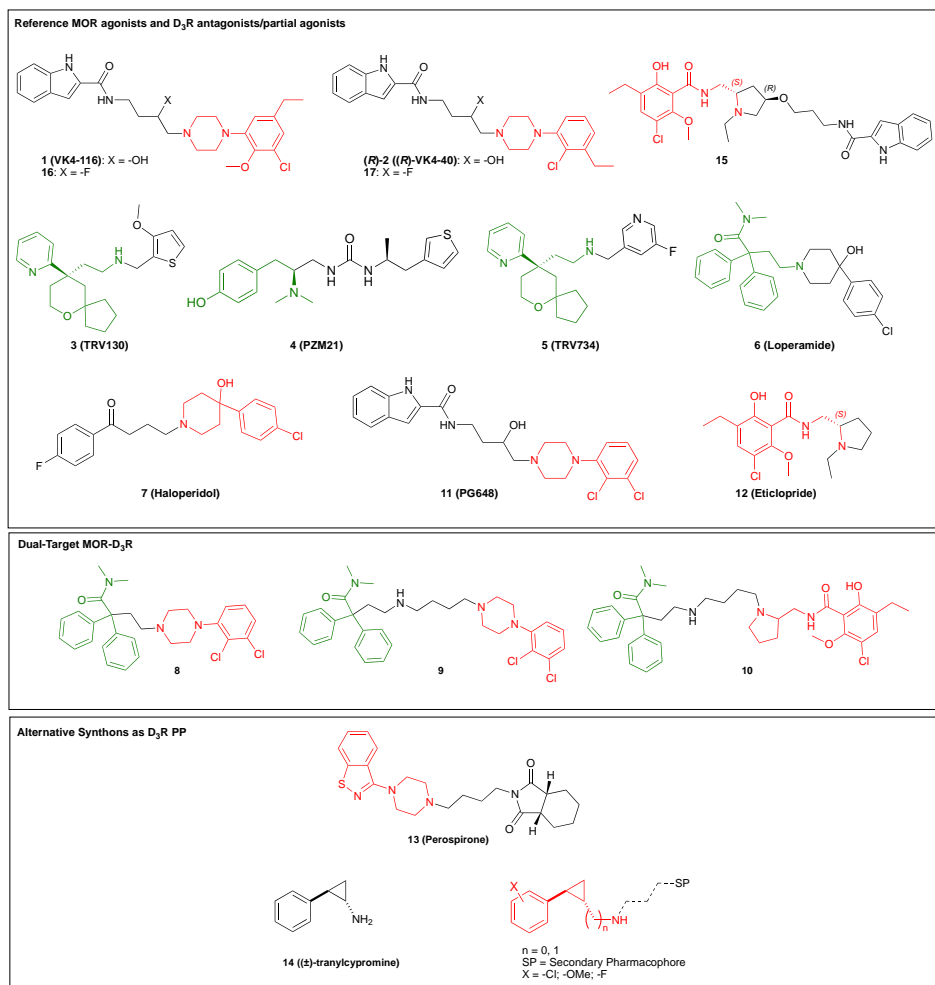


Figure 1. Top panel: MOR agonists and D₃R antagonists/partial agonists used as references to inspire and select MOR (green) and D₃R (red) primary pharmacophores (PP), targeting their respective orthosteric binding sites (OBS). **Middle panel:** First series MOR-D₃R dual-target leads⁴⁷ used as starting point for the optimization campaign. **Bottom panel:** D₃R scaffolds (red) that inspired investigation of new PP chemical space.

Based on our interest in both opioid and dopamine D₂-like receptors systems, we recently developed an innovative drug design approach^{10-12, 48} merging the analgesic properties of MOR agonists with D₃R antagonism/partial agonism predicting reduced addictive liability.⁴⁷ We designed compounds using a bivalent drug design⁴⁹ and scaffold hybridization⁵⁰ strategy, linking together two pharmacophores: i) MOR agonist primary pharmacophore (PP), targeting and activating MOR in its orthosteric binding site (OBS), and ii) D₃R antagonist/partial agonist PP, binding within the D₃R OBS. We also demonstrated that carefully chosen MOR PP can be accommodated in the D₃R secondary binding pocket (SBP)⁴⁷ and, similarly, well-designed D₃R PP can also interact with the MOR SBP, increasing the affinity of these bivalent ligands for both targets.

With this approach, we wanted to provide an alternative drug discovery strategy which could potentially speed up the preclinical development process by simplifying pharmacological and toxicological studies, that until now have been conducted with two different drugs in combination, by obtaining a single molecule with merged pharmacological properties. Considering the need for both centrally as well as peripherally limited analgesics, we took a two-pronged approach to 1) discover safer CNS active analgesics, with reduced addictive liability, as well as 2) generate new families of primarily peripherally acting ligands, for their therapeutic potential in peripheral pain and inflammation. Using the **6**-scaffold, given its structural features resembling classical D₃R ligands such as haloperidol (**7**; **Figure 1**), allowed an initial structure-activity relationships (SAR) campaign,⁴⁷ where we identified and characterized the most potent, first in class, dual-target MOR agonists-D₃R antagonists (**Figure 1**).

In our first reported series,⁴⁷ inspired and designed around **6** as the MOR PP, most of the lead molecules (**8**, **9**, and **10**; **Figure 1** and **Table 1**) presented CNS multiparameter optimization

scores (CNS-MPO; a value indicating the likelihood of a drug to cross the BBB)⁵¹ <2.5, suggesting a more peripherally restricted profile. In this study, we implemented a combination of *in silico* methods to predict the ability of new drugs to target the CNS,² and we sought to expand the SAR by specifically adjusting the physicochemical properties necessary to obtain higher CNS drug-like parameters, while still retaining high affinity agonist and antagonist potencies at both MOR and D₃R targets of interest, respectively.

Since the beginning of this new campaign, the SAR design was assisted by CNS-MPO calculations and predictions, as detailed in depth in the discussion below, and by parallel *in vitro* binding screening to assess the effect of every structural modification. We directed the chemistry and drug design around two MOR agonist pharmacophores: 1) **6**, to continue improving the previous generation of ligands with the aim of increasing potency and CNS profile, allowing the comparison of centrally and peripherally active ligands; and 2) **3**, the well-known potent and centrally active MOR agonist, thus allowing us to specifically improve its pharmacology to reduce addictive liability with the dual target approach. Due to extensive SAR studies already published,³⁶ the most favorable positions to link the D₃R pharmacophores were revealed. Moreover, we were particularly focused on the possibility to use the **3**-scaffold for modulating different maximal efficacy at MOR, creating libraries of full and partial agonists to further establish the correlation between intrinsic efficacy and therapeutic window.³⁰

Herein, we aimed to synthesize dual target compounds with maximized D₃R affinity and subtype preferential selectivity. In addition, we aimed to obtain compounds with moderate MOR affinity and moderate MOR efficacy, still sufficient to elicit significant *in vivo* analgesia, but with reduced receptor desensitization, in contrast to the extremely potent and efficacious addictive synthetic opioids. One of the most important challenges was to find the right balance between

MOR and D₃R affinity, which can be successfully translated in *in vivo* occupancy. Ultimately, to have an effect on limiting the opioid pharmacophore rewarding profile, a significant level of D₃R occupancy^{52, 53} needs to be achieved at the dose used for effective anti-nociception. This would likely require a higher affinity D₃R antagonist/partial agonist, meanwhile a more moderate MOR agonist/partial agonist affinity would be able to elicit relevant analgesia,^{54, 55} due to amplification of the agonist activated cellular signaling cascade and/or MOR receptor reserve.

For the D₃R PP, in addition to the classical high affinity/selectivity-inducing scaffolds, like the 2,3-dichlorophenyl piperazine (inspired by PG648 (**11**))⁵⁶ and the 1-(3-chloro-5-ethyl-2-methoxyphenyl)piperazine (inspired by eticlopride (**12**) and **1**)⁵⁷ (**Figure 1**), we also decided to investigate new chemical space and tether less explored scaffolds, such as 1-(6-(trifluoromethyl)pyridin-2-yl)piperazine (predicted to enhance the D₃R subtype selectivity), the 3-(piperazin-1-yl)benzo[d]isothiazole (inspired by the atypical antipsychotic perospirone⁵⁸⁻⁶⁰ (**13**)), and variously substituted phenyl cyclopropylamines (inspired by tranlycypromine (**14**) and its analogues)⁶¹ (**Figures 1 and 2**). Finally, to evaluate the role of key physicochemical properties, such as pK_a and clogP, a significant effort was directed in designing complex linkers, such as substituted pyrrolidine rings (inspired by **12** and its bitopic analogues, i.e. **15**; **Figure 1**) focusing on the basicity of the harboring amines, effect of electron withdrawing groups (EWG; inspired by **1,16** and **2,17** pairs, **Figure 1**)^{57, 62} or donating substituents, presence of hydrogen bond (H-bond) donor/acceptor groups, and stereochemistry, which we previously reported to be a fundamental factor in bitopic and bivalent drug design, when targeting two sites within the same receptors, exploiting unique ligand poses^{49, 63, 64} (**Figure 2**).

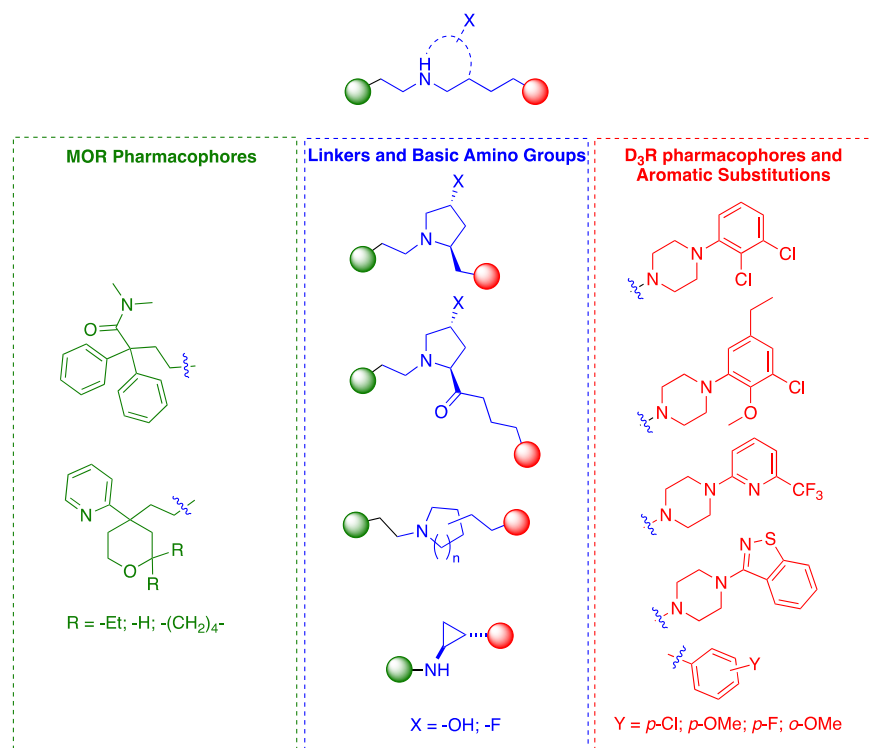


Figure 2. Dual-target drug design to generate the new library of SAR, tethering MOR (green) and D₃R (red) primary pharmacophores by linkers with various substitutions, regiochemistry, and stereochemistry patterns (blue).

RESULTS AND DISCUSSION

Drug Design and Synthesis

This generation of bivalent dual target ligands can be sub-divided into two main categories based on the MOR agonist PP: (A) the *N,N*-dimethyl-2,2-diphenylacetamides, derived from **6**, and (B) the 2-(tetrahydro-2*H*-pyran-4-yl)pyridines, inspired by **3**³⁶ and its analogues (**Figure 2**). For both classes of PPs, variations in the substitution patterns around the MOR agonist scaffold, the length, stereochemistry, and structural composition of the linker, and the connected D₃R

pharmacophores with antagonists or partial agonists functionality were explored to create a large SAR library (**Figure 2**). It was important to not only understand the biological implications of each of the MOR and D₃R substituted pharmacophores attached in a bivalent fashion, but also to investigate the role of the linker in its geometry and chemical space.

All of the compounds were designed and synthesized to retain or improve the desired pharmacological profile and receptor subtype selectivity without neglecting the importance of balanced physicochemical properties essential for CNS activity. The CNS-MPO scores predicting BBB permeability and CNS activity, are based on six factors (**Table S1**): molecular weight (MW), cLogP, cLogD, pK_a of the most basic group, topological polar surface area (TPSA), and number of hydrogen bond donor groups. Molecular weight >360, cLogP >3, and cLogD (at pH 7.4) >2, negatively impact the CNS-MPO scores, with 0 scoring values (T0) for these parameters at 500 for molecular weight, 4 for cLogD, and 5 for cLogP.⁵¹ To fulfill essential bivalent requirements of dual-target D₃R-MOR pharmacophores, we generally end up with unfavorable high molecular weight compounds, along with higher cLogP/cLogD values, and very basic pK_a due to presence of multiple secondary/tertiary basic amine groups, fundamental for the respective target binding. Hence, we implemented the following designs to improve each of the parameters involved in CNS-MPO calculations: i) decreasing MW, cLogP and cLogD; CNS-MPO score tends to add significant penalties on MW and cLogP, however, there are very good reasons to keep these values low. Larger cLogP values can improve rate of penetration across the membranes but, at the same time, large lipophilic molecules also show non-specific protein binding, thus limiting unbound “active” form of the drug (both in plasma and brain); ii) ~~d~~Decreasing pK_a of the basic nitrogen, and incorporating EWGs close to basic amine, which might increase concentration of non-ionized diffusible form, and reduce P-gp recognition;⁶⁵ iii) ~~r~~Reducing H-bond donors by replacement of

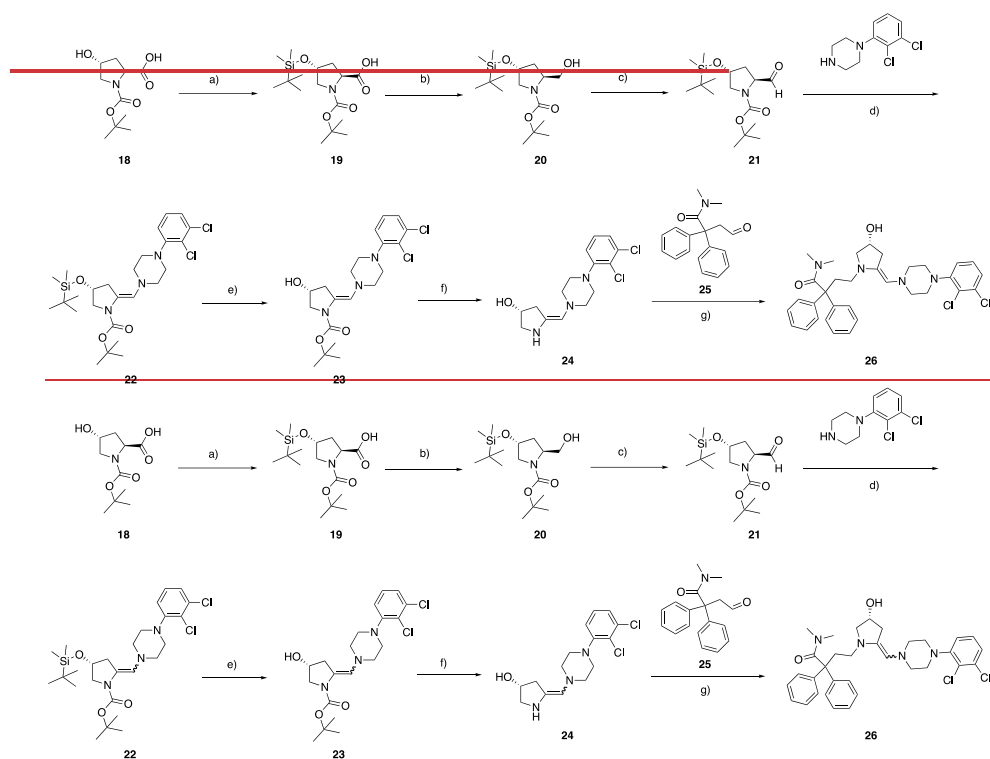
H-bond donor atoms or incorporating H-bond acceptors capable of engaging H-bond donors in intramolecular H-bonds, that reduce availability to water solvent and P-gp, and also reduce flexibility of the molecule. Ultimately, iv) while TPSA was not specifically used as a factor in the design, it is important to note that removal of heteroatoms will reduce TPSA, while including H-bond acceptors will increase the value. CNS-MPO⁶⁶⁻⁶⁸ scores have been calculated for each new candidate and are reported in **Tables 1, 2** and **S1**.

The first series of compounds, based on **6**, was designed using previous SAR⁴⁷ that highlighted the importance of linker rigidity and the presence of basic tertiary amine groups that help to achieve optimal p*K*_a values in comparison to previously reported secondary amines. This led to the use of well-tolerated pyrrolidine (L-proline inspired) linkers. The versatility and importance of using pyrrolidine moieties with specific stereochemistry and substitution patterns when designing D₃R antagonists has been the focus of previous SAR campaigns inspired by **12** (**Figure 1**).⁶³ It was expected that the presence of a hydroxyl group with the well-established optimal trans-(2*S*,4*R*)⁶³ stereochemistry around the pyrrolidine (**Figure 2**) ring would reduce the lipophilicity of these highly functionalized bivalent compounds.

The hydroxy group of commercially available starting material (2*S*,4*R*)-1-(*tert*-butoxycarbonyl)-4-hydroxypyrrolidine-2-carboxylic acid (**18**; **Scheme 1**) was first protected as a *tert*-butyl dimethyl silyl ether (**19**), prior to reducing the carboxylic acid group to the corresponding primary alcohol **20**. Further oxidation, assisted with Dess-Martin periodinane (DMP), provided the aldehyde intermediate for reductive amination. As detailed in the experimental section, due to the poor solubility of the intermediate iminium salt, after work-up, the reductive amination proceeded to the formation of the enamine product **22**, as mixture of diastereoisomers, instead of the fully reduced tertiary amine. Nevertheless, the unsaturated scaffold was considered an

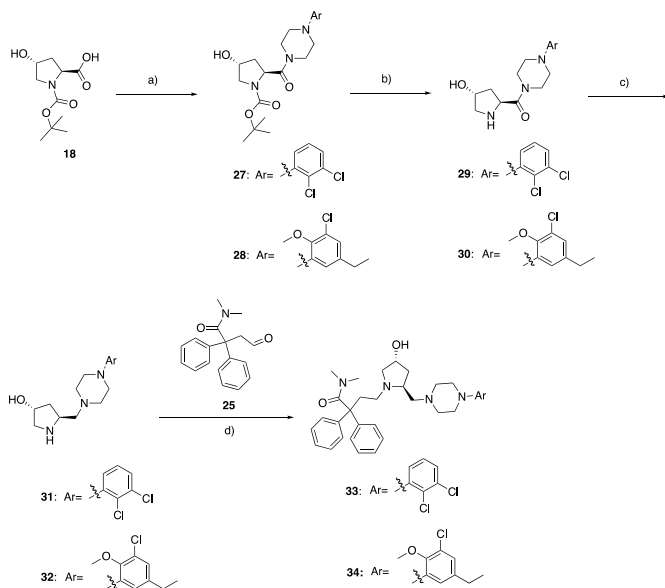
Formatted: Font: Bold

interesting additional derivative. Thus, the deprotection of the silyl ether with TBAF and the Boc-group with TFA allowed the ~~freeing deprotection~~ of the key secondary amine **24** to react with *N,N*-dimethyl-4-oxo-2,2-diphenylbutanamide (**25**)⁴⁷ in a reductive amination to prepare **26**.



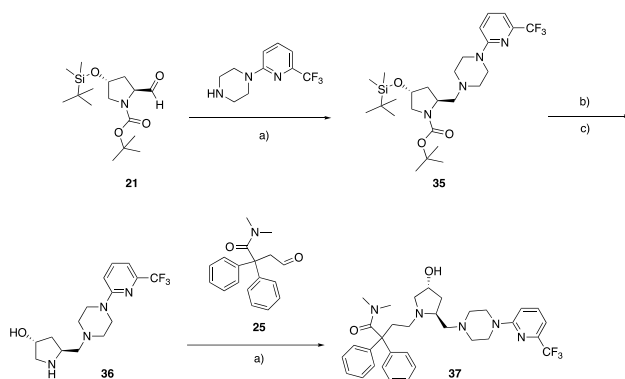
Scheme 1 a) imidazole, *tert*-butylchlorodimethylsilane (TBDMSCl), DCM/DMF; b) borane-methyl sulfide complex (BH₃:DMS), THF, from 0°C to room temperature (RT); c) Dess-Martin periodinane (DMP), DCM, from 0°C to RT; d) sodium triacetoxyborohydride (STAB), cat. acetic acid (AcOH), DCM; 2N aq. NaOH; e) 1M TBAF, THF; f) trifluoroacetic acid (TFA)/DCM, g) STAB, cat. AcOH, DCE.

Obviously, the interest was still in obtaining the fully saturated pyrrolidine analogues, in order to increase chiral complexity and observe the implications on both MOR and D₃R affinity/potency. In **Scheme 2**, **18** underwent amide coupling with 1-(2,3-dichlorophenyl)piperazine. Boc-deprotection with TFA afforded **29**, which was reduced with lithium aluminum hydride (LAH), followed by reductive amination to obtain **33**. The LAH reduction step needed to be carefully monitored, because partial loss of chlorine atoms was observed, and thus only a limited amount of the desired product was isolated by preparative HPLC. To further expand the D₃R SAR, an analogous route replacing 1-(2,3-dichlorophenyl)piperazine with 1-(3-chloro-5-ethyl-2-methoxyphenyl)piperazine yielded **34**.



Scheme 2 a) Appropriate aromatic piperazine, EDC-HCl, HOBt, TEA, DCM; b) TFA/DCM; c) LiAlH₄ (LAH), THF, from 0°C to RT; d) STAB, cat. AcOH, DCE.

To prepare a third analog with 1-(6-(trifluoromethyl)pyridin-2-yl)piperazine as the D₃R pharmacophore, a more succinct route was developed in order to circumvent the amide reduction step, as described in **Scheme 3**. Similarly, in preliminary pilot reactions, a loss of fluorine atoms was observed when exposed to prolonged LAH reduction. Thus, a reductive amination between 1-(6-(trifluoromethyl)pyridin-2-yl)piperazine and the previously reported intermediate **21** afforded the protected **35**. Sequential deprotection of the silyl- and the Boc- protecting groups led to the secondary amine, which was then coupled with **25** to yield **37**.



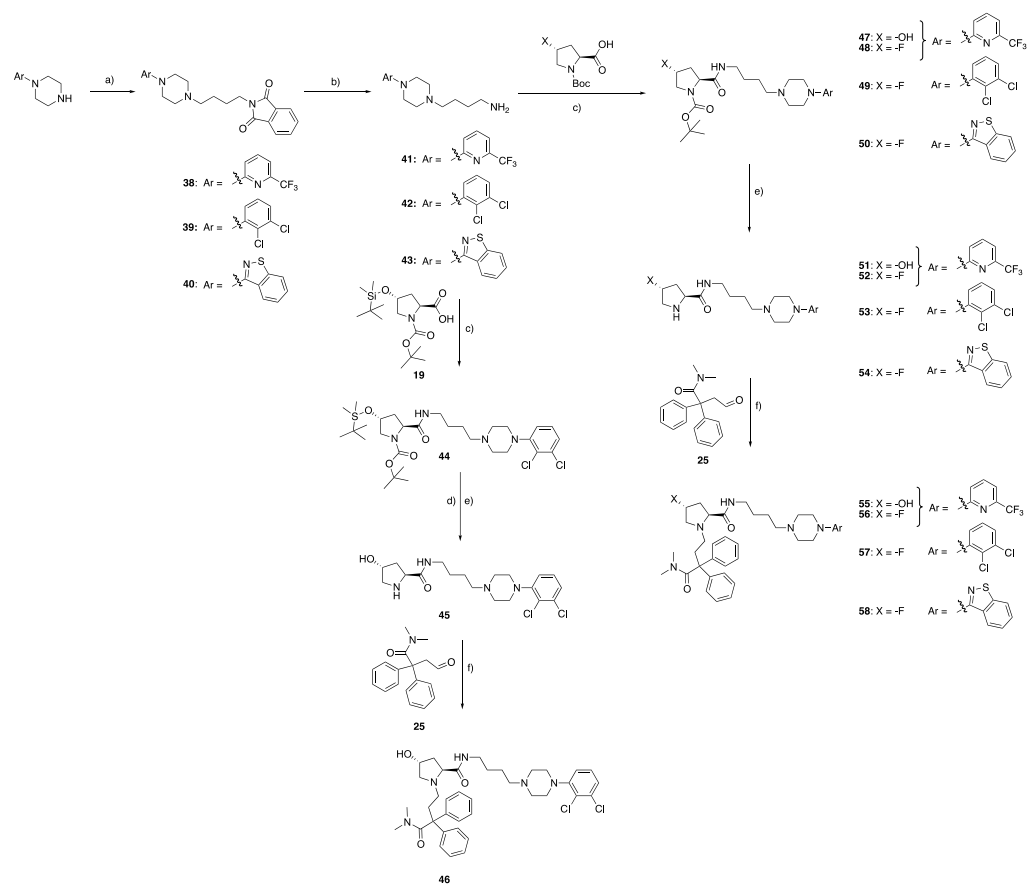
Scheme 3 a) STAB, cat. AcOH, DCE; b) 1M TBAF, THF; c) TFA/DCM.

In the previous schemes, the amide was reduced to add flexibility to the short linker chain. However, the importance of longer linkers, usually 4 to 5 methylene units, in maximizing D₃R binding was previously observed,⁴⁷ thus, a series with a longer carbon chain was synthesized in which the amide was kept in order to examine the effects of a less basic functionality (**Scheme 4**).

Additionally, CNS-MPO predictions suggested that the hydroxy group could be replaced with a fluorine atom, as observed for classic D₃R antagonist reported over the years.⁶² The absolute stereochemistry was maintained identical to previous analogues, and the replacement of the

hydroxy to fluorine helped the CNS-MPO scores, due to the removal of an H-bond donor atom, while still eliciting binding contact within the D₃R.

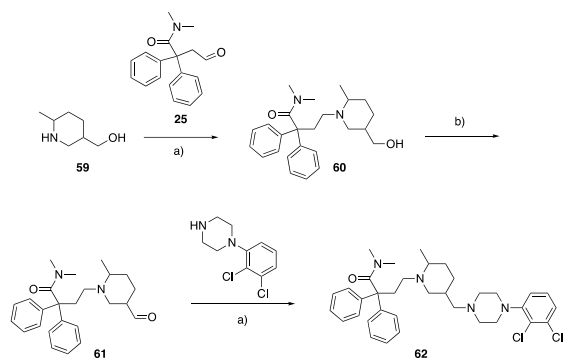
As described in **Scheme 4**, canonical D₃R PPs 1-(2,3-dichlorophenyl)piperazine and 1-(6-(trifluoromethyl)pyridin-2-yl)piperazine were functionalized through *N*-alkylation with 2-(4-bromobutyl)isoindoline-1,3-dione, then deprotected using hydrazine. In order to prepare the pyrrolidinyl compounds, first an amide coupling between **42** and **19** afforded **44**, which was deprotected, followed by a reductive amination between the pyrrolidine and **25** to yield **46**. Similar synthetic procedures were adopted to synthesize compounds **55**, **56** and **57**, containing either (2*S*,4*R*)-4-hydroxy or (2*S*,4*R*)-4-fluoro proline rings, tethered with the desired aromatic piperazine scaffolds. In the quest to keep exploring and designing new D₃R pharmacophores, computer aided drug design (CADD) supported the introduction of the novel less explored 3-(piperazin-1-yl)benzo[*d*]isothiazole as D₃R PP, prompting the synthesis of **58**, as depicted in **Scheme 4** as well.



Scheme 4 a) 2-(4-bromobutyl)isoindoline-1,3-dione, K_2CO_3 , acetonitrile (ACN), reflux; b) NH_2NH_2 , EtOH, reflux; c) EDC·HCl, HOBT, DIPEA, DCM; d) 1M TBAF, THF; e) TFA/DCM; f) STAB, cat. AcOH, DCE.

The effects of increasing the ring size in the linker, while reducing overall distance between PPs, because of the relative regio- and stereochemistry, were probed by replacing the pyrrolidine with a piperidine nucleus, as depicted in **Scheme 5**. First a reductive amination between (6-methylpiperidin-3-yl)methanol (**59**) and **25** afforded intermediate **60**, which was oxidized to aldehyde prior to an additional reductive amination to prepare **62**. This compound lowered the CNS-MPO score, which combined to favor D₂R binding over D₃R (expected from shorter linker analogues^{47, 49, 63}) discouraged further exploration of this linker or the separation of the diastereoisomers. However, a slightly longer linker tethered to the 3-position of an unsubstituted pyrrolidine, ~~the 3-position, as the regiochemical location of the linker,~~ was further explored by ~~reverting the ring to an unsubstituted pyrrolidine, while slightly increasing the chain length~~ to favor D₃R/D₂R selectivity.

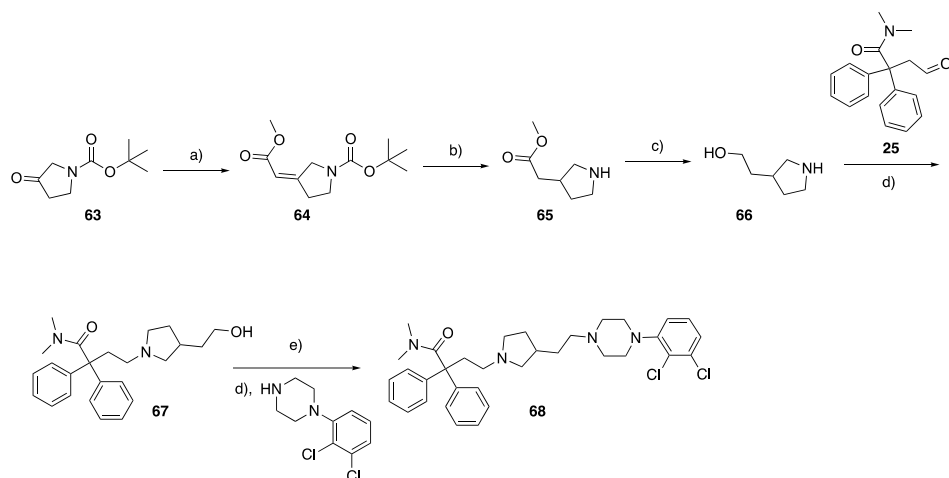
Formatted: Highlight



Scheme 5 a) STAB, cat. AcOH, DCE; b) DMP, DCM, from 0°C to RT

As described in **Scheme 6**, commercially available *tert*-butyl 3-oxopyrrolidine-1-carboxylate (**63**) was homologized to afford **64**, followed by hydrogenation and Boc- deprotection with TFA. Next, the ester was reduced using LAH before the reductive amination of **66** with **25**. Finally, the alcohol

was oxidized, followed by immediate reductive amination with 1-(2,3-dichlorophenyl)piperazine to afford **68**. Similar to **62**, despite the significant improvement on MOR-D₃R dual target affinity and selectivity over D₂R, the poor CNS-MPO score did not support the synthesis of additional analogues.

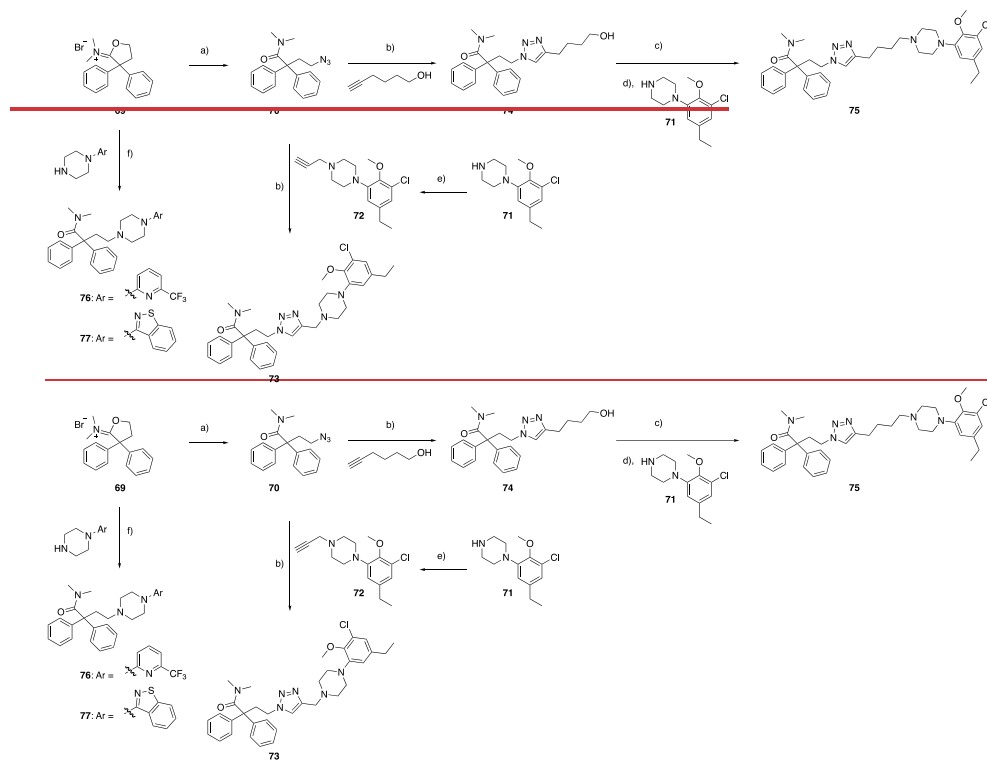


Scheme 6 a) trimethyl phosphonoacetate, NaH, MeOH, from 0°C to RT; b) 5% cat. Pd/C, EtOH, TFA, H₂ 50 psi; c) LAH, THF, from 0°C to RT; d) STAB, cat. AcOH, DCE; e) DMP, DCM, from 0°C to RT.

The linker was further adapted, converted to a triazole, and tethered with both longer and shorter alkyl chains, as shown in **Scheme 7**. When reacted with sodium azide, the commercially available *N*-(3,3-diphenyldihydrofuran-2(3*H*)-ylidene)-*N*-methylmethanaminium bromide (**69**) ring opens and functionalizes as an azide group to yield **70**. 1-(3-chloro-5-ethyl-2-methoxyphenyl)piperazine (**71**)⁵⁷ was *N*-alkylated with 3-bromoprop-1-yne, which was then reacted with **70** in an azide-alkyne click reaction to synthesize the short linker compound, **73**. To produce the longer linker chain analog, **70** was similarly reacted in a click reaction with hex-5-yn-

1-ol in the presence of copper(II) sulfate pentahydrate and sodium ascorbate. Alcohol intermediate **74** was then oxidized to an aldehyde, followed by immediate reductive amination to obtain **75**. Further development of this series was terminated due to the decrease in binding affinities with the triazole linker.

The next approach taken was a series of shorter alkyl linker compounds, achieved through direct alkylation with 1-(6-(trifluoromethyl)pyridin-2-yl)piperazine and 3-(piperazin-1-yl)benzo[*d*]isothiazole by opening the ring through nucleophilic attack of **69** (**Scheme 7**, compounds **76** and **77**, respectively). This approach proved to be extremely successful in generating high potency efficacious MOR agonists,⁴⁷ which tolerate the presence of a large variety of substituted piperazine scaffolds. However, the D₃R affinity appears to be more sensitive to the aryl piperazine used, leading us to further explore additional PPs.

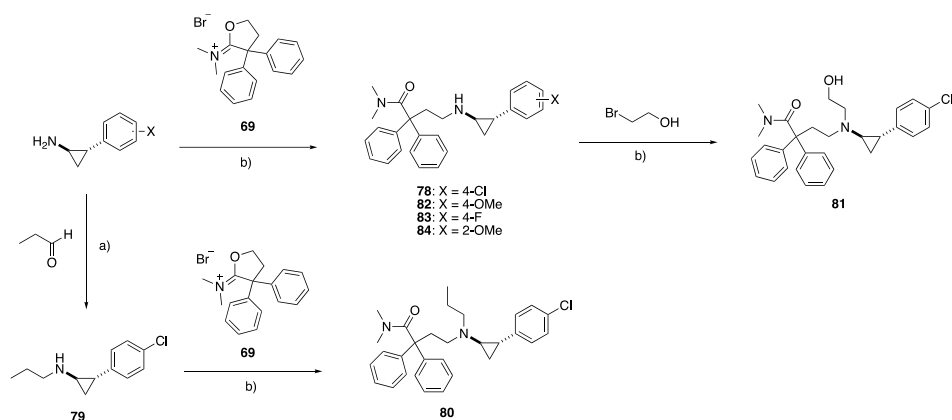


Scheme 7 a) NaN_3 , DMF; b) copper(II) sulfate pentahydrate, sodium (L)-ascorbate, THF/ H_2O ; c) DMP, DCM, from 0°C to RT; d) STAB, cat. AcOH, DCE; e) 3-bromoprop-1-yne, K_2CO_3 , ACN, reflux; f) K_2CO_3 , ACN, reflux.

An analogous route initiated by the ring opening of **69** was probed using a novel D_3R scaffold that contains a cyclopropyl amino group instead of the piperazine (**Scheme 8**), based on a previously reported series of ligands with dopaminergic profiles,^{61, 70, 71} inspired by **14** (**Figures 1 and 2**). The first compound synthesized was **78**, using *trans*-2-(4-chlorophenyl)cyclopropan-1-amine. In order to explore binding affinities for tertiary amines with respect to secondary amines,

Formatted: Font: Bold

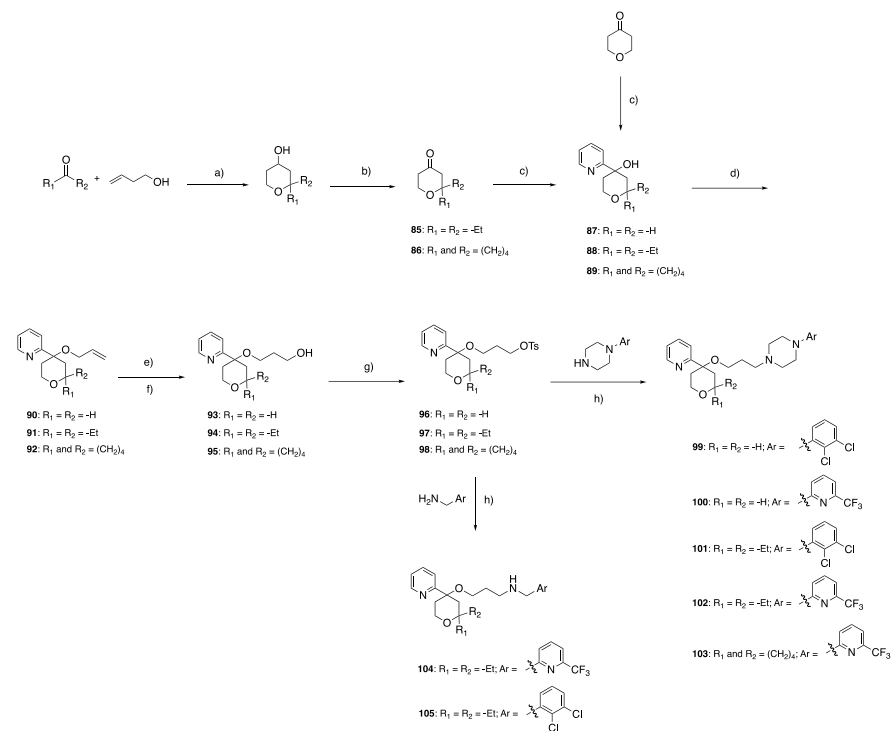
80 was synthesized by *N*-propylation of *trans*-2-(4-chlorophenyl)cyclopropan-1-amine through a reductive amination, followed by nucleophilic ring opening of **69**. While the binding affinities were not affected, the CNS-MPO score declined when switching from a secondary to a tertiary amine, due to increased lipophilicity. In an attempt to improve the CNS-MPO, while keeping the tertiary amine, **81** was synthesized through *N*-alkylation of **78** with 2-bromoethan-1-ol. The binding affinities at D₃R significantly decreased, thus we explored substitutions on the phenyl ring instead, maintaining the secondary amine as the basic moiety. Starting material **69** was reacted with *trans*-2-(4-methoxyphenyl)cyclopropan-1-amine, *trans*-2-(4-fluorophenyl)cyclopropan-1-amine, or *trans*-2-(2-methoxyphenyl)cyclopropan-1-amine to complete the SAR based on **6**, yielding compounds **82**, **83**, and **84**, respectively.



Scheme 8 a) NaBH₄, MeOH; b) K₂CO₃, 90°C, ACN.

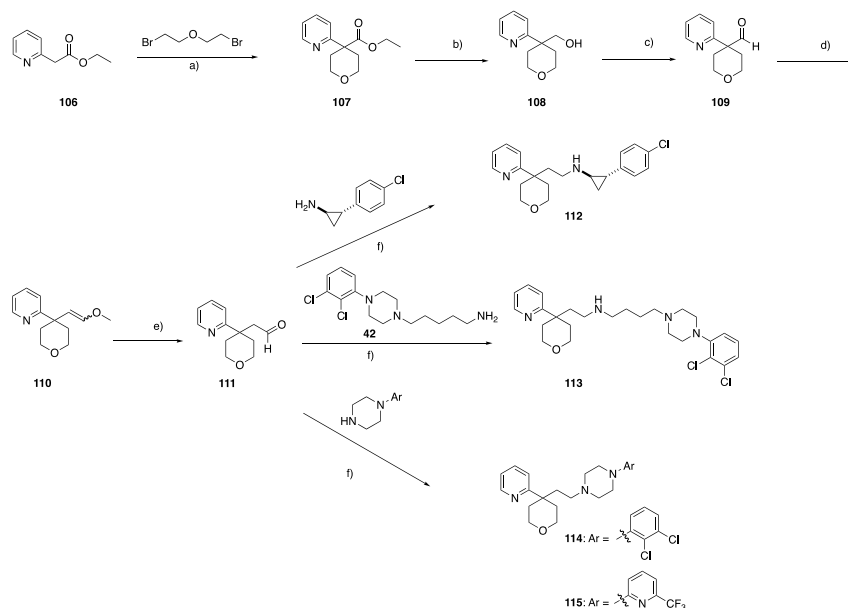
For the second class of MOR PPs, the **3**-scaffold inspired series, three sets of substitutions on the tetrahydropyran (THP) ring were explored (**Figure 2**). As depicted in **Scheme 9**, the first series aimed to reach a longer distance between PPs by including an ether linker. First, a Prins

cyclization³⁶ using 3-pentanone, or cyclopentanone, with but-3-en-1-ol, followed by immediate oxidation, afforded ketones **85** and **86**, respectively. In the case of the unsubstituted tetrahydro-4*H*-pyran-4-one, the material was commercially available. The pyridine scaffold was then introduced via organo-lithium coupling. Next, an *O*-alkylation reaction occurred in the presence of allyl bromide and sodium hydride, and the terminal alkene was subjected to a hydroboration-oxidation, leading to key intermediates **93**, **94** and **95**. Tosylation reaction of the primary alcohols was followed by nucleophilic substitution with the appropriate D₃R piperazines, or (6-(trifluoromethyl)pyridin-2-yl)methanamine (**104**), or (2,3-dichlorophenyl)methanamine (**105**). From studying the role of the substitutions at the 2-position on the THP ring, it was clear that the diethyl and cyclopentyl groups were slightly favorable for higher MOR affinity, however the oxygen bridge pushed the basic nitrogen too far from the MOR PP reducing the MOR binding affinities, and thus it was decided that only the classic ethyl linker chain would be further explored.



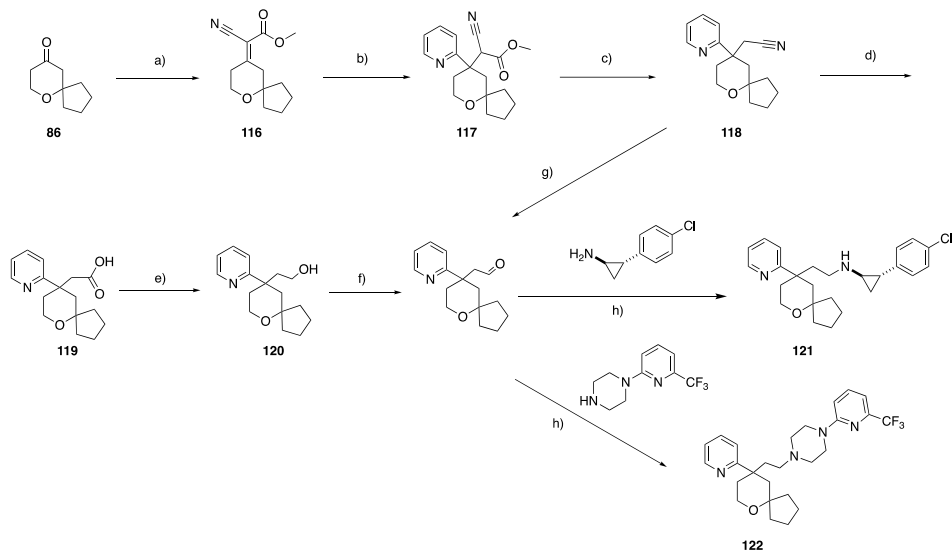
Scheme 9 a) conc. H_2SO_4 , DCM, $-78^\circ C$ to RT; b) DMP, DCM, from $0^\circ C$ to RT; c) 2-bromopyridine, n-butyllithium, methyl *tert*-butyl ether (TBME), from $-78^\circ C$ to RT; d) NaH, allyl bromide, TBME/THF, DMF, from $0^\circ C$ to RT, reflux; e) $BH_3 \cdot THF$, THF, from $0^\circ C$ to RT; f) 2M aq. NaOH, H_2O_2 , from $0^\circ C$ to RT; g) *p*-Toluenesulfonyl chloride (*p*-TsCl), 4-dimethylaminopyridine (DMAP), DCM, from $0^\circ C$ to RT; h) K_2CO_3 , ACN, reflux.

As described in **Scheme 10**, to develop initial SAR, and simplify the overall stereochemistry, the unsubstituted THP MOR pharmacophore was used. First, the THP (**107**) ring was prepared by cyclization of 1-bromo-2-(2-bromoethoxy)ethane with ethyl 2-(pyridin-2-yl)acetate (**106**) under basic conditions, followed by LAH reduction, then oxidation of **108** to aldehyde **109**. Next, a Wittig reaction homologized the linker chain, affording **110**, which was hydrolyzed to the corresponding aldehyde. Finally the reductive amination of **111** with *trans*-2-(4-chlorophenyl)cyclopropan-1-amine, 1-(2,3-dichlorophenyl)piperazine, or 1-(6-(trifluoromethyl)pyridin-2-yl)piperazine, afforded the desired products **112**, **114** and **115**, respectively. In order to directly compare the same D₃R PP with shorter and longer linker chains, reductive amination of **111** with **42** was also conducted to obtain **113**.



Scheme 10 a) NaH, DMF, 40°C; b) LAH, THF, from 0°C to RT, 2N aq. NaOH, MeOH; c) DMP, DCM, from 0°C to RT; d) (methoxymethyl)triphenylphosphonium chloride, *t*-BuOK, THF, from 0°C to RT; e) HCl (37% in H₂O), DCM; f) STAB, cat. AcOH, DCE.

To synthesize analogues of **3** with the 2-cyclopentyl substitution (**Scheme 11**), reported to favorably modulate MOR pharmacology,³⁶ the key intermediate **118** was either obtained from commercial sources, or de-novo synthesized adapting previously reported procedures.⁷²⁻⁷⁵ In particular, **86**, prepared using the Prins reaction, was first reacted with methyl 2-cyanoacetate assisted by ammonium acetate and acetic acid, followed by 2-bromopyridine under turbo-Grignard conditions to prepare **117**. De-carboxylation of the ester, nitrile hydrolysis to the acid, and BH₃:DMS reduction afforded the primary alcohol **120**, which was oxidized to the aldehyde for reductive amination with selected D₃R PPs: *trans*-2-(4-chlorophenyl)cyclopropan-1-amine and 1-(6-(trifluoromethyl)pyridin-2-yl)piperazine to yield **121** and **122**, respectively. While being able to synthesize key intermediates, such as nitrile, carboxylic acid, and primary alcohol is fundamental to direct future synthetic routes towards different scaffolds and more diverse chemical space, for our purposes an alternative more succinct, and efficient route^{74, 75} was also applied, by directly converting the nitrile **118** to the aldehyde, using DIBAL-H, followed by one-pot reductive amination with any desired amine.



Scheme 11 a) Methyl 2-cyanoacetate, AcOH, AcONH₄, toluene, reflux; b) 2-bromopyridine, isopropyl magnesium chloride (iPrMgCl), CuI, THF, from 0°C to RT; c) and d) KOH, ethylene glycol, 110-120°C; e) BH₃:DMS, THF, from 0°C to RT; f) DMP, DCM, from 0°C to RT; g) DIBAL-H, toluene, from -78°C to RT; h) STAB, cat. AcOH, DCE.

Structure-Activity Relationships and CNS-MPO Analysis

All the new analogues were evaluated for their binding affinities at hMOR, hD_{2L}R and hD₃R, using stable expressing HEK293 cell lines, in competition with [³H]-DAMGO and [³H]-*N*-methylspiperone, respectively. The affinity values are reported as $K_i \pm$ S.E.M. in **Table 1** for all the **6**-based derivatives, and in **Table 2** for the bivalent analogues constructed using **3** as the MOR PP.

Reference compounds **3**, **5**, **6** and previously reported lead molecules⁴⁷ **8**, **9** and **10** (**Figure 1**) are included in the binding tables for comparison. Finally, to obtain a better in-depth overview

of the CNS penetrability of these new analogues, CNS-MPO scores are also reported in the tables (additional detailed values are in **Table S1**). In particular, as mentioned before, the drug design and *in vitro* screening was directed toward identifying new leads with improved D₃R selectivity over the D₂R subtype, with improved CNS-MPO values (e.g., >3), while ultimately still retaining affinity and desired efficacies for both targets of interest (i.e. MOR full or partial agonists; D₃R partial agonists or antagonists).

Although we aimed to develop ligands with CNS-MPO scores >3, there are certain other known factors for brain penetration that are not accounted in the scores: i) flexibility/number of rotatable bonds; ii) impact of acidic moieties; iii) TPSA as a relatively simplistic measure of polar surface area which does not account for 3D conformations; iv) internal H-bonds are relatively beneficial for BBB penetration, while general H-bond donor count in the CNS-MPO score does not differentiate between types of hydrogen bond donors. Given these caveats, we decided to also consider promising compounds, in terms of their *in vitro* pharmacological profiles, even with lower CNS-MPO values of 2.8-2.9. Moreover, too often in the development of analgesics the attention is focused on centrally acting drugs, forgetting the importance of peripherally mediated pain events, often chronic, for which potent, but more peripherally limited MOR agonists could be extremely beneficial therapeutics, with reduced central effects. Thus, we aimed to characterize a large library of compounds, to provide tools for studying and uncovering the multiple facets of the central vs peripheral pain/analgesia mechanisms, as well.

Starting from the previously reported leads **9** and **10**, we observed that both compounds presented 13 rotatable bonds and large molecular weights. According to Pajouhesh and Lenz,⁷⁶ the number of rotatable bonds should be <8 or in general, molecules should be less flexible. Moreover, the presence of a secondary amine in the linker, with its higher p*K*_a, was also detrimental for the

overall score. Thus, inclusion of internal H-bonds to reduce flexibility, combined with the decrease in pKa, was proposed to bring further improvements. Based on this strategy, we synthesized new derivatives by using a pyrrolidine moiety in the linker, with its increased rigidity and decreased pKa due to the tertiary amine group. Moreover, the presence of the hydroxy substitution and its absolute stereochemistry, was supported by previous studies to be optimal for D₃R affinity, and possibly selectivity.^{49, 62, 63} With the first analog **26**, promising MOR affinity was observed (MOR K_i = 23.8 nM), however very poor binding at D₂R and D₃R (D₂R K_i = 1400 nM and D₃R K_i = 705 nM) was likely due to the extra-rigidity induced by the exocyclic alkene linker, and the overall short distance between the two pharmacophores. Saturation of the double bond in the preferred pyrrolidine stereochemistry (2*S*,4*R*)⁶³ was indeed beneficial to rescue binding at D₃R (D₃R K_i = 247 nM and 111 nM for **33** and **34**, respectively), but positioning of the basic nitrogen with respect to the linker and D₃R piperazine PP decreased MOR binding (MOR K_i = 529 nM and 377 nM for **33** and **34**, respectively). Replacing the highly lipophilic piperazines of **33** and **34** with the 1-(6-(trifluoromethyl)pyridin-2-yl)piperazine significantly improved the CNS-MPO score, but negatively affected the overall binding profile. With shorter linker chains, within the D₃R, the pyrrolidine ring appears to clash with neighboring residues, therefore extension of flexible linkers was designed to mitigate these clashes. In particular, compound **46** presented one of the highest D₃R affinities in the series (D₃R K_i = 7.26 nM), selectivity over D₂R (D₂R/D₃R = 19.4), while still maintaining a promising MOR affinity (K_i = 564 nM), suggesting that longer linkers are still tolerated for MOR binding, while being more beneficial for D₃R. Overall, across this SAR campaign, the 1-(6-(trifluoromethyl)pyridin-2-yl)piperazine scaffold appears to cause loss of D₃R affinity, but this loss is compensated for by an increase in D₃R selectivity and CNS-MPO scores, suggesting it as an extremely valuable D₃R PP. Thus, **55** was prepared and tested, and it presented

not just an improved CNS-MPO value >3 , but it also retained good affinities at both D₃R and MOR, with a D₃R subtype selectivity >10 -fold.

A decrease in p*K*_a, can be achieved not only by converting secondary to tertiary amines, but also by introduction of electron withdrawing fluorine atom in the linker. It has been previously observed how fluorine atoms are well tolerated in linker chains for potent and selective D₃R antagonists/partial agonists (**Figure 1**).^{13, 49, 62} Replacement of hydroxy to fluorine atom not only decreases p*K*_a of the basic nitrogen, but it also reduces the number of H-bond donors, and it can form internal H-bonds with protonated nitrogens, thus potentially shielding it from solvent water and further improving BBB penetration. These improvements may not be reflected in the CNS-MPO scores because, the concomitant increase in molecular weight and clogP/clogD account for half of the scores, but for the other half of the parameters potential improvements could still be achieved (**Table S1**). Indeed, replacement of the hydroxy substituent of **55** (p*K*_a = 8.24; **Table S1**) with a fluorine atom, generated **56** (p*K*_a = 7.9; **Table S1**), presenting reasonable affinities at both MOR (*K*_i = 192 nM) and D₃R (*K*_i = 87.3 nM), with the best subtype selectivity observed in the pyrrolidine series (D₂R/D₃R = 23), despite a slight drop in CNS-MPO score with respect to its hydroxy analog (2.8 vs 3.1). This proved the value of the new 1-(6-(trifluoromethyl)pyridin-2-yl)piperazine D₃R PP (**56**), which despite a slight loss of D₃R binding, compared to the classic 2,3-dichlorophenyl piperazine (**57**), is an optimal scaffold to retain moderate-high MOR affinity, and achieve D₃R subtype selectivity in more distal bivalent pharmacophores.

In an attempt to explore newer D₃R PP chemical space, replacement of 2,3-dichlorophenyl with benzothiazole (inspired by **13**) was synthesized, obtaining compound **58**. This yielded one of the most favorable MOR (*K*_i = 146 nM) and D₃R (*K*_i = 53 nM) dual-target affinity ligands, similarly to **56**, despite an undesired drop in D₃R selectivity over D₂R (**58**: D₂R/D₃R = 6.1). Given

Formatted: Font: Italic

Formatted: Font: Bold

Formatted: Font: Bold

Formatted: Font: Bold

Formatted: Font: Bold

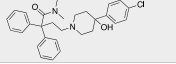
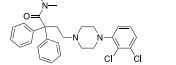
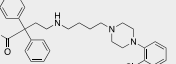
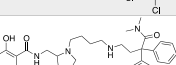
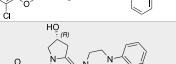

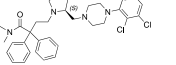
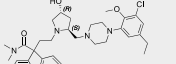
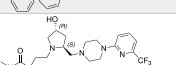
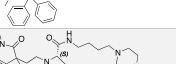
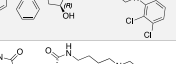
the promising results observed for **56** and **58**, the new 1-(6-(trifluoromethyl)pyridin-2-yl)piperazine and 3-(piperazin-1-yl)benzo[*d*]isothiazole PPs were introduced as replacements to further investigate SAR around the aromatic region of **6**-derivatives, such as **76** and **77**.

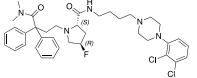
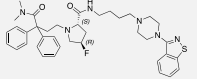
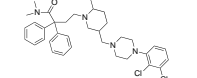
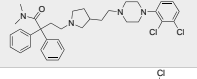
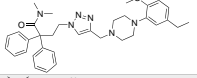
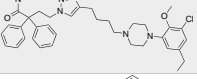
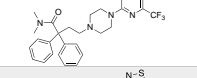
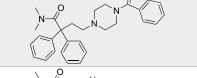
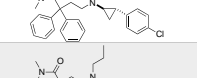
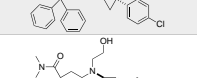
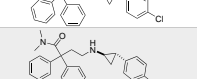
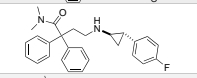
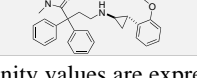
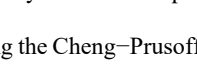
PP replacement started to decrease cLogP, cLogD and p*K*_a, while also positively increasing TPSA enough to significantly impact the CNS-MPO scores (**Table S1**). However, despite presenting some very high affinities for MOR (**76**: MOR *K*_i = 1.23 nM; **77**: MOR *K*_i = 0.364 nM) both analogues lost D₃R affinity, thus making them unsuitable for further dual-target investigation but leaving them as potentially promising selective MOR ligands. This underscored how important different aromatic groups are in the D₃R PP region, when directly linked to the di-phenyl **6**-PP, while sharing the same basic nitrogen for both scaffolds.

With the idea to continue working with lower MW derivatives and optimizing the D₃R PP chemical space, we decided to test a new series of *trans*-cyclopropyl amine scaffolds, inspired by **14** and its D₃R derivatives.⁶¹ Preliminary docking studies predicted that a decreased size of the ring system (from piperazine to cyclopropyl-amine), and more flexible moieties, would have been well tolerated in MOR, while providing better D₃R binding. Indeed, **78**, with a *trans*-2-(4-chlorophenyl)cyclopropan-1-amine as D₃R PP, when compared to **8**, showed better D₃R affinity (*K*_i = 80.1 nM), high MOR binding (*K*_i = 12.3) and >10 fold D₃R selectivity over D₂R. Starting from these observations, we focused the design towards improving CNS-MPO scores (**Table S1**). Unlike *N*-alkylation on the secondary nitrogen which proved to be detrimental for either increasing the lipophilicity too much (**80**, *N*-propyl negatively affected the CNS-MPO value), or abolishing D₃R affinity (**81**), SAR studying substitution patterns around the cyclopropyl phenyl ring proved to be the key to obtain new first in class leads. In particular, replacing the *p*-Cl (**78**), with *p*-OMe (**82**), or *p*-F (**83**) led to significant decreases in D₂-like binding, however shifting the methoxy

substituent from the *para*- to the *ortho*- position, gave **84**, which retained high to moderate MOR ($K_i = 55.2$ nM) and D₃R ($K_i = 382$ nM) affinities, respectively, with the best CNS-MPO score of the series (CNS-MPO = 3.7).

Table 1. Binding affinity for the **6**-based dual-target ligands

Compounds	[³ H]-DAMGO	[³ H]- <i>N</i> -Methylspiperone			CNS MPO Score ^b
	hMOR K_i (nM) ± SEM	hD ₂₁ R K_i (nM) ± SEM	hD ₃ R K_i (nM) ± SEM	Selectivity ratio D ₂ R/D ₃ R	
6 (Loperamide) ^a	 0.268 ± 0.0227 (n=3)	5790 ± 366 (n=4)	1940 ± 78.8 (n=3)	2.99	2.9
8^a	 0.832 ± 0.121 (n=3)	74.7 ± 7.50 (n=3)	171 ± 49.2 (n=3)	0.437	2.3
9^a	 23.8 ± 4.91 (n=3)	43.9 ± 9.04 (n=3)	39.2 ± 11.3 (n=3)	1.12	2.1
10^a	 106 ± 3.25 (n=3)	502 ± 32 (n=3)	135 ± 13.2 (n=3)	3.72	1.4
26	 23.8 ± 3.58 (n=3)	1400 ± 166 (n=3)	705 ± 264 (n=3)	1.99	2.5
33	 529 ± 145 (n=3)	1180 ± 33.3 (n=3)	247 ± 14.9 (n=3)	4.78	2.4
34	 377 ± 37.5 (n=3)	870 ± 117 (n=3)	111 ± 38 (n=3)	7.84	2.3
37	 782 ± 98.7 (n=3)	4660 ± 1660 (n=3)	2700 ± 1800 (n=3)	1.73	3.2
46	 564 ± 185 (n=3)	141 ± 38.7 (n=3)	7.26 ± 2.27 (n=3)	19.4	2.8
55	 791 ± 95.3 (n=3)	2220 ± 190 (n=3)	220 ± 56.2 (n=3)	10.1	3.1
56	 192 ± 47.6 (n=3)	2010 ± 505 (n=3)	87.3 ± 19.9 (n=3)	23.0	2.8

57		787 ± 51 (n=4)	272 ± 55.6 (n=3)	12.5 ± 1.11 (n=3)	21.8	2.8
58		146 ± 38 (n=3)	322 ± 86.4 (n=3)	53.0 ± 4.46 (n=3)	6.08	2.8
62		867 ± 104 (n=4)	146 ± 41.2 (n=3)	309 ± 52.2 (n=3)	0.472	1.5
68		23.5 ± 4.06 (n=3)	117 ± 4.36 (n=3)	20.2 ± 3.24 (n=3)	5.79	1.8
73		2380 ± 819 (n=3)	1440 ± 592 (n=3)	929 ± 492 (n=3)	1.55	3.0
75		2120 ± 374 (n=3)	286 ± 57.6 (n=3)	74.6 ± 48 (n=3)	3.83	3.0
76		1.23 ± 0.384 (n=3)	1480 ± 656 (n=3)	2300 ± 742 (n=3)	0.643	2.8
77		0.364 ± 0.141 (n=3)	465 ± 75 (n=3)	986 ± 87.6 (n=3)	0.472	2.7
78		12.3 ± 2.97 (n=3)	851 ± 25.1 (n=3)	80.1 ± 22.6 (n=3)	10.6	2.5
80		31.2 ± 9.61 (n=3)	978 ± 162 (n=3)	82.0 ± 35.8 (n=3)	11.9	1.4
81		26.9 ± 5.86 (n=4)	7330 ± 1440 (n=4)	3260 ± 1440 (n=4)	2.25	2.8
82		81.8 ± 11.6 (n=3)	8640 ± 3070 (n=4)	1090 ± 254 (n=5)	7.93	3.5
83		47.0 ± 13.2 (n=3)	8010 ± 712 (n=4)	2330 ± 490 (n=4)	3.44	3.0
84		55.2 ± 21.2 (n=4)	1550 ± 336 (n=3)	382 ± 38.8 (n=3)	4.06	3.7

All the affinity values are expressed as $K_i \pm$ standard error of the mean (SEM), derived from IC_{50} values using the Cheng–Prusoff⁷⁷ equation and calculated as the mean of at least three independent experiments (n = number of independent experiments), each performed in triplicate. ^aData previously reported.⁴⁷ ^bCalculated based on the method^{51, 66} previously reported and using

Chemicalize for obtaining physicochemical properties values. All the physicochemical properties and values used to calculate the CNS-MPO score for each compound are reported in the S.I. (**Table S1**).

As expected, compound **3** has an excellent CNS-MPO score of 4.8 (**Table 2**). Interestingly, when the compound, and particularly its basic secondary amine, is protonated, both hydrogens can be shielded by intramolecular hydrogen bonds with the pyridine nitrogen and methoxy group. Based on SAR generated from the **6**-based series, when designing this new library of compounds inspired by **3**, we focused on the effects of alkyl substitutions in the 2-position of the tetrahydropyran (THP) ring, different linker lengths, particularly to evaluate the necessary distance between the aromatic regions of the two pharmacophores and the shared basic nitrogen, and lastly comparison between aryl-piperazines and aryl-cyclopropyl amines as D₃R scaffolds.

In the first groups of analogues, D₃R PPs were connected in position 4 of the THP ring via an ether linkage, which created a favorable linker length to accommodate the compounds within the D₃R. Indeed, most of the new ligands exhibited a consistently high affinity at D₃R, in particular **99** (D₃R $K_i = 22.1$ nM) and **102** (D₃R $K_i = 96.3$ nM), with the latter also presenting D₃R selectivity over D₂R (13-fold). However, extending the basic amine group 4-atom units away from the pyridine aromatic moiety negatively impacted MOR affinity, with most of the ligands presenting K_{iS} in the low micromolar range. Interestingly, and supported by previous literature reports,³⁶ introducing alkyl substitution in position 2 of the THP ring elicits positive pharmacological responses, not just in terms of agonist potency and efficacy, but we also observed improvements in affinity. Of course, adding an alkyl group to the ligands affected the CNS-MPO scores, due to the increased MW and lipophilicity, but nevertheless all the analogues still presented CNS-MPO scores >3.0. Alkyl substitutions were well tolerated in D₃R, with **100** (unsubstituted analog), **102**

(di-ethyl substitution), and **103** (spiro-cyclopentyl substitution) all presenting similar D₃R K_is. The best combination for dual-target affinity was observed with **102**, with a sub-micromolar affinity for MOR (K_i = 745 nM), combined with a high D₃R binding and selectivity, as discussed above.

On the other end, shortening the distance between the D₃R aromatic group and its basic nitrogen, as in **104** and **105**, was detrimental for affinity across the entire spectrum of receptors. A similar outcome, but with loss of binding at MOR, was also observed with the over-extended linker analog **113**.

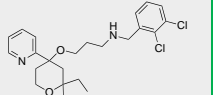
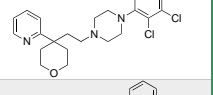
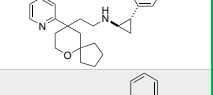
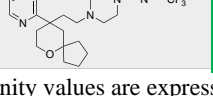
After deciding that the 2-methylene linker (as in **3** and **5**) was likely the most favorable length for the dual-target design, and particularly for MOR affinity, we proceeded to test the new set of piperazine bound analogues, with or without cyclopentyl substitution in the 2-THP ring. When selecting D₃R piperazines, we considered that despite the advantage of presenting lower *p*K_a than secondary amines, they precluded formation of internal H-bonds. Predictions based on the **13**-like benzothiazole scaffold suggested possible CNS-MPO improvement, but the moiety was not used in this set, after observing that in the **6**-series it preferentially favored D₂R affinity, instead of D₃R, when in a short linker combination (**77**), and it did not show any major improvement in affinity or selectivity with extended linkage, if compared to the highly selective 1-(6-(trifluoromethyl)pyridin-2-yl)piperazine. Thus, the design proceeded with the 2,3-dichlorophenyl piperazine and the 1-(6-(trifluoromethyl)pyridin-2-yl)piperazine as the D₃R PP, which showed important features in either achieving low nanomolar D₃R affinity, or D₃R/D₂R subtype selectivity, respectively. Within the unsubstituted THP ring group, **114** showed the most promising dual-target profile, with CNS-MPO = 3.4. Introducing the cyclopentyl substitution as a spiro-ring would have induced a drop in the CNS-MPO, already close to the set threshold, thus **114** was deemed not suitable for further modification. Instead, **115**, with a 4.9 CNS-MPO due to

the hydrophilic 1-(6-(trifluoromethyl)pyridin-2-yl)piperazine D₃R PP, was a good candidate for 2-THP substitution, which yielded **122**, exhibiting a >10-fold improved MOR affinity with respect to its unsubstituted analog (**115**) and retained a >3 CNS-MPO score. Unfortunately, low D₃R binding precluded further development.

Lastly, in **Table 1**, we observed the positive impact on the dual-target and CNS profiles of replacing piperazine rings with *trans*-cyclopropyl amine moieties. The *trans*-cyclopropyl relative configuration has been extensively characterized as favorable to achieve D₂-like receptor affinity and subtype selectivity,⁶¹ and it was the same relative configuration that we continued pursuing.

In silico CNS-MPO predictions suggested that H-bond acceptor in the phenyl ortho-position, when the cyclopropyl is in a *rel-cis* conformation could allow more favorable internal hydrogen bonds, however based on the literature this would have likely led to decreased affinity. Nevertheless, when the D₃R PP *trans*-2-(4-chlorophenyl)cyclopropan-1-amine was linked to the **3** scaffold, the most promising lead molecules within the series was obtained: **121** exhibited comparable affinity at both MOR ($K_i = 85.2$ nM), consistently >10-fold higher with respect to its 2-THP unsubstituted analog **112**, and D₃R ($K_i = 361$ nM), with one of the highest D₃R subtype selectivity in the series (D₂R/D₃R = 15-fold) and CNS-MPO of 3.2.

In the **6**-based series, we reported how introducing an ortho-methoxy group in the phenyl-cyclopropyl amine scaffold can significantly improve the CNS-MPO score, due to its hydrogen bond acceptor status, enabling the creation of intramolecular hydrogen-bonds. However, when comparing **78** (*p*-Cl) with **84** (*o*-OMe), the substitution switch resulted in a loss of D₃R affinity of ~5-fold. This precluded an attempt to perform a similar switch in the **3**-based lead **121**; because starting from a more moderate D₃R K_i , a 5-fold loss of affinity might cause a shift into the micromolar range binding affinities, not suitable for future applications.

104		2520 ± 599 (n=4)	>100000 (n=3)	2700 ± 722 (n=3)	>37.0	4.1
105		540 ± 76.4 (n=3)	13400 ± 2910 (n=3)	1180 ± 279 (n=3)	11.4	2.9
112		1580 ± 158 (n=4)	4070 ± 1040 (n=3)	258 ± 82.4 (n=3)	15.8	4.5
113		1460 ± 101 (n=3)	963 ± 70.9 (n=3)	96.5 ± 24.1 (n=3)	9.98	3.3
114		691 ± 189 (n=6)	121 ± 14 (n=3)	46.5 ± 3.75 (n=3)	2.60	3.4
115		1670 ± 593 (n=4)	7460 ± 605 (n=3)	899 ± 123 (n=3)	8.30	4.9
121		85.2 ± 32.7 (n=7)	5520 ± 1960 (n=5)	361 ± 131 (n=5)	15.3	3.2
122		166 ± 26.5 (n=3)	5430 ± 561 (n=4)	734 ± 101 (n=3)	7.40	3.4

All the affinity values are expressed as $K_i \pm$ standard error of the mean (SEM), derived from IC50 values using the Cheng–Prusoff⁷⁷ equation and calculated as the mean of at least three independent experiments (n = number of independent experiments), each performed in triplicate. ^bCalculated based on the method^{51, 66} previously reported and using Chemicalize for obtaining physicochemical properties values. All of the physicochemical properties and values used to calculate the CNS-MPO score for each compound are reported in the S.I. (**Table S1**).

BRET Functional Studies at MOR and D₃R

Based on their structures, binding affinities and CNS-MPO scores, 13 compounds were selected for functional *in vitro* studies using a range of BRET assays, alongside reference ligands such as DAMGO, morphine and **3** for MOR full, partial, and weak partial agonists respectively, and for D₃R, dopamine and quinpirole as full agonists and **7** as an antagonist. In the **6**-based series, 7 compounds were selected from the pyrrolidine-linked derivatives (**33**, **34**, **46**, **55**, **56**, **58**, and **68**) and 3 compounds from the trans-cyclopropyl amine derivatives (**78**, **80** and **84**). The final 3 compounds were selected from the **3**-based series (**102**, **114** and **121**). At the MOR, all compounds were tested for their ability to activate MOR by measuring recruitment of a conformationally selective nanobody (Nb33) that recognizes and binds to the active conformation of MOR, to promote heterotrimeric G protein dissociation using G α_{i2} G protein activation (GPA) assays at MOR (G α_{i2}) and D₃R (G α_{oA}), and to induce arrestin-3 recruitment to the MOR. Together, these assays measuring proximal, non-amplified signals (Nb33 and arrestin 3) as well as highly amplified signals (GPA), allow for a clear characterization of opioid agonist efficacy such that weak partial agonists can be distinguished from antagonists in the GPA assay and efficacious partial agonist can be distinguished from the reference full agonist DAMGO in the Nb33 and arrestin3 recruitment assays [ref]. At the D₃R, compounds were tested for their ability to promote G α_{oA} GPA as this receptor has been shown to selectively couple to this G protein. The compounds that showed weak or no agonist activity at the D₃R were then tested as antagonists, using the same GPA G α_{oA} assay, in the presence of 3 nM quinpirole. Results are shown in **Figures 3, 4 and 5** and **Table 3**.

In the **6**-based pyrrolidine-linked series (**Figure 3**), all compounds tested were partial agonists at the MOR, except **58** which did not induce any agonist response, all less potent and

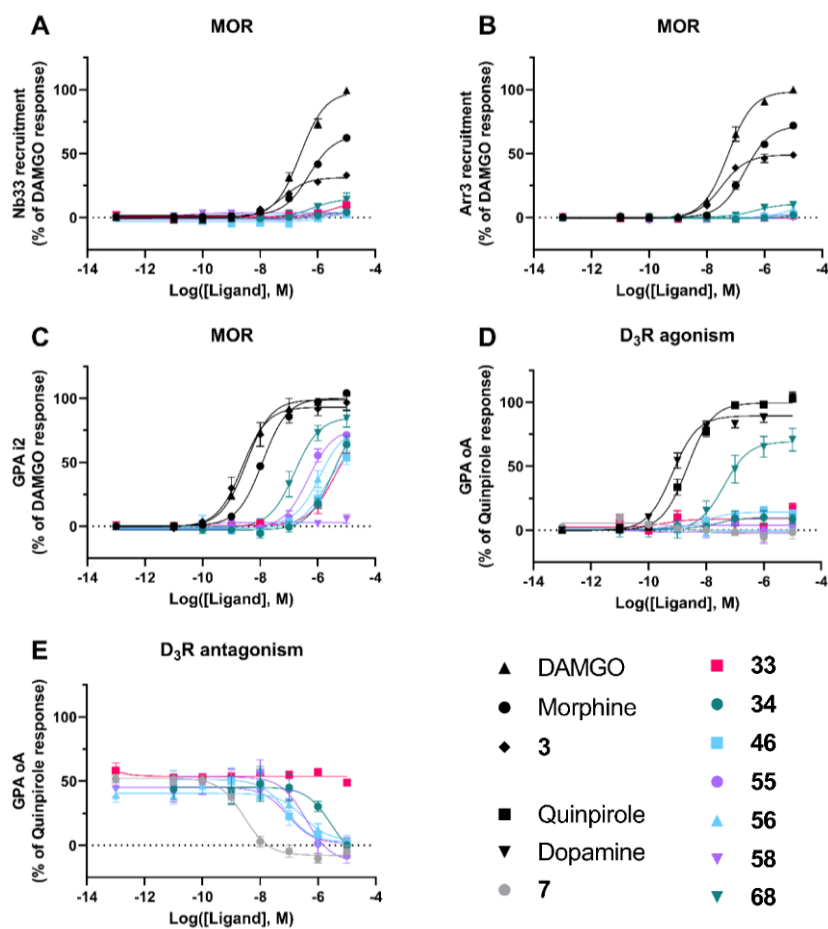
Commented [MC(1): Add references here:
<https://pubmed.ncbi.nlm.nih.gov/32234959/>
<https://pubmed.ncbi.nlm.nih.gov/34158473/>

Commented [MC(2): Reference:
10.1016/j.tips.2020.09.009

Formatted: Highlight

Commented [RL3]: Lane JR, Powney B, Wise A, Rees S, Milligan G. G protein coupling and ligand selectivity of the D2L and D3 dopamine receptors. *J Pharmacol Exp Ther.* 2008 Apr;325(1):319-30. doi: 10.1124/jpet.107.134296. Epub 2008 Jan 24. PMID: 18218829.

efficacious than our 3 reference ligands. The most potent and efficacious ligand at the MOR of this panel is **68**, which is also the only D₃R partial agonist of this subgroup and has a modified



linker compared to the rest of the pyrrolidine-linked derivatives. Although this modified linker prevents from making more analogs of **68** as it decreases its CNS-MPO score, it seems to be beneficial for agonist activity at both receptors. However, a weaker partial agonist or antagonist at the D₃R seems more desirable to reduce potential D₂R/D₃R-mediated side effects.

Figure 3. Functional profiles of selected 6-based pyrrolidine-linked compounds. Each panel shows a different signaling readout: **A.** Nb33 recruitment at MOR, **B.** Arrestin-3 recruitment at MOR in the presence of overexpressed GRK2, **C.** MOR-mediated $G\alpha_{i2}$ protein activation, **D.** D₃R-mediated $G\alpha_{oA}$ protein activation and **E.** Antagonism at D₃R using $G\alpha_{oA}$ GPA in the presence of 3 nM of quinpirole. Data represent mean \pm SEM of 3-9 independent experiments performed in duplicate.

The other 6 compounds of this subgroup did not induce more than 15 % response as D₃R agonists, so they were tested as D₃R antagonists, using the GPA $G\alpha_{oA}$ assay in antagonist mode. They were all able to inhibit the quinpirole-mediated signal except **33**, which had one of the lowest binding affinities at D₃R (**Table 1**). The most potent antagonist of this subgroup and the entire series is **46**. It is a weak partial agonist at the MOR as shown by its weak by detectable response in GPA but not in arrestin-3 or Nb33 recruitment, with a good D₂R/D₃R selectivity ratio and a CNS-MPO score close to 3 which is the desired profile.

In the trans-cyclopropyl amine derivatives (**Figure 4**), all 3 compounds tested had similar profiles. They were all MOR partial agonists and D₃R antagonists, the most potent of them for both receptors being **84**, which makes it a great candidate for future studies and further analog design. With a 6-based MOR PP, the trans-cyclopropyl amine type of linker seems to be better tolerated for MOR activation, particularly for the more proximal assays like Nb33 and arrestin-3 recruitment.

In the 3-based series (**Figure 5**), all 3 compounds showed some agonist activity at the MOR, with **121** exhibiting a similar profile to **3** and being the best MOR agonist tested. At the D₃R, **121** did not induce any agonist activity, but it did inhibit the quinpirole-mediated response

with an inhibitory potency of 271 nM which makes it another good candidate for future studies. Compounds **114** and **102** both showed weak partial agonism at the D₃R, with a potency of 98 nM for **114**, which makes it another interesting ligand to investigate.

To further inform analog design and lead optimization, molecular docking studies were performed on some of the potential lead compounds identified in the BRET functional studies.

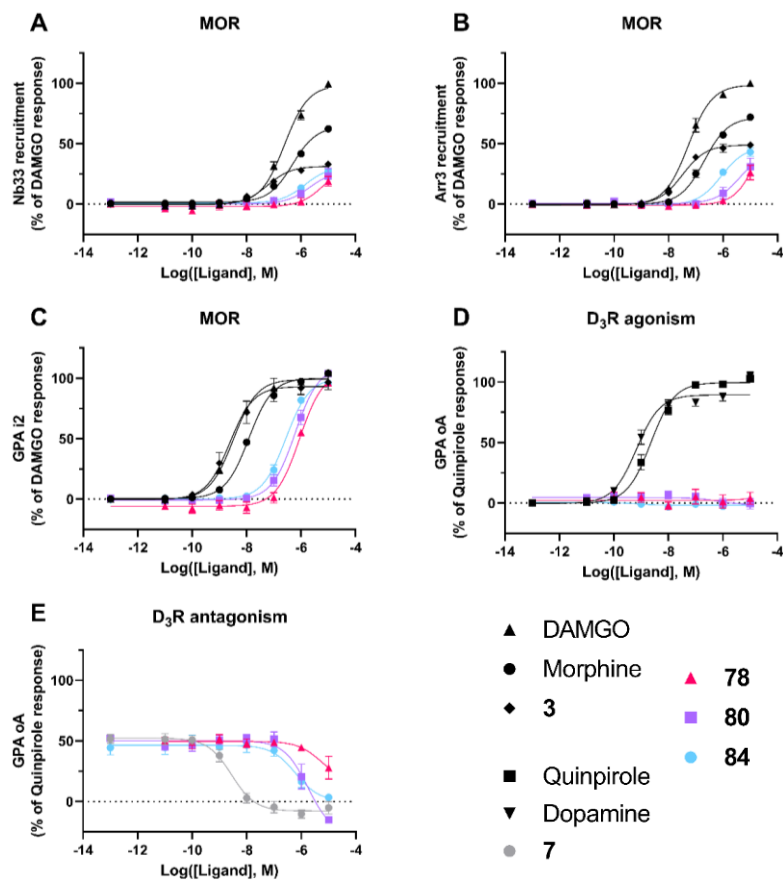


Figure 4. Functional profiles of selected 6-based trans-cyclopropyl amine compounds. Each panel shows a different signaling readout: **A.** Nb33 recruitment at MOR, **B.** Arrestin-3 recruitment at MOR in the presence of overexpressed GRK2, **C.** MOR-mediated $G\alpha_{i2}$ protein activation, **D.** D₃R-mediated $G\alpha_{oA}$ protein activation and **E.** Antagonism at D₃R using $G\alpha_{oA}$ GPA in the presence of 3 nM of quinpirole. Data represent mean \pm SEM of 3-9 independent experiments performed in duplicate.

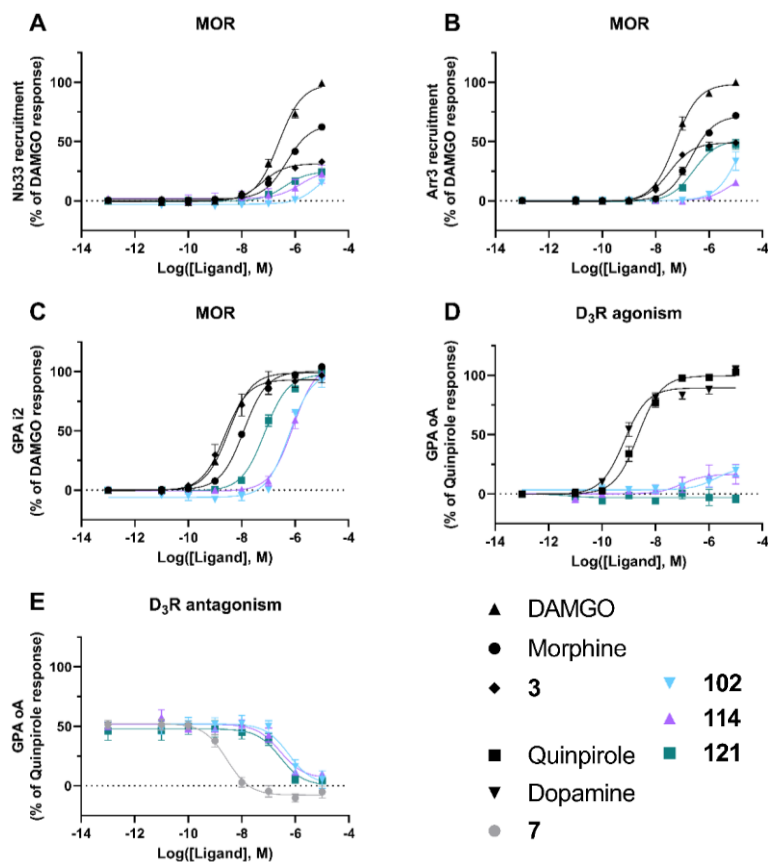


Figure 5. Functional profiles of selected 3-based compounds. Each panel shows a different signaling readout: **A.** Nb33 recruitment at MOR, **B.** Arrestin-3 recruitment at MOR in the presence of overexpressed GRK2, **C.** MOR-mediated $G\alpha_{i2}$ protein activation, **D.** D₃R-mediated $G\alpha_{oA}$ protein activation and **E.** Antagonism at D₃R using $G\alpha_{oA}$ GPA in the presence of 3 nM of quinpirole. Data represent mean \pm SEM of 3-9 independent experiments performed in duplicate

Table 3. Potencies and efficacies at MOR and D₃R

Compound	MOR Nb33 recruitment		MOR G ₁₂ activation		MOR arr3 recruitment (+ GRK2)		D ₃ R G _{oA} activation		
	pEC ₅₀ ± SEM [nM] (n=9)	E _{max} ± SEM (%)	pEC ₅₀ ± SEM [nM] (n=9)	E _{max} ± SEM (%)	pEC ₅₀ ± SEM [nM] (n=9)	E _{max} ± SEM (%)	pEC ₅₀ ± SEM [nM]	E _{max} ± SEM (%)	pIC ₅₀ ± SEM [nM]
DAMGO	6.61 ± 0.05 [248] (n=9)	98.5 ± 2.1	8.48 ± 0.03 [3.28] (n=9)	99.0 ± 0.8	7.26 ± 0.05 [54.4] (n=9)	98.7 ± 1.7	-	-	-
Morphine	6.31 ± 0.04 [491] (n=9)	64.4 ± 1.3	7.92 ± 0.03 [12.1] (n=9)	100.2 ± 1.2	6.68 ± 0.05 [207] (n=9)	71.9 ± 1.4	-	-	-
3	7.23 ± 0.08 [58.5] (n=3)	31.4 ± 0.9	8.62 ± 0.13 [2.40] (n=3)	93.2 ± 3.3	7.49 ± 0.07 [32.5] (n=3)	49.1 ± 1.2	-	-	-
Quinpirole	-	-	-	-	-	-	8.64 ± 0.06 [2.27] (n=9)	99.6 ± 1.7	-
Dopamine	-	-	-	-	-	-	9.17 ± 0.08 [0.68] (n=9)	89.5 ± 2.1	-
7 (Haloperidol)	-	-	-	-	-	-	NA	NA	8.56 ± 0.14 [2.76] (n=9)
33	5.48 ± 0.45 [3,329] (n=3)	12.7 ± 4.0	5.46 ± 0.14 [3,447] (n=3)	73.6 ± 7.5	NA	NA	NA	NA	NA
34	NA	NA	5.48 ± 0.16 [3,314] (n=3)	86.1 ± 10.6	NA	NA	7.60 ± 0.99 [25.4] (n=4)	10.0 ± 3.0	5.53 ± 0.53 [2,962] (n=3)
46	NA	NA	5.74 ± 0.17 [1,810] (n=3)	63.7 ± 7.2	NA	NA	8.01 ± 0.29 [9.84] (n=4)	14.2 ± 1.2	7.10 ± 0.35 [78.9] (n=4)
55	NA	NA	6.33 ± 0.11 [470] (n=3)	76.7 ± 4.0	NA	NA	NA	NA	6.41 ± 0.26 [386] (n=4)
56	5.24 ± 0.50 [5,751] (n=3)	15.0 ± 6.0	5.94 ± 0.08 [1,159] (n=3)	77.6 ± 3.4	6.4% at 10μM (n=3)	ND	NA	NA	6.50 ± 0.27 [316] (n=4)

58	NA	NA	NA	NA	NA	NA	NA	NA	7.04 ± 0.23 [90.9] (n=4)
68	6.18 ± 0.40 [658] (n=3)	14.6 ± 3.1	6.80 ± 0.10 [158] (n=3)	85.4 ± 3.8	6.33 ± 0.20 [470] (n=3)	10.5 ± 1.0	7.38 ± 0.20 [41.7] (n=3)	69.3 ± 4.9	-
78	18.9 % at 10µM (n=3)	ND	6.05 ± 0.07 [890] (n=3)	106.0 ± 4.5	26.2% at 10µM (n=3)	ND	NA	NA	5.26 ± 0.80 [5,446] (n=3)
80	5.68 ± 0.27 [2,100] (n=3)	27.7 ± 4.9	6.21 ± 0.06 [611] (n=3)	110.0 ± 3.3	5.38 ± 0.31 [4,206] (n=3)	43.7 ± 10.6	NA	NA	5.76 ± 0.71 [1,737] (n=3)
84	5.86 ± 0.12 [1,386] (n=3)	31.0 ± 2.3	6.56 ± 0.05 [278] (n=3)	100.5 ± 2.1	6.06 ± 0.08 [876] (n=3)	47.5 ± 2.1	NA	NA	6.21 ± 0.25 [616] (n=4)
102	15.5 % at 10µM (n=3)	ND	6.22 ± 0.08 [604] (n=3)	100.1 ± 4.5	33.5% at 10µM (n=3)	ND	19.8% at 10µM (n=4)	ND	6.25 ± 0.26 [566] (n=4)
114	5.80 ± 0.50 [1,587] (n=3)	25.7 ± 7.4	6.07 ± 0.07 [848] (n=3)	107.4 ± 4.2	5.19 ± 0.32 [6,478] (n=3)	25.1 ± 7.7	7.01 ± 0.59 [98.0] (n=3)	16.6 ± 4.1	6.57 ± 0.20 [269] (n=3)
121	6.39 ± 0.12 [406] (n=3)	24.9 ± 1.4	7.14 ± 0.06 [73.4] (n=3)	97.6 ± 2.2	6.58 ± 0.08 [261] (n=3)	51.3 ± 1.9	NA	NA	6.57 ± 0.27 [271] (n=4)

All data represent the mean of at least three independent experiments (n = number of independent experiments), each performed in duplicate. Potency values are expressed as pEC₅₀ ± SEM with the corresponding EC₅₀ in nM in brackets. Efficacy values are calculated as a percentage of a reference ligand (DAMGO or quinpirole for MOR and D₃R, respectively) and expressed as E_{max} ± SEM (%). NA = No Activity, the compound presents no agonist or antagonist activity at the highest tested concentration; ND = Not determined.

Molecular Docking

For the rational design of our dual-target molecules, we used structure-based molecular modeling techniques. The inactive-state D₃R (PDB: 3PBL)⁷⁸ and active-state MOR (PDB: 5C1M)⁷⁹ were used for all atom docking investigations, and ICM-Pro (Molsoft LLC)⁸⁰ was used to locally optimize receptor–ligand interactions utilizing energy-based Monte Carlo minimization techniques.

As depicted in **Figure 6**, the optimal binding modes of the most promising dual-target ligands, **3**-based **121**, and **6**-based **84** show salt bridge interactions between the basic nitrogen and the conserved D110^{3.32} of the antagonist-state D₃R receptor. The hydrophobic residues V111^{3.33}, V189^{5.39}, W342^{6.48}, F345^{6.51}, F346^{6.52}, and H349^{6.55} define the OBS of the D₃R, that surrounds the *para*-Cl-substituted phenyl residue of the trans-cyclopropyl amine scaffold of **121** (**Figure 6A**). The OBS in D₃R is located between TM3, TM5, and TM6 and represented by semi-transparent molecular surface. The spiro-cyclopentyl substituted tetrahydropyran ring in **3**-based **121** effectively targets the SBP of D₃R, lined with hydrophobic L89^{2.64} and C181^{ECL2} residues from the one side and polar Y365^{7.35}, Y32^{1.35} and S182^{ECL2} from the other (**Figure 6B**). The binding poses of *p*-Cl-phenyl moiety in **121** and the *o*-OMe substituted phenyl moiety of **84** are overlapping, acquiring *N,N*-dimethyl-2,2-diphenylacetamide in **84** to be additionally stabilized by hydrogen bonding interactions with Y365^{7.35} when targeting D₃R OBS located between TM3, TM5, and TM6.

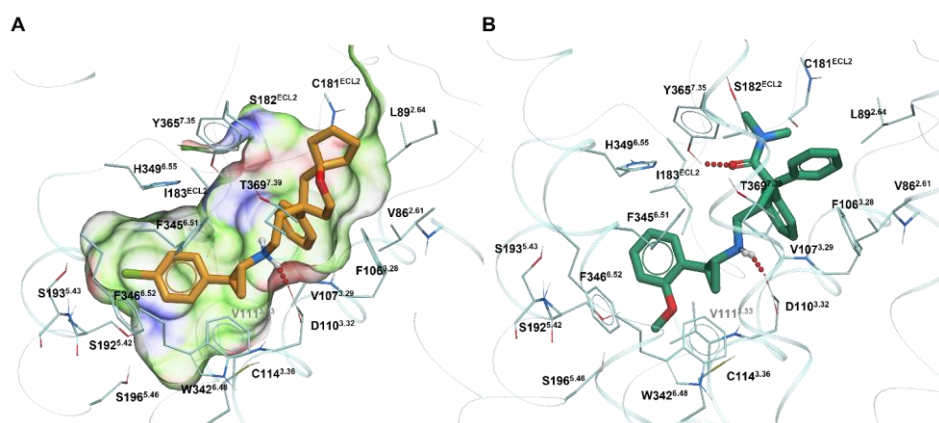


Figure 6. Binding mode of **121** (orange sticks, panel A) and **84** (green sticks, panel B) inside the D3R (cyan; PDB: 3PBL). A semi-transparent skin reveals the receptor's molecular surface, which is colored by the residue properties (red (acidic), blue (basic), green (hydrophobic)).

In **121**, the *p*-Cl phenyl-cyclopropyl amine PP of the D₃R is tethered to MOR PP tetrahydropyran ring, occupying the SBP and OBS sites of MOR receptor correspondingly (**Figure 7A**). The MOR hydrophobic OBS is formed within TM3, TM5, TM6, and TM7 helices and inner pocket water-mediated hydrogen bonding interactions with Y150^{3.33} and H299^{6.52}. When targeting OBS, the trans-cyclopropyl amine moiety of **121** is producing a salt bridge interaction ~~between the basic nitrogen of the cyclopropyl amine moiety and with~~ the conserved D149^{3.32} in OBS (**Figure 7A**). Similar to **121**, the *N,N*-dimethyl-2,2-diphenylacetamide PP of the canonical MOR in **84** occupies the OBS pocket of MOR receptor in the active state, defined by the Y150^{3.33}, M153^{3.35}, V238^{5.42}, W295^{6.48}, I298^{6.51}, H299^{6.52}, V302^{6.55}, W320^{7.35}, G327^{7.42}, I324^{7.39}, and Y328^{7.43} residues (**Figure 7B**). The trans-cyclopropyl amine moiety links the *N,N*-dimethyl-2,2-diphenylacetamide residue to the *o*-methoxy phenyl PP of D₃R, which targets the SBP of MOR which is defined by transmembrane 5 (TM5) and extracellular loop (ECL2) domains. The engagement of the TM5-

found to occupy the SBP whereas the aryl-piperazine moiety comfortably targets the hydrophobic OBS of the D₃R (**Figure 8B**).

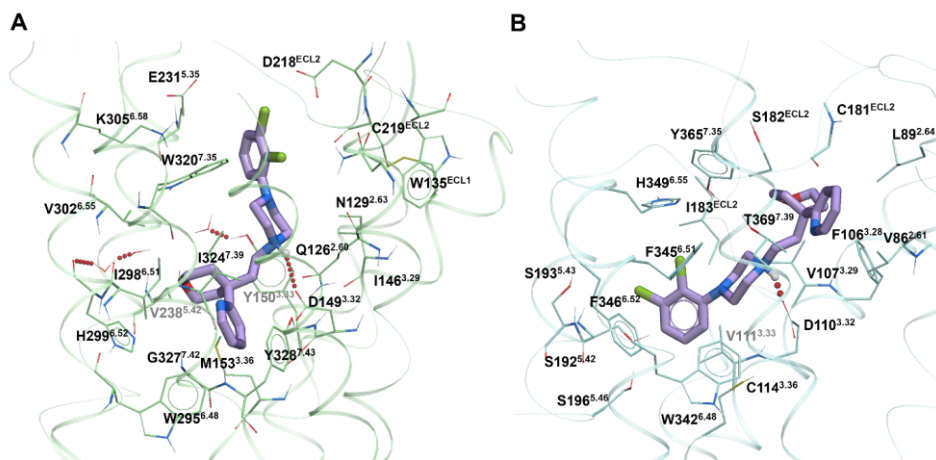


Figure 8. Binding mode of **114** (purple sticks) inside the (A) MOR (light green; PDB: 5C1M) and (B) D₃R (cyan; PDB: 3PBL).

The conformationally flexible 3-based dual-target **102** ligand revealed similar docking modes for MOR and D₃R to the more rigid analog **114** (**Figure 9**). Thus, the extended 2,3-dichlorophenyl moiety of **102** has been moved slightly further into the subpocket between TM5-ECL2 of MOR (**Figure 6A**). The di-ethyl substituted tetrahydropyran moiety of **102** has been shown to fit well into the OBS of MOR justifying its PP origin. In addition to the salt bridge interaction between the 2-trifluoro-substituted pyridine-piperazine D₃R PP motif and D110^{3.32}, the tetrahydropyran moiety in **102** is effectively targeting the SBP of D₃R as well (**Figure 9B**). Furthermore, as expected, the hydrophobic trifluoro-substituent residue of pyridine moiety is well tolerated in the hydrophobic OBS of the D₃R.

diphenylbutanamide moiety of **55** and **46** is well tolerated in the SBP of the D₃R with the hydroxy substituent of the pyrrolidine-like linker and the amide tether forming hydrogen bonds with L89^{2,64} and T369^{7,39} correspondingly. The F-substituted pyrrolidine-linked **6**-based **56** and **58** dual-target ligands revealed the same well fitted binding motifs into the solvent-accessible active MOR and inactive state dopamine receptors, albeit lacking the hydrogen bonding interaction with L89^{2,64} in D3 (Figure S1, S2).

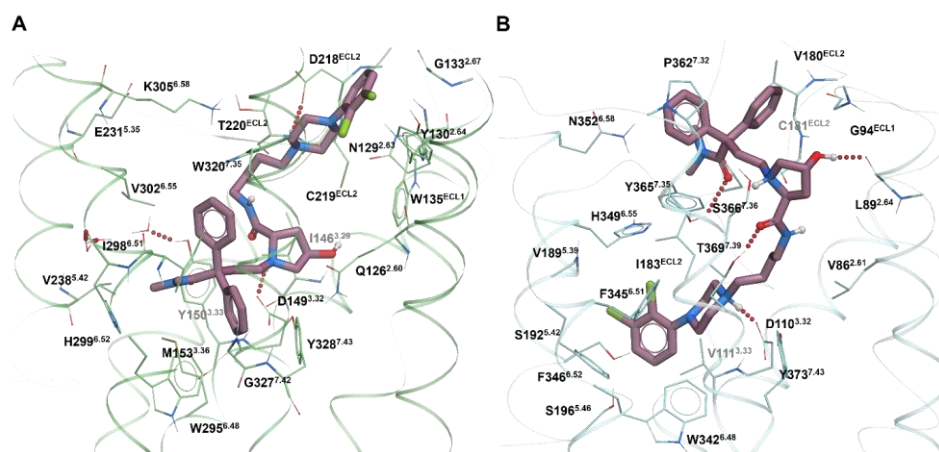


Figure 10. Binding modes of **46** (mate purple) inside the (A) MOR (light green; PDB: 5C1M) and (B) D₃R (cyan; PDB: 3PBL).

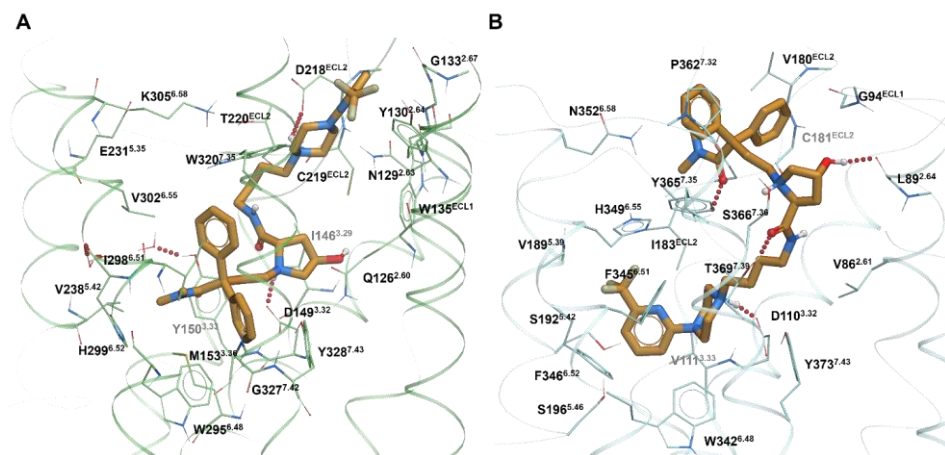


Figure 11. Binding modes of **55** (mate purple) inside the (A) MOR (light green; PDB: 5C1M) and (B) D₃R (cyan; PDB: 3PBL).

CONCLUSIONS

It is evident how challenging it is to combine drug design features that satisfy multiple-receptor affinity, subtype selectivity, and exploration of innovative chemical space resulting in retention of pharmacologically desired efficacy at both receptor targets, while attempting to also optimize peripheral versus CNS activity. Often chemical modifications that improve CNS penetrability are not favorable for dual receptor engagement and, on the contrary, highly decorated scaffolds that can push the limit of drug design to extremely high affinity and potency, exploiting the nuances of structure-based drug design, tend to be detrimental for brain/plasma distribution and CNS activity. Ultimately, the key resides in being able to find the right compromise. Herein, we reported an extensive SAR study conducted in parallel between *in vitro* cell-based assays screening and *in silico* prediction models, that ultimately identified promising leads, based on **6** (i.e. **46**, **55**, **56**, **58** and **84**) and **3** (**102**, **114** and **121**), which presented high to moderate affinities and selectivity for both MOR and D₃R, while still retaining CNS-MPO scores between 2.8-3.7.

We not only introduced an innovative approach for dual-target pharmacology, but with a highly methodical synthetic work, supported by computer aided drug design, the we exploration explored of untapped chemical space, probing the respective receptor's binding sites and thus identifying scaffold compositions for maximized pharmacological profiles.

The new leads offer potential for *in vivo* analgesia with reduced addictive liability, and possibly present a new direction to develop safer pain medications. In addition, ~~some~~ of the most ~~active and~~ potent ~~and~~ active compounds, demonstrating the desired dual-pharmacology profile, ~~endowed with the desired dual pharmacological profile, have been despite being~~ predicted to be more peripherally limited (CNS-MPO <2.5: compounds **8, 9, and 10** from the ~~previous generation;~~⁴⁷ ~~compounds 34, 68, 78, and 80 from this new series~~), ~~yet~~ may be valuable therapeutics for inflammation and pain mediated by peripheral MOR mechanisms. From a medicinal chemistry perspective, these new leads offer ~~extended further~~ additional opportunities for future optimization campaigns. Moreover, they underscore how starting from selective ligands for specific receptor families, it is possible to identify shared structural moieties to design and synthesize unique dual target pharmacotherapeutics.

EXPERIMENTAL METHODS

Chemistry

All chemicals and solvents were purchased from chemical suppliers unless otherwise stated and used without further purification. All melting points were determined (when obtainable) on an OptiMelt automated melting point system and are uncorrected. Reactions were not yield optimized. The ¹H and ¹³C NMR spectra were recorded on a Varian Mercury Plus 400 instrument. Proton chemical shifts are reported as parts per million (δ ppm) relative to tetramethylsilane (0.00 ppm) as an internal standard, or to deuterated solvents. Coupling constants are measured in Hz.

Formatted: Font: Bold

Formatted: Font: Bold

Formatted: Font: Bold

Formatted: Font: Bold

Formatted: Font: Bold

Formatted: Font: Bold

Formatted: Font: Bold

Chemical shifts for ^{13}C NMR spectra are reported as parts per million (δ ppm) relative to deuterated CHCl_3 or deuterated MeOH (CDCl_3 77.5 ppm, CD_3OD 49.3 ppm). Chemical shifts, multiplicities and coupling constants (J) have been reported and calculated using Vnmrj Agilent-NMR 400Mr or MNova 9.0 software. Gas chromatography-mass spectrometry (GC/MS) data were acquired (where obtainable) using an Agilent Technologies (Santa Clara, CA) 7890B GC equipped with an HP-5MS column (cross-linked 5% PH ME siloxane, 30 m \times 0.25 mm i.d. \times 0.25 μm film thickness) and a 5977B mass-selective ion detector in electron-impact mode. Ultrapure grade helium was used as the carrier gas at a flow rate of 1.2 mL/min. The injection port and transfer line temperatures were 250 and 280 $^\circ\text{C}$, respectively, and the oven temperature gradient used was as follows: the initial temperature (70 $^\circ\text{C}$) was held for 1 min and then increased to 300 $^\circ\text{C}$ at 20 $^\circ\text{C}/\text{min}$ and maintained at 300 $^\circ\text{C}$ for 4 min, total run time 16.5 min. Column chromatography was performed using a Teledyne Isco CombiFlash RF flash chromatography system, or a Teledyne Isco EZ-Prep chromatography system. Preparative thin layer chromatography was performed on Analtech silica gel plates (1000 μm). When %DMA is reported as eluting system, it stands for % of methanol in DCM, in presence of 1% NH_4OH . Preparative chiral HPLC was performed using a Teledyne Isco EZ-Prep chromatography system with DAD (Diode Array Detector) and ELS detectors. HPLC analysis was performed using an Agilent Technologies 1260 Infinity system coupled with DAD. For each analytical HPLC run multiple DAD λ absorbance signals were measured in the range of 210-280 nm. Separation of the analyte, purity and enantiomeric/diastereomeric excess determinations were achieved at 40 $^\circ\text{C}$ using the materials and methods reported in each detailed reaction description (general eluting condition: 0-10 min at 10% ACN in water; 10-20 min gradient increase to 40% ACN in water, maintained at 40% ACN from 20-30 min; 30-40 min gradient increase to 80% ACN in water, maintained at 80% ACN until the

end of the 60 min total maximum run time; either 0.1% TFA or 0.1% DEA were used as mobile phase additives, as detailed in each compound analytical reports). Preparative and analytical HPLC columns were purchased from Daicel corporation, Agilent or Phenomenex. Preparative HPLC methods and conditions are reported in the descriptions of the chemical reactions where they were applied. Microanalyses were performed by Atlantic Microlab, Inc. (Norcross, GA) and agree with $\pm 0.4\%$ of calculated values. In Electrospray Ionization Mass Spectrometry (ESI-MS) neat solutions of samples were dissolved and diluted in acetonitrile (ACN). Samples were analyzed by direct injection (10 μ L) using a Vanquish UHPLC system (ThermoFisher, Waltham, MA) with tandem Orbitrap Exploris 120 mass spectrometer (ThermoFisher). The flow rate was 200 μ L/min with an isocratic mobile phase of 80% ACN for the four-minute run. Analysis was performed using a heated electron spray ionization (HESI) source in positive ion mode. In MS mode, the mass resolution was set at 120,000 while in MS/MS mode the mass resolution was set at 15,000. In Matrix-Assisted Laser Desorption/Ionization Mass Spectrometry (MALDI-MS) neat solutions of samples were dissolved and diluted in methanol (MeOH). Samples were mixed with the MALDI matrix prior to spotting 1 μ L of the sample/matrix solution on the sample target. Alpha-cyano-4-hydroxycinnamic acid (CHCA) prepared at 10 mg/mL in ACN/EtOH/0.003%TFA in water (84/13/3 v/v/v) and 2,6-dihydroxyacetophenone (DHA) prepared as a saturated solution in 50% EtOH were used as MALDI matrices. Mass analysis was conducted using a LTQ-XL-Orbitrap with a MALDI ion source (Thermo Fisher Scientific, San Jose, CA) in positive ion mode. In MS mode, the mass resolution was set at 100,000 while in MS/MS mode the mass resolution was set at 15,000. Unless otherwise stated, all the test compounds were evaluated to be >95% pure based on combustion analysis, NMR, GC-MS, and HPLC-DAD-HRMS-MS/MS. The detailed analytical results are reported in the characterization of each final compound and in the S.I..

(2*S*,4*R*)-1-(*tert*-Butoxycarbonyl)-4-((*tert*-butyldimethylsilyl)oxy)pyrrolidine-2-carboxylic acid (19**)** *tert*-Butylchlorodimethylsilane (6.52 g, 43.2 mmol) was added portion-wise to a solution of **18** (5.00 g, 21.6 mmol) and imidazole (2.94 g, 43.2 mmol) in DCM (20 mL) and DMF (5 mL). The reaction was stirred at RT for 2 h, the mixture was washed with 0.1N HCl and sat. NH₄Cl, dried over Na₂SO₄, filtered, and the solvents were evaporated under vacuum. The residue was used in the following step without further purification (6.80 g, 91% yield). ¹H NMR (400 MHz, CDCl₃) (mixture of rotamers) δ 4.51 – 4.14 (m, 2H), 3.57 (ddd, *J* = 19.8, 11.0, 5.3 Hz, 1H), 3.33 (ddd, *J* = 41.1, 11.1, 3.9 Hz, 1H), 2.18 (dddd, *J* = 18.4, 13.3, 8.3, 5.3 Hz, 1H), 2.10 – 1.91 (m, 1H), 1.43 (2 x s, 9H), 0.99 – 0.73 (2 x s, 9H), 0.36 – 0.19 (2 x s, 6H).

***tert*-Butyl (2*S*,4*R*)-4-((*tert*-butyldimethylsilyl)oxy)-2-(hydroxymethyl)pyrrolidine-1-carboxylate (**20**)** A solution of **19** (4.00 g, 11.6 mmol) was dissolved in THF (20 mL), followed by drop-wise addition of borane-methyl sulfide complex (28.9 mL, 2M in THF, 57.9 mmol) at 0°C. The reaction mixture allowed to warm to RT and stirred overnight under argon atmosphere. The reaction was quenched with sat. aq. NH₄Cl and extracted with EtOAc. The organic phase was dried over Na₂SO₄, filtered, and the solvent was evaporated under vacuum. The crude material was purified by flash chromatography, eluting with 40% EtOAc in hexanes to yield the desired product (2.20 g, 57% yield). ¹H NMR (400 MHz, CDCl₃) δ 4.89 (d, *J* = 8.2 Hz, 1H), 4.28 (br s, 1H), 4.17 – 4.09 (m, 1H), 3.69 (t, *J* = 9.9 Hz, 1H), 3.54 (t, *J* = 9.5 Hz, 1H), 3.43 (d, *J* = 11.7 Hz, 1H), 3.34 (dd, *J* = 11.6, 4.1 Hz, 1H), 1.95 (m, 1H), 1.60 (m, 1H), 1.47 (s, 9H), 0.87 (s, 9H), 0.06 (s, 6H).

***tert*-Butyl (R)-4-((*tert*-butyldimethylsilyloxy)-2-((4-(2,3-dichlorophenyl)piperazin-1-yl)methylene)pyrrolidine-1-carboxylate (22)** DMP (2.8 g, 1 equiv, 6.6 mmol) was added portion-wise, at 0°C, to a solution of **20** (2.2 g, 6.6 mmol) in DCM (30 mL). The mixture was warmed to RT and stirred for additional 1 h. The mixture was washed with sat. aq. NaHCO₃, dried over Na₂SO₄ and filtered. 3 drops of AcOH were added to the stirring solution of crude aldehyde **21**, followed by the addition of 1-(2,3-dichlorophenyl)piperazine (1.5 g, 6.6 mmol). The reaction was stirred at RT for 30 min. Immediate precipitation of the iminium salt intermediate was observed, then sodium triacetoxyborohydride (STAB, 1.4 g, 6.6 mmol) was added portion-wise. The precipitate never went back into DCM solution, and thus, the expected reduction never occurred. After 2 h, the reaction was quenched, and the organic phase washed with 2N aq. NaOH and brine. The organic layer was dried over Na₂SO₄, filtered, evaporated under vacuum, and the residue purified by flash chromatography. The enamine product eluted with 2% DMA (2% MeOH with 0.5% NH₄OH, in DCM) (2.0 g, 55% yield). ¹H NMR (400 MHz, CDCl₃) δ 7.13 (m, 2H), 6.92 (t, *J* = 7.4 Hz, 1H), 5.36 – 5.25 (m, 1H), 4.39 (m, 1H), 4.01 (m, 1H), 3.38 (m, 1H), 3.02 (br s, 4H), 2.72 – 2.60 (m, 4H), 2.33 (dt, *J* = 13.6, 4.2 Hz, 1H), 1.99 (br s, 1H), 1.49 (m, 9H), 0.90 (m, 9H), 0.06 (dd, *J* = 4.2, 2.1 Hz, 6H).

(R)-5-((4-(2,3-Dichlorophenyl)piperazin-1-yl)methylene)pyrrolidin-3-ol (24) TBAF (1 M in THF; 12 mL, 12 mmol) was added to a stirring solution of **22** (2.2 g, 4.1 mmol) in THF (20 mL). The mixture was stirred for 45 min until complete deprotection of the silyl ether was observed in TLC. The solvent was evaporated under vacuum, and the crude intermediate **23** was dissolved in DCM (20 mL), followed by addition of TFA (10 mL). The mixture was stirred overnight at RT. The excess of TFA was evaporated under vacuum, and the residue was basified with 2N aq. NaOH

and extracted with DCM:2-PrOH (3:1). The organic phase was dried over Na₂SO₄, filtered, and evaporated under vacuum to obtain the crude material which was used in the next step without further purification.

(R)-4-(2-((4-(2,3-Dichlorophenyl)piperazin-1-yl)methylene)-4-hydroxypyrrolidin-1-yl)-N,N-dimethyl-2,2-diphenylbutanamide (26) Compound **25**⁴⁷ (1.1 g, 3.9 mmol) was dissolved in DCE (15 mL), followed by the addition of cat. AcOH (3-4 drops) and a solution of **24** (1.3 g, 3.9 mmol) in DCE (15 mL). The mixture was stirred for 30 min, then STAB (0.83 g, 3.9 mmol) was added portion-wise. The reaction was stirred overnight at RT. The reaction was diluted with a solution of 0.5% NH₄OH in MeOH, the solvents were evaporated under vacuum, and the residue was purified by flash chromatography eluting with 10% DMA (0.57 g, 24% yield). ¹H NMR (400 MHz, CDCl₃) δ 7.65 (br s, 1H), 7.57 (d, *J* = 1.6 Hz, 2H), 7.57 – 7.46 (m, 2H), 7.44 (dt, *J* = 9.2, 1.6 Hz, 1H), 7.37 (ddt, *J* = 12.4, 10.3, 3.1 Hz, 3H), 7.33 – 7.16 (m, 2H), 7.16 – 7.08 (m, 1H), 6.94 (dtd, *J* = 11.4, 5.7, 4.9, 2.9 Hz, 1H), 5.33 – 5.24 (m, 1H), 4.44 (br s, 1H), 3.79 (br s, 1H), 2.95 (m, 9H), 2.45 (2 x br s, 10H), 1.86 (dd, *J* = 28.4, 19.6 Hz, 3H). ¹³C NMR (101 MHz, CDCl₃) δ 173.38, 152.41, 140.00, 135.06, 130.87, 129.30, 129.26, 129.08, 128.39, 128.12, 125.40, 119.54, 71.76, 64.13, 63.51, 54.56, 51.98, 41.43, 40.29, 38.49. The free base was converted into the corresponding oxalate salt, obtained as a white solid (m.p. >165°C decomposition). HRMS-MS/MS C₃₃H₃₈Cl₂N₄O₂ + H⁺ calculated 593.24446, found 593.24552. Elemental analysis (C₃₃H₃₈Cl₂N₄O₂ + 2.5 H₂C₂O₄ + 2.5 H₂O) calculated C 52.84, H 5.60, N 6.49, found C 52.54, H 5.24, N 6.87.

***tert*-Butyl (2*S*,4*R*)-2-(4-(2,3-dichlorophenyl)piperazine-1-carbonyl)-4-hydroxypyrrolidine-1-carboxylate (27)** EDC HCl salt (1.66 g, 8.65 mmol) and HOBt (1.17 g, 8.65 mmol) were added to a solution of **18** (2.00 g, 8.65 mmol) in DCM (50 mL), followed by the addition of TEA (2.41 mL, 17.3 mmol). The mixture was stirred at RT for 30 min, followed by dropwise addition of 1-(2,3-dichlorophenyl)piperazine⁵⁷ (2.00 g, 8.65 mmol) dissolved in DCM (50 mL). The reaction was stirred at RT for an additional 2 h. The solvents were evaporated under vacuum, and the residue was purified by flash chromatography eluting with 100% EtOAc (2.3 g, 60% yield). ¹H NMR (400 MHz, CDCl₃) (mixture of rotamers) δ 7.17 (ddd, *J* = 7.4, 4.6, 1.7 Hz, 2H), 6.96 – 6.88 (m, 1H), 4.91 – 4.76 (m, 1H), 4.51 (2 x br s, 1H), 3.87 (s, 2H), 3.79 – 3.66 (m, 4H), 3.61 - 3.50 (2 x d, *J* = 11.8, 11.7 Hz, 1H), 3.07 - 3.00 (m, 4H), 1.80 (m, 2H), 1.44 (dt, *J* = 13.5, 2.8 Hz, 9H).

***tert*-Butyl (2*S*,4*R*)-2-(4-(3-chloro-5-ethyl-2-methoxyphenyl)piperazine-1-carbonyl)-4-hydroxypyrrolidine-1-carboxylate (28)** The desired product was prepared as described for **27**, starting from 1-(3-chloro-5-ethyl-2-methoxyphenyl)piperazine⁵⁷ (0.300 g, 1.18 mmol), in presence of TEA (0.492 mL, 3.53 mmol) and purified by flash chromatography eluting with 10% DMA (0.500 g, 91% yield). ¹H NMR (400 MHz, CDCl₃) (mixture of rotamers) δ 6.90 (d, *J* = 7.8 Hz, 1H), 6.59 (s, 1H), 4.83 (dt, *J* = 34.4, 7.7 Hz, 1H), 4.52 (2 x br s, 1H), 3.85 (d, *J* = 3.1 Hz, 3H), 3.68 (dd, *J* = 27.6, 12.7 Hz, 4H), 3.49 (d, *J* = 2.1 Hz, 4H), 3.39 – 2.83 (m, 4H), 2.55 (d, *J* = 7.9 Hz, 2H), 1.45 (d, *J* = 14.1 Hz, 9H), 1.20 (t, *J* = 7.6 Hz, 3H).

(3*R*,5*S*)-5-((4-(2,3-Dichlorophenyl)piperazin-1-yl)methyl)pyrrolidin-3-ol (31)

The intermediate **29** was prepared by -Boc deprotection, mediated by TFA, as described for **24**, starting from **27** (2.30 g, 5.18 mmol). The obtained crude material was immediately dissolved in

THF (15 mL) and added dropwise to a stirring suspension of LAH (500 mg, 13.2 mmol) in THF (15 mL) at 0°C under argon atmosphere. After the dropwise addition was completed, the reaction was allowed to warm to RT and stirred overnight. The mixture was cooled to 0°C, and the reaction quenched by slow dropwise addition of sat. aq. Na₂SO₄. The suspension was filtered, and the solvents were evaporated under vacuum to yield the crude material, which was used in the following step without further purification (0.470 g, 99% yield).

(3*R*,5*S*)-5-((4-(3-Chloro-5-ethyl-2-methoxyphenyl)piperazin-1-yl)methyl)pyrrolidin-3-ol

(32) The desired product was prepared as described for **31**, starting from **28** (500 mg, 1.07 mmol) and used in the following step without further purification (290 mg, 77% yield).

4-((2*S*,4*R*)-2-((4-(2,3-Dichlorophenyl)piperazin-1-yl)methyl)-4-hydroxypyrrolidin-1-yl)-

***N,N*-dimethyl-2,2-diphenylbutanamide (33)** The compound was prepared following the general reductive amination procedure described for **26**, starting from **31** (780 mg, 2.37 mmol) and **25** (930 mg, 3.31 mmol), and isolated by C18 preparative HPLC as TFA salt (Phenomenex Gemini NX-C18 110 Å, AXIA Packed, 150 x 30 mm, 5 µm; gradient 10%-80% ACN in water + 0.1% TFA; 60 min run; injection 4mL (~10-15 mg/mL); temperature 25 C; DAD λ₂₁₄ nm and λ₂₅₄ nm) (324 mg, 17% yield, yellow oil). ¹H NMR (400 MHz, CDCl₃) δ 7.49 – 7.17 (m, 12H), 6.98 (dd, *J* = 7.9, 1.7 Hz, 1H), 4.53 (s, 1H), 4.16 (br s, 1H), 3.84 (d, *J* = 12.1 Hz, 1H), 3.52 (d, *J* = 13.3 Hz, 1H), 3.40 – 3.20 (m, 9H), 2.99 (br s, 4H), 2.86 (m, 2H), 2.70 (t, *J* = 11.5 Hz, 1H), 2.60 – 2.40 (m, 2H), 2.31 (s, 3H), 2.14 – 1.99 (m, 2H). ¹³C NMR (101 MHz, CDCl₃) δ 173.49, 149.38, 139.49, 138.00, 134.33, 129.30, 129.20, 129.08, 128.34, 128.25, 127.95, 127.83, 127.72, 127.58, 125.91, 118.95, 68.77, 61.60, 60.20, 59.68, 56.72, 53.53, 48.67, 39.85, 39.51, 39.26, 37.36. HRMS-

MS/MS $C_{33}H_{40}Cl_2N_4O_2 + H^+$ calculated 595.26011, found 595.25984. Analytical HPLC: Agilent poroshell C-18 4.6 x 50 mm, 2.7 μ m; gradient 10%-80% ACN in water + 0.1% TFA; 60 min run; injection 20 μ L (1 mg/mL); temperature 40°C; R 22.862 min, purity >99%.

4-((2*S*,4*R*)-2-((4-(3-Chloro-5-ethyl-2-methoxyphenyl)piperazin-1-yl)methyl)-4-

hydroxypyrrolidin-1-yl)-*N,N*-dimethyl-2,2-diphenylbutanamide (34) The compound was prepared following the general reductive amination procedure described for **26**, starting from **32** (290 mg, 0.819 mmol) and **25** (231 mg, 0.819 mmol). The desired product was isolated by flash chromatography eluting with 15% DMA (180 mg, 36% yield). 1H NMR (400 MHz, $CDCl_3$) δ 7.41 – 7.30 (m, 9H), 7.30 – 7.16 (m, 1H), 6.88 – 6.83 (s, 1H), 6.60 (s, 1H), 4.50 (q, $J = 3.6$ Hz, 1H), 3.93 (dd, $J = 12.4, 4.9$ Hz, 1H), 3.78 (s + m, 3H + 1H), 3.56 (d, $J = 12.4$ Hz, 1H), 2.95 (s, 3H), 2.85 (m, 7H), 2.70 – 2.53 (m, 6H), 2.37 – 2.22 (m, 6H), 1.98 (dd, $J = 8.6, 5.6$ Hz, 2H), 1.24 (t, $J = 7.6$ Hz, 3H). ^{13}C NMR (101 MHz, $CDCl_3$) δ 176.56, 176.52, 174.49, 173.37, 146.25, 146.06, 140.73, 128.86, 128.79, 128.20, 128.08, 127.87, 127.54, 127.43, 127.28, 122.15, 116.65, 92.93, 68.90, 60.78, 59.35, 58.93, 57.85, 53.43, 49.82, 40.34, 39.19, 38.57, 37.31, 28.55, 22.70, 15.53. The free base was converted into the corresponding oxalate salt, obtained as a white solid (m.p. 115-117°C). HRMS-MS/MS $C_{36}H_{47}ClN_4O_3 + H^+$ calculated 619.34095, found 619.33962. Elemental analysis ($C_{36}H_{47}ClN_4O_3 + 2 H_2C_2O_4 + 2 H_2O$) calculated C 57.51, H 6.64, N 6.71, found C 57.44, H 6.26, N 6.64

***tert*-Butyl (2*S*,4*R*)-4-((*tert*-butyldimethylsilyloxy)-2-((4-(6-(trifluoromethyl)pyridin-2-yl)piperazin-1-yl)methyl)pyrrolidine-1-carboxylate (35)** The compound was prepared following the same procedure described for **26** starting from 1-(6-(trifluoromethyl)pyridin-2-

yl)piperazine (0.94 g, 4.1 mmol) and **21** (1.5 g; 4.5 mmol). The desired product was partially purified by flash chromatography eluting with 40% EtOAc in hexanes (0.62 g, 25% yield) and used in the following step without further purification.

(3R,5S)-5-((4-(6-(Trifluoromethyl)pyridin-2-yl)piperazin-1-yl)methyl)pyrrolidin-3-ol (36)

The compound was prepared following the same procedure described for **24** starting from **35** (620 mg, 1.14 mmol). The crude material obtained was used in the following step without further purification.

4-((2S,4R)-4-Hydroxy-2-((4-(6-(trifluoromethyl)pyridin-2-yl)piperazin-1-

yl)methyl)pyrrolidin-1-yl)-N,N-dimethyl-2,2-diphenylbutanamide (37) The compound was

prepared following the same procedure described for **26** starting from **36** (200 mg, 0.605 mmol) and **25** (187 mg, 0.666 mmol). The desired product was isolated by flash chromatography eluting with 25% DMA (120 mg, 33% yield). ¹H NMR (400 MHz, CDCl₃) δ 7.56 (t, *J* = 8.0 Hz, 1H), 7.43 – 7.29 (m, 8H), 7.28 – 7.19 (m, 2H), 6.93 (d, *J* = 7.3 Hz, 1H), 6.73 (d, *J* = 8.6 Hz, 1H), 4.36 – 4.28 (m, 1H), 3.44 (m, 5H), 2.88 (br s, 3H), 2.80 (m, 1H), 2.64 – 2.49 (m, 3H), 2.42 – 2.23 (m, 9H), 2.17 – 2.09 (m, 2H), 1.80 (m, 2H). ¹³C NMR (101 MHz, CDCl₃) δ 172.80, 158.26, 137.45, 127.75, 127.66, 127.23, 126.16, 126.06, 108.70, 108.07, 69.47, 61.55, 59.17, 52.64, 44.00, 39.88. The free base was converted into the corresponding oxalate salt, obtained as an off-white solid (m.p. 75–77°C). HRMS-MS/MS C₃₃H₄₀F₃N₅O₂ + H⁺ calculated 596.32069, found 596.31987. Elemental analysis (C₃₃H₄₀F₃N₅O₂ + 2.5 H₂C₂O₄ + 0.5 H₂O) calculated C 55.00, H 5.59, N 8.44, found C 55.04, H 5.66, N 8.72

2-(4-(4-(6-(Trifluoromethyl)pyridin-2-yl)piperazin-1-yl)butyl)isoindoline-1,3-dione (38) A solution of 1-(6-(trifluoromethyl)pyridin-2-yl)piperazine (5.0 g, 22 mmol), 2-(4-bromobutyl)isoindoline-1,3-dione (5.5 g, 20 mmol) and K_2CO_3 (15.0 g, 108 mmol) in ACN (100 mL) was stirred at reflux 3 h. The mixture was filtered, the solvent evaporated under vacuum, and the desired product isolated by flash chromatography eluting with 5% DMA (4.0 g, 40% yield). 1H NMR (400 MHz, $CDCl_3$) δ 7.76 (dd, $J = 5.4, 3.1$ Hz, 2H), 7.63 (dd, $J = 5.5, 3.1$ Hz, 2H), 7.49 (d, $J = 8.0$ Hz, 1H), 6.84 (d, $J = 7.3$ Hz, 1H), 6.67 (d, $J = 8.7$ Hz, 1H), 3.65 (t, $J = 7.1$ Hz, 2H), 3.51 (t, $J = 5.1$ Hz, 4H), 2.44 (t, $J = 5.1$ Hz, 4H), 2.34 (t, $J = 7.6$ Hz, 2H), 1.66 (t, $J = 7.6$ Hz, 2H), 1.54 – 1.45 (m, 2H).

2-(4-(4-(Benzo[*d*]isothiazol-3-yl)piperazin-1-yl)butyl)isoindoline-1,3-dione (40) The compound was prepared following the same procedure described for **38**, starting from 3-(piperazin-1-yl)benzo[*d*]isothiazole (1.0 g, 5.0 mmol). The desired product was isolated by flash chromatography eluting with 100% EtOAc (1.3 g, 70% yield). 1H NMR (400 MHz, $CDCl_3$) δ 7.97 – 7.77 (m, 4H), 7.73 (br s, 2H), 7.47 (br s, 1H), 7.37 (br s, 1H), 3.75 (br s, 2H), 3.56 (br s, 4H), 2.67 (br s, 4H), 2.48 (br s, 2H), 1.77 (br s, 2H), 1.61 (br s, 2H).

4-(4-(6-(Trifluoromethyl)pyridin-2-yl)piperazin-1-yl)butan-1-amine (41) Hydrazine (0.65 g, 20 mmol) was added to a solution of **38** (0.88 g, 2.0 mmol) in EtOH (15 mL) and the mixture was stirred at reflux for 12 h. The solvent was evaporated, the residue suspended in 20% aq. K_2CO_3 and extracted with DCM. The organic phase was dried over Na_2SO_4 , filtered, and evaporated under vacuum. The crude material obtained was used in the next step without further purification (0.59 g, 95% yield). 1H NMR (400 MHz, $CDCl_3$) δ 7.56 (t, $J = 8.0$ Hz, 1H), 6.93 (d, $J = 7.3$ Hz, 1H),

6.76 (d, $J = 8.7$ Hz, 1H), 3.68 – 3.55 (m, 4H), 2.73 (t, $J = 6.8$ Hz, 2H), 2.58 – 2.49 (m, 4H), 2.45 – 2.35 (m, 2H), 1.65 – 1.42 (m, 4H), 1.26 (br s, 2H).

4-(4-(Benzo[*d*]isothiazol-3-yl)piperazin-1-yl)butan-1-amine (43) The compound was prepared following the same procedure described for **41**, starting from **40** (1.3 g, 3.0 mmol). The crude material obtained was used in the next step without further purification (0.40 g, 45% yield). ¹H NMR (400 MHz, CDCl₃) δ 7.91 (d, $J = 8.2$ Hz, 1H), 7.81 (d, $J = 8.0$ Hz, 1H), 7.46 (t, $J = 7.6$ Hz, 1H), 7.38 – 7.31 (m, 1H), 3.65 – 3.51 (m, 4H), 2.72 – 2.63 (m, 6H), 2.51 – 2.40 (m, 2H), 1.98 (br s, 2H), 1.67 – 1.46 (m, 4H).

***tert*-Butyl (2*S*,4*R*)-4-((*tert*-butyldimethylsilyloxy)-2-((4-(4-(2,3-dichlorophenyl)piperazin-1-yl)butyl)carbamoyl)pyrrolidine-1-carboxylate (44)** The compound was prepared following the same procedure described for **28** starting from **19** (1.7 g, 5.0 mmol) and **42**⁸² (1.5 g, 5.0 mmol), in presence of DIPEA (0.86 mL, 5.0 mmol). The desired product was isolated by flash chromatography eluting with 5% DMA (1.9 g, 61% yield). ¹H NMR (400 MHz, CDCl₃) (mixture of rotamers) δ 7.21 – 7.11 (m, 2H), 7.06 (br s, 1H), 7.02 – 6.92 (m, 1H), 4.36 (2 x br s, 2H), 3.45 – 3.39 (m, 1H), 3.35 (br s, 1H), 3.28 (br s, 1H), 3.08 (br s, 4H), 2.64 (br s, 4H), 2.44 (br s, 3H), 1.76 (br s, 2H), 1.51 (br s, 4H), 1.46 (s, 9H), 0.92 – 0.84 (m, 9H), 0.08 (br s, 6H).

(2*S*,4*R*)-*N*-(4-(4-(2,3-Dichlorophenyl)piperazin-1-yl)butyl)-4-hydroxypyrrolidine-2-carboxamide (45) The compound was prepared following the same procedure described for **24** starting from **44** (1.9 g, 3.0 mmol), and using consecutive deprotecting steps with TBAF (1M THF

solution, 9 mL, 9 mmol) and TFA (1.2 mL, 15 mmol). The crude material obtained was used in the following step without further purification.

(2*S*,4*R*)-*N*-(4-(4-(2,3-Dichlorophenyl)piperazin-1-yl)butyl)-1-(4-(dimethylamino)-4-oxo-3,3-diphenylbutyl)-4-hydroxypyrrolidine-2-carboxamide (46) The compound was prepared

following the same procedure described for **26** starting from **45** (1.48 g, 3.55 mmol). The desired product was isolated by flash chromatography eluting with 10% DMA (0.24 g, 10% yield). ¹H NMR (400 MHz, CDCl₃) δ 7.57 (s, 1H), 7.40 – 7.29 (m, 7H), 7.29 – 7.23 (m, 3H), 7.21 – 7.11 (m, 2H), 7.00 (m, 1H), 4.30 (dq, *J* = 10.1, 4.8 Hz, 1H), 3.38 (dd, *J* = 10.3, 5.3 Hz, 1H), 3.19 - 3.11 (m, 9H), 2.96 (s, 3H), 2.75 (br s, 4H), 2.52 (d, *J* = 7.7 Hz, 2H), 2.44 - 2.30 (m, 6H), 2.11 (ddt, *J* = 12.9, 8.7, 5.1 Hz, 2H), 1.91 (ddd, *J* = 13.6, 8.0, 6.2 Hz, 1H), 1.60 (m, 4H). ¹³C NMR (101 MHz, CDCl₃) δ 175.09, 173.77, 173.28, 150.90, 140.64, 139.73, 134.01, 128.55, 128.51, 127.78, 127.50, 127.48, 126.98, 126.93, 124.76, 118.69, 70.48, 66.36, 60.96, 59.76, 57.79, 53.64, 52.85, 50.62, 50.45, 44.50, 39.96, 39.13, 38.48, 37.19, 27.58, 23.41, 21.75. The free base was converted into the corresponding oxalate salt, obtained as a white solid (m.p. 182-184°C). HRMS-MS/MS C₃₇H₄₇Cl₂N₅O₃ + H⁺ calculated 680.31287, found 680.31183. Elemental analysis (C₃₇H₄₇Cl₂N₅O₃ + 2 H₂C₂O₄ + 2 H₂O) calculated C 54.91, H 6.18, N 7.81, found C 54.77, H 5.87, N 7.63.

tert-Butyl **(2*S*,4*R*)-4-hydroxy-2-((4-(4-(6-(trifluoromethyl)pyridin-2-yl)piperazin-1-yl)butyl)carbamoyl)pyrrolidine-1-carboxylate (47)**

The compound was prepared following the same procedure described for **28** starting from **41** (3.54 g; 9.25 mmol) and **18** (2.14 g; 9.25 mmol), in presence of DIPEA (1.61 mL, 9.25 mmol). The desired product was isolated by flash chromatography eluting with 5% DMA (3.2 g, 67% yield).

¹H NMR (400 MHz, CDCl₃) (mixture of rotamers) δ 8.13 (s, 1H), 7.80 (d, *J* = 8.7 Hz, 1H), 7.59 (d, *J* = 7.5 Hz, 1H), 7.28 – 7.19 (m, 1H), 4.42 (2 x br s, 2H), 3.67 (dd, *J* = 13.4, 6.6 Hz, 3H), 3.52 (dd, *J* = 11.6, 5.0 Hz, 1H), 3.09 (q, *J* = 7.4 Hz, 2H), 2.82 – 1.98 (m, 15H), 1.46 (d, *J* = 15.3 Hz, 9H).

***tert*-Butyl (2*S*,4*R*)-4-fluoro-2-((4-(4-(6-(trifluoromethyl)pyridin-2-yl)piperazin-1-yl)butyl)carbamoyl)pyrrolidine-1-carboxylate (48)** The compound was prepared following the same procedure described for **28**, starting from **41** (566 mg, 1.87 mmol) and (2*S*,4*R*)-1-(*tert*-butoxycarbonyl)-4-fluoropyrrolidine-2-carboxylic acid (480 mg, 2.06 mmol), in presence of DIPEA (0.359 mL, 2.06 mmol). The desired product was isolated by flash chromatography eluting with 5% DMA (980 mg, >99% yield). ¹H NMR (400 MHz, CDCl₃) δ 7.57 (t, *J* = 8.0 Hz, 1H), 7.03 (br s, 1H), 6.94 (d, *J* = 7.3 Hz, 1H), 6.76 (d, *J* = 8.6 Hz, 1H), 5.20 (d, *J* = 52.8 Hz, 1H), 4.42 (br s, 1H), 3.90 (m, 1H), 3.62 (br s, 4H), 3.61-3.28 (m, 3H), 3.08 (q, *J* = 7.5 Hz, 1H), 2.55 (br s, 4H), 2.42 (br s, 2H), 1.55 (d, *J* = 16.5 Hz, 5H), 1.47 (s, 9H).

***tert*-Butyl (2*S*,4*R*)-2-((4-(4-(2,3-dichlorophenyl)piperazin-1-yl)butyl)carbamoyl)-4-fluoropyrrolidine-1-carboxylate (49)** The compound was prepared following the same procedure described for **28**, starting from **42** (800 mg, 2.65 mmol) and (2*S*,4*R*)-1-(*tert*-butoxycarbonyl)-4-fluoropyrrolidine-2-carboxylic acid (680 mg, 2.91 mmol), in presence of DIPEA (0.507 mL, 2.91 mmol). The desired product was isolated by flash chromatography eluting with 5% DMA (1.03 g, 75% yield). ¹H NMR (400 MHz, CDCl₃) δ 7.16 (s, 2H), 7.05 (s, 1H), 6.97 (s, 1H), 5.14 (2 x br s, 1H), 4.39 (m, 2H), 3.98 (m, 1H), 3.60-3.39 (m, 3H), 3.07 (br s, 4H), 2.63 (br s, 4H), 2.44 (br s, 3H), 1.58 (br s, 4H), 1.47 (s, 9H).

***tert*-Butyl (2*S*,4*R*)-2-((4-(4-(benzo[*d*]isothiazol-3-yl)piperazin-1-yl)butyl)carbamoyl)-4-fluoropyrrolidine-1-carboxylate (50)** The compound was prepared following the same procedure described for **28**, starting from **43** (396 mg, 1.36 mmol) and (2*S*,4*R*)-1-(*tert*-butoxycarbonyl)-4-fluoropyrrolidine-2-carboxylic acid (350 mg, 1.50 mmol), in presence of DIPEA (0.261 mL, 1.50 mmol). The desired product was isolated by flash chromatography eluting with 5% DMA (560 mg, 81% yield). ¹H NMR (400 MHz, CDCl₃) δ 8.00 – 7.78 (m, 2H), 7.45 (m, 2H), 7.04 (s, 1H), 5.25 (d, *J* = 53.9 Hz, 1H), 4.46 (br s, 1H), 3.96 (br s, 1H), 3.58 (br s, 4H), 3.32 (br s, 3H), 2.70 (br s, 4H), 2.48 (br s, 2H), 1.62 (br s, 6H), 1.52 (s, 9H).

(2*S*,4*R*)-4-Fluoro-*N*-(4-(4-(6-(trifluoromethyl)pyridin-2-yl)piperazin-1-yl)butyl)pyrrolidine-2-carboxamide (52) TFA (1.6 mL) was added dropwise to a stirring solution of **48** (980 mg, 1.89 mmol) in DCM (20 mL). The mixture was stirred at RT overnight, the solvent was evaporated under vacuum, the residue was basified with 2N aq. NaOH and extracted with DCM. The organic phase was dried over Na₂SO₄, filtered, and evaporated under vacuum to yield the desired product, which was used in the following step without further purification (720 mg, 91% yield). ¹H NMR (400 MHz, CDCl₃) δ 7.68 (s, 1H), 7.57 (t, *J* = 8.0 Hz, 1H), 6.93 (d, *J* = 7.2 Hz, 1H), 6.76 (d, *J* = 8.7 Hz, 1H), 5.19 (d, *J* = 53.6 Hz, 1H), 3.99 (t, *J* = 8.2 Hz, 1H), 3.61 (br s, 4H), 3.30 (m, 3H), 2.75 (dd, *J* = 13.2 Hz, *J* = 13.8 Hz, 1H), 2.53 (br s, 5H), 2.40 (s, 2H), 2.15 – 1.95 (m, 2H), 1.56 (s, 4H).

(2*S*,4*R*)-*N*-(4-(4-(2,3-Dichlorophenyl)piperazin-1-yl)butyl)-4-fluoropyrrolidine-2-carboxamide (53) The compound was prepared following the same procedure described for **52**, starting from **49** (1.03 g, 1.99 mmol). The desired product was used in the following step without further purification (0.60 g, 73% yield). ¹H NMR (400 MHz, CDCl₃) δ 7.69 (br s, 1H), 7.16 (br s,

2H), 6.96 (br s, 1H), 5.19 (d, $J = 53.8$ Hz, 1H), 4.00 (d, $J = 7.9$ Hz, 1H), 3.30 (br s, 3H), 3.08 (br s, 4H), 2.87 – 2.25 (m, 9H), 2.08 (m, 1H), 1.57 (s, 4H).

(2*S*,4*R*)-*N*-(4-(4-(Benzo[*d*]isothiazol-3-yl)piperazin-1-yl)butyl)-4-fluoropyrrolidine-2-

carboxamide (54) The compound was prepared following the same procedure described for **52**, starting from **50** (560 mg, 1.11 mmol). The desired product was used in the following step without further purification (325 mg, 72% yield). ^1H NMR (400 MHz, CDCl_3) δ 7.91 (d, $J = 8.0$ Hz, 1H), 7.81 (d, $J = 8.1$ Hz, 1H), 7.69 (s, 1H), 7.47 (t, $J = 7.5$ Hz, 1H), 7.36 (t, $J = 7.4$ Hz, 1H), 5.19 (d, $J = 53.8$ Hz, 1H), 4.00 (t, $J = 8.3$ Hz, 1H), 3.62 – 3.51 (m, 4H), 3.41 – 3.15 (m, 3H), 2.80 – 2.62 (m, 5H), 2.47 (m, 3H), 2.35 (s, 1H), 2.18 – 1.94 (m, 1H), 1.58 (s, 4H).

(2*S*,4*R*)-1-(4-(Dimethylamino)-4-oxo-3,3-diphenylbutyl)-4-hydroxy-*N*-(4-(4-(6-

(trifluoromethyl)pyridin-2-yl)piperazin-1-yl)butyl)pyrrolidine-2-carboxamide (55) TFA (25 mL) was added to a solution of **47** (1.83 g, 3.55 mmol) in DCM (50 mL), and stirred at RT until reaction completion, monitored by TLC. The solvent was evaporated under vacuum, the residue was basified with 2N aq. NaOH and extracted with DCM. The organic phase was dried over Na_2SO_4 , filtered, and evaporated under vacuum. The crude was immediately reacted with the aldehyde via reductive amination conditions as described for **26**. The desired product was isolated by flash chromatography eluting with 10% DMA (0.18 g, 15% yield). ^1H NMR (400 MHz, CDCl_3) δ 7.57 (t, $J = 8.0$ Hz, 1H), 7.40 – 7.32 (m, 8H), 7.26 (q, $J = 2.6, 2.0$ Hz, 3H), 6.94 (d, $J = 7.4$ Hz, 1H), 6.77 (d, $J = 8.7$ Hz, 1H), 4.29 (m, 1H), 3.62 (d, $J = 5.9$ Hz, 4H), 3.38 (dd, $J = 10.6, 5.3$ Hz, 1H), 3.20 (m, 3H), 2.96 (s, 3H), 2.53 (s, 4H), 2.43 – 2.18 (m, 8H), 2.08 (m, 2H), 1.91 (dt, $J = 13.5, 7.0$ Hz, 1H), 1.72 (br s, 2H), 1.50 (br s, 4H). ^{13}C NMR (101 MHz, CDCl_3) δ 173.85, 173.20,

158.80, 140.60, 138.23, 128.52, 128.11, 127.86, 126.93, 109.38, 108.79, 70.65, 66.42, 61.04, 59.73, 58.26, 53.67, 52.88, 44.71, 40.06, 38.62, 27.69, 24.18. The free base was converted into the corresponding oxalate salt, obtained as a white solid (m.p. 122-124°C). HRMS-MS/MS $C_{37}H_{47}F_3N_6O_3 + H^+$ calculated 681.37345, found 681.37253. Elemental analysis ($C_{37}H_{47}F_3N_6O_3 + 2.5 H_2C_2O_4 + H_2O$) calculated C 54.60, H 5.89, N 9.10, found C 54.74, H 5.72, N 9.10. Analytical HPLC: Agilent poroshell C-18 4.6 x 50 mm, 2.7 μ m; gradient 10%-80% ACN in water + 0.1% TFA; 60 min run; injection 20 μ L (1 mg/mL); temperature 40°C; 'R 20.759 min, purity >99%.

(2*S*,4*R*)-1-(4-(Dimethylamino)-4-oxo-3,3-diphenylbutyl)-4-fluoro-*N*-(4-(4-(6-(trifluoromethyl)pyridin-2-yl)piperazin-1-yl)butyl)pyrrolidine-2-carboxamide (56) The compound was prepared following the same reductive amination conditions described for **26**, starting from **52** (62.0 mg, 0.15 mmol). The desired product was isolated by flash chromatography eluting with 5% DMA (78 mg, 77% yield, hygroscopic solid/colorless oil). 1H NMR (400 MHz, $CDCl_3$) δ 7.58 (t, $J = 7.9$ Hz, 1H), 7.47 (s, 1H), 7.37 (d, $J = 6.0$ Hz, 7H), 7.28 (d, $J = 7.0$ Hz, 2H), 6.95 (d, $J = 7.3$ Hz, 1H), 6.77 (d, $J = 8.7$ Hz, 1H), 5.04 (d, $J = 55.7$ Hz, 1H), 3.64 (s, 4H), 3.51 – 3.34 (m, 1H), 3.20 (d, $J = 16.9$ Hz, 3H), 2.97 (s, 3H), 2.71- 2.62 (m, 5H), 2.50 – 2.21 (m, 8H), 2.01 (br s, 2H), 1.79 (m, 1H), 1.56 (s, 4H). ^{13}C NMR (101 MHz, $CDCl_3$) δ 173.20, 173.16, 158.77, 146.93, 146.59, 146.26, 145.92, 140.86, 139.69, 138.28, 128.55, 128.52, 128.19, 127.77, 127.00, 126.93, 122.99, 120.27, 109.43, 108.94, 108.91, 93.80, 92.05, 66.34, 59.74, 59.39, 59.16, 58.04, 53.48, 52.62, 44.78, 44.47, 39.09, 38.59, 38.51, 38.29, 37.17, 27.64, 23.80. Analytical HPLC: Phenomenex Gemini C18 4.6 x 50 mm, 3 μ m; gradient 10%-80% ACN in water + 0.1% TFA; 60 min run; injection 20 μ L (1 mg/mL); temperature 40°C; 'R 18.701, 18.940 min, purity >99%; gradient 10%-80% ACN in water + 0.1% DEA; 60 min run; injection 20 μ L (1 mg/mL);

temperature 40°C; *t*_R 36.909 min, purity >99%. HRMS-MS/MS C₃₇H₄₆F₄N₆O₂ + H⁺ calculated 683.36911, found 683.36857; C₃₇H₄₆F₄N₆O₂ + Na⁺ calculated 705.35106, found 705.35075

(2*S*,4*R*)-*N*-(4-(4-(2,3-Dichlorophenyl)piperazin-1-yl)butyl)-1-(4-(dimethylamino)-4-oxo-3,3-diphenylbutyl)-4-fluoropyrrolidine-2-carboxamide (57) The compound was prepared following the same reductive amination conditions described for **26**, starting from **53** (494 mg, 1.18 mmol). The desired product was isolated by flash chromatography eluting with 5% DMA (420 mg, 52% yield, white solid m.p. 91-94°C). ¹H NMR (400 MHz, CDCl₃) δ 7.38 - 7.16 (m, 12H), 6.97 (s, 1H), 5.04 (d, *J* = 54.4 Hz, 1H), 3.43 (dd, *J* = 32.4, 13.7 Hz, 1H), 3.21 (br s, 3H), 3.10 (s, 4H), 2.97 (s, 3H), 2.65 (s, 5H), 2.54 – 2.24 (m, 9H), 2.06 (s, 1H), 1.70 (br s, 1H), 1.55 - 1.41 (br s, 4H). ¹³C NMR (101 MHz, CDCl₃) δ 173.10, 151.21, 140.84, 139.72, 134.03, 128.51, 128.17, 127.76, 127.44, 126.97, 126.90, 124.59, 118.62, 93.78, 92.02, 66.34, 59.73, 59.38, 59.16, 58.12, 53.44, 53.20, 51.14, 44.76, 39.08, 38.63, 38.51, 38.30, 37.17, 27.69, 24.06. Analytical HPLC: Phenomenex Gemini C18 4.6 x 50 mm, 3 μm; gradient 10%-80% ACN in water + 0.1% TFA; 60 min run; injection 20 μL (1 mg/mL); temperature 40°C; *t*_R 19.291 min, purity >99%. HRMS-MS/MS C₃₇H₄₆Cl₂FN₅O₂ + H⁺ calculated 682.30854, found 682.30829; C₃₇H₄₆Cl₂FN₅O₂ + 2H⁺ calculated 341.65791, found 341.65774.

(2*S*,4*R*)-*N*-(4-(4-(Benzo[*d*]isothiazol-3-yl)piperazin-1-yl)butyl)-1-(4-(dimethylamino)-4-oxo-3,3-diphenylbutyl)-4-fluoropyrrolidine-2-carboxamide (58) The compound was prepared following the same reductive amination conditions described for **26**, starting from **54** (110 mg, 0.270 mmol). The desired product was isolated by flash chromatography eluting with 5% DMA (177 mg, 99% yield, white solid m.p. 68-71°C). ¹H NMR (400 MHz, CDCl₃) δ 7.90 (d, *J* = 8.4 Hz, 1H), 7.82 (d, *J* = 8.3 Hz, 1H), 7.51 – 7.42 (m, 2H), 7.37 (d, *J* = 6.1 Hz, 7H), 7.26 (s, 3H), 5.04 (d,

$J = 53.4$ Hz, 1H), 3.58 (d, $J = 9.8$ Hz, 4H), 3.51 – 3.35 (m, 1H), 2.97 (s, 3H), 2.72 (br s, 6H), 2.54 – 2.25 (m, 9H), 2.06 (d, $J = 8.6$ Hz, 3H), 1.91 – 1.69 (m, 1H), 1.57 (s, 4H). ^{13}C NMR (101 MHz, CDCl_3) δ 174.28, 173.18, 173.17, 163.80, 152.80, 140.87, 139.70, 128.55, 128.53, 128.21, 128.03, 127.78, 127.54, 127.00, 126.92, 123.90, 123.89, 120.58, 93.82, 92.06, 66.35, 59.75, 59.40, 59.17, 58.14, 53.46, 52.77, 49.76, 44.79, 38.63, 38.53, 38.31, 27.71, 23.85. Analytical HPLC: Phenomenex Gemini C18 4.6 x 50 mm, 3 μm ; gradient 10%-80% ACN in water + 0.1% TFA; 60 min run; injection 20 μL (1 mg/mL); temperature 40°C; t_{R} 18.227 min, purity >99%; gradient 10%-80% ACN in water + 0.1% DEA; 60 min run; injection 20 μL (1 mg/mL); temperature 40°C; t_{R} 36.075 min, purity >99%. HRMS-MS/MS $\text{C}_{38}\text{H}_{47}\text{FN}_6\text{O}_2\text{S} + \text{H}^+$ calculated 671.35380, found 671.35299; $\text{C}_{38}\text{H}_{47}\text{FN}_6\text{O}_2\text{S} + \text{Na}^+$ calculated 693.33574, found 693.33545.

4-(5-(Hydroxymethyl)-2-methylpiperidin-1-yl)-*N,N*-dimethyl-2,2-diphenylbutanamide (60)

The compound was prepared following the same procedure described for **26**, starting from **59** (101 mg, 0.782 mmol) and **25** (220 mg, 0.782 mmol). The desired product was isolated by flash chromatography eluting with 10% DMA (170 mg, 55% yield). Diastereomeric ratio/excess and relative configurations have not been determined. ^1H NMR (400 MHz, CDCl_3) δ 7.51 – 7.24 (m, 10H), 3.62 (d, $J = 11.4$ Hz, 1H), 3.19 (d, $J = 14.6$ Hz, 1H), 2.99 (s, 3H), 2.74 - 2.61 (m, 5H), 2.29 (s, 3H), 2.04 – 1.87 (m, 3H), 1.77 (m, 3H), 1.55 (ddd, $J = 14.3, 9.5, 4.8$ Hz, 1H), 1.24 (td, $J = 12.6, 10.8, 3.8$ Hz, 1H), 1.14 (d, $J = 6.3$ Hz, 3H).

4-(5-((4-(2,3-Dichlorophenyl)piperazin-1-yl)methyl)-2-methylpiperidin-1-yl)-*N,N*-dimethyl-2,2-diphenylbutanamide (62) DMP (0.13 g, 2 equiv, 0.30 mmol) was added portion-wise to a solution of **60** (60 mg, 0.15 mmol) in DCM (10 mL), at 0°C. The mixture was allowed to warm to RT and stirred for 2 h. The suspension was washed sat. aq. NaHCO_3 , the organic phase was dried

over Na₂SO₄, filtered, and evaporated under vacuum to yield the crude aldehyde **61**, which was reacted with 1-(2,3-dichlorophenyl)piperazine (42 mg, 0.18 mmol) following the same procedure described for **26**. The desired product was isolated by C18 preparative HPLC as TFA salt (Phenomenex Gemini NX-C18 110 Å, AXIA Packed, 150 x 30 mm, 5 µm; gradient 10%-80% ACN in water + 0.1% TFA; 60 min run; injection 4mL (~10-15 mg/mL); temperature 25°C; DAD λ₂₁₄ nm and λ₂₅₄ nm) (21 mg, 23% yield, hygroscopic solid/off-white oil). Diastereomeric ratio/excess and relative configurations have not been determined. ¹H NMR (400 MHz, CDCl₃) δ 7.39 (m, 10H), 7.20 (dd, *J* = 17.4, 9.6 Hz, 2H), 6.99 (d, *J* = 7.8 Hz, 1H), 3.89 (br s, 1H), 3.71 (m, 2H), 3.41 – 3.22 (m, 5H), 2.98 (m + s, 1H + 3H), 2.85 (m, 5H), 2.54 (br s, 2H), 2.30 (s, 3H), 1.70 – 1.95 (m, 3H), 1.31 (m, 3H), 1.16 (d, *J* = 6.0 Hz, 3H). ¹³C NMR (101 MHz, CDCl₃) δ 173.26, 148.84, 138.91, 138.48, 134.34, 134.29, 129.15, 129.09, 127.98, 127.82, 127.78, 127.69, 126.18, 126.08, 119.14, 119.03, 60.05, 58.82, 58.48, 54.56, 51.42, 48.28, 47.94, 43.88, 39.26, 38.06, 37.38, 30.93, 29.66, 26.77, 17.25. HRMS-MS/MS C₃₅H₄₄Cl₂N₄O + H⁺ calculated 607.29649, found 607.29620. Analytical HPLC: Agilent poroshell C-18 4.6 x 50 mm, 2.7 µm; gradient 10%-80% ACN in water + 0.1% TFA; 60 min run; injection 20 µL (1 mg/mL); temperature 40°C; Rt 22.013 min, purity >99%.

***tert*-Butyl-3-(2-methoxy-2-oxoethylidene)pyrrolidine-1-carboxylate (64)** Trimethyl phosphonoacetate (2.36 g, 13.0 mmol) was dissolved in MeOH (10 mL), and the solution was cooled to 0°C. Sodium hydride (0.33 g, 95% wt, 13.0 mmol) was added portion-wise, and the mixture was allowed to warm to RT and stirred for 30 min, followed by drop-wise addition of **63** (2.00 g, 10.8 mmol) dissolved in MeOH (10 mL). The reaction was stirred overnight at RT, quenched with addition of sat. aq. NH₄Cl, MeOH was evaporated under vacuum, and the aq. layer

extracted with DCM. The organic phase was dried over Na₂SO₄, filtered, and evaporated under vacuum. The desired product was isolated, as E and Z mixture, via flash chromatography, eluting with a gradient from 0% to 60% EtOAc in hexanes (0.92 g, 35% yield). GC/MS ^tR 8.428 min, m/z 421.1

Methyl 2-(pyrrolidin-3-yl)acetate (65) Pd/C (20.3 mg, 0.19 mmol) was added to a solution of **64** (920 mg, 3.81 mmol) in EtOH (20 mL) and TFA (0.4 mL), and shaken in a Parr apparatus overnight at 50 psi H₂ pressure. The reaction was filtered over Celite, the solvent was evaporated under vacuum, the residue was dissolved in DCM and stirred for additional 30 min in presence of TFA (3 mL). The solution was evaporated, the residue suspended in 2N aq. NaOH (pH>9) and extracted with DCM. The organic phase was dried over Na₂SO₄, filtered, and evaporated under vacuum. The crude material obtained was used in the following step without further purification (350 mg, 64% yield). ¹H NMR (400 MHz, CDCl₃) δ 3.68 (s, 3H), 3.15 (dd, *J* = 10.5, 6.6 Hz, 1H), 2.99 – 2.88 (m, 2H), 2.56 – 2.35 (m, 4H), 2.06 – 1.93 (m, 2H), 1.38 (dq, *J* = 12.6, 7.3 Hz, 1H).

2-(Pyrrolidin-3-yl)ethan-1-ol (66) LAH (280 mg, 7.33 mmol) was suspended in THF (10 mL), followed by dropwise addition of **65** (350 mg, 2.44 mmol) dissolved in THF (10 mL), at 0°C. The mixture was allowed to reach RT and stirred for additional 4 h. The reaction was quenched with sat. aq. Na₂SO₄, filtered, and the solvent was evaporated under vacuum. The crude material was used without further purification.

4-(3-(2-Hydroxyethyl)pyrrolidin-1-yl)-*N,N*-dimethyl-2,2-diphenylbutanamide (67) The compound was prepared following the same procedure described for **26**, starting from **66** (240 mg,

2.08 mmol). The desired product was isolated by flash chromatography eluting with 25% DMA (40 mg, 5% yield). ¹H NMR (400 MHz, CDCl₃) δ 7.36 (m, 7H), 7.27 (m, 3H), 3.68 – 3.47 (m, 2H), 2.98 (s, 3H), 2.81 (td, *J* = 9.2, 4.5 Hz, 1H), 2.53 – 2.34 (m, 4H), 2.31 (m + s, 2H + 3H), 2.19 (q, *J* = 7.1 Hz, 2H), 2.02 (s, 1H), 1.96 – 1.82 (m, 1H), 1.65 (m, 1H), 1.57 – 1.46 (m, 2H).

4-(3-(2-(4-(2,3-Dichlorophenyl)piperazin-1-yl)ethyl)pyrrolidin-1-yl)-*N,N*-dimethyl-2,2-diphenylbutanamide (68) The compound was prepared following the same procedure described for **62**, starting with oxidation of **67** (40 mg, 0.11 mmol) to aldehyde and subsequent reductive amination in presence of 1-(2,3-dichlorophenyl)piperazine hydrochloride (27 mg, 0.13 mmol). The desired product was isolated by preparative reverse phase HPLC as TFA salt (Phenomenex C-18 Gemini preparative HPLC column) eluting with a gradient starting from 10% ACN to 80% ACN in 2-PrOH + 0.1% TFA (flow rate 25-30 mL/min; injection of 4 mL – 5 mg/mL) for a total run time of 60 min (35 mg, 56% yield, yellow oil). ¹H NMR (400 MHz, CDCl₃) δ 7.41 - 7.33 (m, 10H), 7.27 – 7.12 (m, 2H), 7.01 – 6.93 (m, 1H), 3.66 (m, 3H), 3.38 (br s, 2H), 3.25 (br s, 2H), 3.08 (br s, 4H), 2.99 (m + s, 1H + 3H), 2.76 (br s, 3H), 2.54 (br d, *J* = 29.4 Hz, 3H), 2.30 (s, 3H), 2.23 (m, 1H), 1.96 (m, 2H), 1.80 (m, 2H). ¹³C NMR (101 MHz, CDCl₃) δ 173.41, 168.32, 148.84, 141.38, 138.70, 138.53, 134.31, 132.72, 131.42, 129.07, 127.82, 127.77, 127.75, 127.73, 126.13, 119.04, 109.56, 94.43, 59.73, 58.38, 56.80, 55.50, 55.07, 53.93, 53.55, 52.64, 52.53, 52.52, 48.19, 40.77, 39.19, 37.30, 34.83, 34.37, 29.73, 28.83, 26.93, 26.73. HRMS-MS/MS C₃₄H₄₂Cl₂N₄O + H⁺ calculated 593.28084, found 593.28053. Analytical HPLC: Phenomenex Gemini C18 4.6 x 50 mm, 3 μm; gradient 10%-80% ACN in water + 0.1% TFA; 60 min run; injection 20 μL (1 mg/mL); temperature 40°C; ^tR 19.638 min, purity 93%. Elemental analysis (C₃₄H₄₂Cl₂N₄O + 3.5 CF₃COOH + 2.5 H₂O) calculated C 47.45, H 4.91, N 5.40, found C 47.56, H 4.64, N 5.43.

4-Azido-*N,N*-dimethyl-2,2-diphenylbutanamide (70) A solution of **69** (2.0 g, 7.5 mmol) and sodium azide (0.49 g, 7.5 mmol) in DMF (10 mL) was stirred at RT, overnight.

The mixture was diluted with DCM and washed with brine. The organic phase was dried over Na₂SO₄, filtered, and evaporated under vacuum. The desired product was isolated by flash chromatography eluting with 20% EtOAc in hexanes (1.6 g, 69% yield). ¹H NMR (400 MHz, CDCl₃) δ 7.53 – 7.15 (m, 10H), 3.10 – 2.85 (m, 5H), 2.55 – 2.43 (m, 2H), 2.31 (s, 3H). GC/MS ^rR 11.973, m/z 308.2.

4-((4-(3-Chloro-5-ethyl-2-methoxyphenyl)piperazin-1-yl)methyl)-1*H*-1,2,3-triazol-1-yl)-*N,N*-dimethyl-2,2-diphenylbutanamide (73) A solution of 3-bromoprop-1-yne (0.158 g, 1.06 mmol), **71**⁵⁷ (0.300 g, 1.18 mmol) and K₂CO₃ (1.63 g, 11.8 mmol) in ACN (20 mL) was stirred at reflux for 2 h. The mixture was filtered, and the solvent was evaporated under vacuum. The residue, redissolved in DCM, was filtered through a silica plug and washed with 10% DMA. The obtained material **72** was dried and solubilized in THF:water (1:1, 20 mL), followed by addition of **70** (0.363 g, 1.18 mmol), copper(II) sulfate pentahydrate (0.0588 g, 0.236 mmol) and sodium (L)-ascorbate (46.7 mg, 0.236 mmol). The reaction was stirred overnight at RT, the solvents evaporated under vacuum and the desired product isolated by flash chromatography eluting with 15% DMA (90 mg, 13% yield, yellow oil). ¹H NMR (400 MHz, CDCl₃) δ 7.44 – 7.38 (s + m, 8H), 7.38 – 7.26 (m, 3H), 6.81 (s, 1H), 6.60 (s, 1H), 4.13 – 4.04 (m, 2H), 3.81 (s, 3H), 3.67 (s, 2H), 3.15 – 3.08 (m, 4H), 3.04 (s, 3H), 2.83 – 2.74 (m, 2H), 2.64 (m, 4H), 2.54 (q, *J* = 7.6 Hz, 2H), 2.34 (s, 3H), 1.24 – 1.15 (t, *J* = 7.6 Hz, 3H). ¹³C NMR (101 MHz, CDCl₃) δ 173.27, 146.30, 146.11, 143.87, 140.75, 139.46, 128.85, 128.17, 127.95, 127.34, 122.82, 122.11, 116.69, 59.72, 59.01, 53.40, 53.37, 50.08, 48.46, 46.27, 39.14, 37.20, 31.43, 30.95, 28.46, 15.41. HRMS-MS/MS

$C_{34}H_{41}ClN_6O_2 + H^+$ calculated 601.30523, found 601.30477. Analytical HPLC: Agilent poroshell C-18 4.6 x 50 mm, 2.7 μ m; gradient 10%-80% ACN in water + 0.1% TFA; 60 min run; injection 20 μ L (1 mg/mL); temperature 40°C; t_R 32.832 min, purity >95%. Elemental analysis ($C_{34}H_{41}ClN_6O_2 + H_2O$) calculated C 65.95, H 7.00, N 13.57, found C 65.70, H 6.91, N 13.62.

4-(4-(4-Hydroxybutyl)-1*H*-1,2,3-triazol-1-yl)-*N,N*-dimethyl-2,2-diphenylbutanamide (74)

Copper(II) sulfate pentahydrate (81.0 mg, 0.324 mmol) and sodium (L)-ascorbate (64.2 mg, 0.324 mmol) were added to a solution of **70** (500 mg, 1.62 mmol) and hex-5-yn-1-ol (159 mg, 1.62 mmol) in THF:water (1:1, 40 mL). The mixture was stirred at RT for 1 h, the solvents were evaporated under vacuum, and the desired product was partially purified by flash chromatography eluting with 10% DMA, then used in the following step without further purification (630 mg, 96% yield).

4-(4-(4-(4-(3-Chloro-5-ethyl-2-methoxyphenyl)piperazin-1-yl)butyl)-1*H*-1,2,3-triazol-1-yl)-*N,N*-dimethyl-2,2-diphenylbutanamide (75) Primary alcohol **74** (500 mg, 1.23 mmol) was oxidized to aldehyde, followed by reductive amination in presence of **71** (313 mg, 1.23 mmol), as described for **62**. The desired product was isolated by flash chromatography eluting with 15% DMA (110 mg, 14% yield, yellow oil). 1H NMR (400 MHz, $CDCl_3$) δ 7.44 – 7.34 (m, 7H), 7.34 – 7.22 (m, 4H), 6.84 (s, 1H), 6.61 (s, 1H), 4.06 - 3.98 (m, 3H), 3.82 (s, 3H), 3.63 (t, $J = 6.4$ Hz, 1H), 3.17 (br s, 3H), 3.02 (s, 3H), 2.79 - 2.64 (m, 8H), 2.58 – 2.45 (m, 3H), 2.33 (s, 3H), 1.75 – 1.54 (m, 4H), 1.18 (t, $J = 7.6$ Hz, 3H). ^{13}C NMR (101 MHz, $CDCl_3$) δ 173.30, 147.60, 147.48, 146.37, 145.93, 140.86, 139.48, 128.82, 127.95, 127.31, 122.37, 120.88, 116.80, 62.45, 59.68, 59.09, 58.11, 53.43, 49.74, 48.32, 46.30, 39.14, 37.20, 32.19, 28.46, 27.32, 25.81, 25.52, 25.42, 25.24,

15.43. HRMS-MS/MS $C_{37}H_{47}ClN_6O_2 + H^+$ calculated 643.35218, found 643.35140. Analytical HPLC: Agilent poroshell C-18 4.6 x 50 mm, 2.7 μ m; gradient 10%-80% ACN in water + 0.1% TFA; 60 min run; injection 20 μ L (1 mg/mL); temperature 40°C; t_R 33.416 min, purity >95%. Elemental analysis ($C_{37}H_{47}ClN_6O_2 + H_2O$) calculated C 67.20, H 7.47, N 12.71, found C 67.49, H 7.23, N 12.36.

***N,N*-Dimethyl-2,2-diphenyl-4-(4-(6-(trifluoromethyl)pyridin-2-yl)piperazin-1-**

yl)butanamide (76) A solution of **69** (1.00 g, 2.89 mmol), 1-(6-(trifluoromethyl)pyridin-2-yl)piperazine (0.670 g, 2.89 mmol) and K_2CO_3 (2.00 g, 14.4 mmol) in ACN (20 mL) was stirred at reflux overnight. The mixture was filtered, the solvent was evaporated under vacuum, and the residue was purified by flash chromatography, eluting with 5% DMA, to yield the desired product (0.95 g, 66% yield). 1H NMR (400 MHz, $CDCl_3$) δ 7.51 (t, $J = 8.0$ Hz, 1H), 7.46 – 7.33 (m, 7H), 7.32 – 7.24 (m, 3H), 6.88 (d, $J = 7.2$ Hz, 1H), 6.69 (d, $J = 8.7$ Hz, 1H), 3.50 (t, $J = 5.0$ Hz, 4H), 2.98 (s, 3H), 2.51 – 2.38 (m, 6H), 2.35 (s, 3H), 2.16 – 2.07 (m, 2H). ^{13}C NMR (101 MHz, $CDCl_3$) δ 173.48, 158.81, 146.84, 146.51, 146.17, 145.84, 140.75, 138.07, 128.40, 128.13, 126.77, 123.00, 120.28, 116.65, 116.63, 116.59, 109.29, 108.53, 108.50, 59.78, 55.84, 53.42, 52.83, 44.77, 42.46, 39.17, 37.23. The free base was converted into the corresponding oxalate salt, obtained as a white solid (m.p. 196-199°C). HRMS-MS/MS $C_{28}H_{31}F_3N_4O + H^+$ calculated 497.25227, found 497.25185. Elemental analysis ($C_{28}H_{31}F_3N_4O + H_2C_2O_4$) calculated C 61.43, H 5.67, N 9.55, found C 61.02, H 5.99, N 9.32.

4-(4-(Benzo[*d*]isothiazol-3-yl)piperazin-1-yl)-*N,N*-dimethyl-2,2-diphenylbutanamide (77)

The compound was prepared following the same procedure described for **76**, starting from 3-(piperazin-1-yl)benzo[*d*]isothiazole (500 mg, 2.28 mmol). The desired product was isolated by

flash chromatography eluting with 10% MeOH in DCM (770 mg, 70% yield, white solid m.p. 73-76°C). ¹H NMR (400 MHz, CDCl₃) δ 7.85 (d, *J* = 8.1 Hz, 1H), 7.78 (d, *J* = 8.1 Hz, 1H) 7.47 – 7.26 (m, 12H), 3.53 – 3.41 (m, 4H), 2.99 (s, 3H), 2.58 (t, *J* = 4.9 Hz, 4H), 2.54 – 2.45 (m, 2H), 2.34 (s, 3H), 2.22 – 2.11 (m, 2H). ¹³C NMR (101 MHz, CDCl₃) δ 173.48, 164.02, 152.67, 140.79, 128.38, 128.35, 128.14, 128.11, 127.40, 126.73, 123.96, 123.75, 120.47, 59.78, 55.91, 53.01, 50.11, 42.26, 39.15, 37.24. Analytical HPLC: Phenomenex Gemini C18 4.6 x 50 mm, 3 μm; gradient 10%-80% ACN in water + 0.1% TFA; 60 min run; injection 20 μL (1 mg/mL); temperature 40°C; *t*_R 20.645 min, purity >99%; HRMS-MS/MS C₂₉H₃₂N₄OS + H⁺ calculated 485.23696, found 485.23622.

rel-*trans*-4-((2-(4-Chlorophenyl)cyclopropyl)amino)-*N,N*-dimethyl-2,2-diphenylbutanamide

(78) The compound was prepared following the same procedure described for **76**, starting from *rel-trans*-2-(4-chlorophenyl)cyclopropan-1-amine HCl (200 mg, 0.98 mmol). The mixture was stirred for 3 h at 90°C in a sealed pressure vessel. The solvent was evaporated under vacuum, and the residue purified by flash chromatography, eluting with 5% DMA (210 mg, 50% yield, yellow oil). ¹H NMR (400 MHz, CDCl₃) δ 7.40 – 7.32 (m, 7H), 7.28 (d, *J* = 8.7 Hz, 3H), 7.15 (d, *J* = 8.0 Hz, 2H), 6.84 (d, *J* = 8.2 Hz, 2H), 2.97 (s, 3H), 2.41 (d, *J* = 4.1 Hz, 4H), 2.32 (s, 3H), 2.15 – 2.13 (m, 1H), 2.02 (br s, 1H), 1.70 (br s, 1H), 1.00-0.88 (m, 1H), 0.84 – 0.76 (m, 1H). ¹³C NMR (101 MHz, CDCl₃) δ 173.57, 163.41, 141.03, 140.85, 140.73, 130.80, 129.73, 128.67, 128.44, 128.39, 128.11, 128.10, 128.07, 127.18, 126.73, 60.13, 59.96, 59.00, 46.81, 46.24, 45.79, 41.49, 37.17, 31.51, 24.53, 17.02. Analytical HPLC: Phenomenex Gemini C18 4.6 x 50 mm, 3 μm; gradient 10%-80% ACN in water + 0.1% TFA; 40 min run; injection 20 μL (1 mg/mL); temperature 40°C; *t*_R 22.323 min, purity >99%; HRMS-MS/MS C₂₇H₂₉ClN₂O + H⁺ calculated 433.20412, found 433.20366.

rel-*trans*-2-(4-Chlorophenyl)-*N*-propylcyclopropan-1-amine (79) Propionaldehyde (47.7 μ L, 0.661 mmol) was added to a solution of rel-*trans*-2-(4-chlorophenyl)cyclopropan-1-amine HCl (150 mg, 0.735 mmol) in MeOH (10 mL). The reaction was stirred at RT for 25 min. NaBH₄ (69.5 mg, 1.84 mmol) was added and stirred for 20 min. Water was added to quench the reaction and the solvent was evaporated under vacuum. The mixture was extracted with EtOAc, the organic phase was dried over Na₂SO₄, filtered, and evaporated under vacuum to yield the desired product, which was used in the following step without further purification.

rel-*trans*-4-((2-(4-Chlorophenyl)cyclopropyl)(propyl)amino)-*N,N*-dimethyl-2,2-diphenylbutanamide (80) The compound was prepared following the same procedure described for **76**, starting from **69** (229 mg, 0.661 mmol) and **79** (154 mg, 0.734 mmol). The mixture was stirred for 3 h at 90°C in a sealed pressure vessel. The solvent was evaporated under vacuum, and the residue was purified with flash chromatography, eluting with 5% DMA, to obtain the desired product (37 mg, 11% yield, yellow oil). ¹H NMR (400 MHz, CDCl₃) δ 7.42 – 7.30 (m, 9H), 7.27 (d, J = 7.8 Hz, 1H), 7.15 (d, J = 8.4 Hz, 2H), 6.82 (d, J = 8.4 Hz, 2H), 2.97 (s, 3H), 2.53 – 2.23 (m, 9H), 1.76 (dt, J = 7.2, 4.1 Hz, 1H), 1.68 (m, 1H), 1.49 – 1.28 (m, 2H), 0.91 (m, 1H), 0.85 – 0.73 (m, 4H). ¹³C NMR (101 MHz, CDCl₃) δ 173.53, 141.10, 141.05, 140.92, 130.79, 128.32, 128.16, 128.10, 128.06, 127.12, 126.63, 126.61, 59.95, 56.85, 51.73, 47.64, 42.10, 29.70, 25.39, 20.35, 17.08, 12.03. Analytical HPLC: Phenomenex Gemini C18 4.6 x 50 mm, 3 μ m; gradient 10%-80% ACN in water + 0.1% TFA; 30 min run; injection 20 μ L (1 mg/mL); temperature 40°C; ^tR 23.653 min, purity >99%; HRMS-MS/MS C₃₀H₃₅ClN₂O + H⁺ calculated 475.25107, found

475.25072. Elemental analysis ($C_{30}H_{35}ClN_2O + 0.25H_2O$) calculated C 75.14, H 7.46, N 5.84, found C 75.19, H 7.51, N 5.84

rel-*trans*-4-((2-(4-Chlorophenyl)cyclopropyl)(2-hydroxyethyl)amino)-*N,N*-dimethyl-2,2-diphenylbutanamide (81) A solution of **78** (140 mg, 0.32 mmol), 2-bromoethan-1-ol (40 mg, 0.32 mmol) and K_2CO_3 (223 mg, 1.62 mmol) in ACN (20 mL) was heated at 90°C and stirred in a sealed vessel overnight. The solvent was evaporated under vacuum, and the desired product was isolated by flash chromatography eluting with 10% DMA (32 mg, 21% yield, colorless oil). 1H NMR (400 MHz, $CDCl_3$) δ 7.42 – 7.32 (m, 8H), 7.31 – 7.25 (m, 2H), 7.16 (d, $J = 8.4$ Hz, 2H), 6.83 (d, $J = 8.4$ Hz, 2H), 3.45 (s, 2H), 2.97 (s, 3H), 2.82 – 2.63 (m, 3H), 2.45 – 2.38 (m, 4H), 2.31 (s, 3H), 1.93 – 1.82 (m, 1H), 1.75 – 1.64 (m, 1H), 0.97 – 0.80 (m, 2H). ^{13}C NMR (101 MHz, $CDCl_3$) δ 173.43, 140.68, 140.41, 131.09, 128.45, 128.20, 128.08, 128.05, 127.15, 126.81, 59.94, 58.47, 55.96, 51.63, 47.33, 42.40, 39.17, 37.20, 25.18, 16.84. Analytical HPLC: Phenomenex Gemini C18 4.6 x 50 mm, 3 μ m; gradient 10%-80% ACN in water + 0.1% TFA; 50 min run; injection 20 μ L (1 mg/mL); temperature 40°C; t_R 21.685, 22.035 min, purity >99%. HRMS-MS/MS $C_{29}H_{33}ClN_2O_2 + H^+$ calculated 477.23033, found 477.22983. Elemental analysis ($C_{29}H_{33}ClN_2O_2 + 0.75H_2O$) calculated C 71.00, H 7.09, N 5.71, found C 71.17, H 6.79, N 5.75

rel-*trans*-4-((2-(4-Methoxyphenyl)cyclopropyl)amino)-*N,N*-dimethyl-2,2-diphenylbutanamide (82) The compound was prepared following the same procedure described for **76**, starting from rel-*trans*-2-(4-methoxyphenyl)cyclopropan-1-amine (85 mg, 0.52 mmol). The mixture was stirred for 3 h at 90°C in a sealed pressure vessel. The desired product was isolated by C18 preparative HPLC as TFA salt (Phenomenex Gemini NX-C18 110 Å, AXIA Packed, 150 x 30 mm, 5 μ m; gradient 10%-80% ACN in water + 0.1% TFA; 60 min run; injection 4mL (~10-

15 mg/mL); temperature 25°C; DAD λ 214 nm and λ 254 nm) (50 mg, 12% yield, yellow oil). An analytical amount was converted into the free base: ^1H NMR (400 MHz, CDCl_3) δ 7.36 (d, J = 10.9 Hz, 10H), 6.86 (d, J = 7.6 Hz, 2H), 6.75 (d, J = 7.1 Hz, 2H), 3.76 (s, 3H), 2.97 (br s, 3H), 2.42 (br s, 4H), 2.32 (br s, 3H), 2.09 (s, 1H), 1.66 (m, 2H), 0.75 (m, 2H). ^{13}C NMR (101 MHz, CDCl_3) δ 173.58, 157.51, 140.94, 140.88, 134.54, 128.66, 128.36, 128.12, 127.58, 127.00, 126.68, 113.60, 60.13, 55.30, 46.84, 45.79, 40.89, 24.25, 16.38. Analytical HPLC: Phenomenex Gemini C18 4.6 x 50 mm, 3 μm ; gradient 10%-80% ACN in water + 0.1% TFA; 60 min run; injection 20 μL (1 mg/mL); temperature 40°C; R 19.984 min, purity >99%. HRMS-MS/MS $\text{C}_{28}\text{H}_{32}\text{N}_2\text{O}_2 + \text{H}^+$ calculated 429.25365, found 429.25306.

rel-*trans*-4-((2-(4-Fluorophenyl)cyclopropyl)amino)-*N,N*-dimethyl-2,2-diphenylbutanamide

(83) The compound was prepared following the same procedure described for **76**, starting from *rel-trans*-2-(4-fluorophenyl)cyclopropan-1-amine HCl (200 mg, 1.07 mmol). The mixture was stirred for 3 h at 90°C in a sealed pressure vessel. The desired product was isolated by C18 preparative HPLC (Phenomenex Gemini NX-C18 110 Å, AXIA Packed, 150 x 30 mm, 5 μm ; gradient 10%-80% ACN in water + 0.1% TFA; 60 min run; injection 4mL (~10-15 mg/mL); temperature 25°C; DAD λ 214 nm and λ 254 nm) as TFA salt, basified with conc. NH_4OH aq. solution and extracted with DCM (30 mg, 6.8% yield, orange oil). Free base ^1H NMR (400 MHz, CDCl_3) δ 7.41 – 7.30 (m, 7H), 7.26 (s, 3H), 6.87 (d, J = 6.8 Hz, 4H), 2.97 (s, 3H), 2.41 (s, 4H), 2.32 (s, 3H), 2.10 (s, 1H), 1.72 – 1.57 (m, 2H), 0.88 (d, J = 4.9 Hz, 1H), 0.76 (s, 1H). ^{13}C NMR (101 MHz, CDCl_3) δ 173.58, 162.19, 159.78, 140.93, 140.83, 138.08, 138.05, 128.38, 128.13, 128.11, 127.33, 127.25, 126.71, 114.89, 114.68, 60.15, 46.84, 45.86, 41.20, 24.39, 16.73. Analytical HPLC: Phenomenex Gemini C18 4.6 x 50 mm, 3 μm ; gradient 10%-80% ACN in water

+ 0.1% TFA; 60 min run; injection 20 μ L (1 mg/mL); temperature 40°C; t_R 20.440 min, purity >99%. HRMS-MS/MS $C_{27}H_{29}FN_2O + H^+$ calculated 417.23367, found 417.23305.

rel-trans-4-((2-(2-Methoxyphenyl)cyclopropyl)amino)-N,N-dimethyl-2,2-

diphenylbutanamide (84) The compound was prepared following the same procedure described for **76**, starting from rel-trans-2-(2-methoxyphenyl)cyclopropan-1-amine HCl (200 mg, 1.00 mmol). The reaction was heated to 90°C and stirred in a sealed pressure vessel for 1.5 h. The solvent was evaporated under vacuum, and the crude product was purified through flash chromatography, eluting with 10% DMA, followed by C18 preparative HPLC (Phenomenex Gemini NX-C18 110 Å, AXIA Packed, 150 x 30 mm, 5 μ m; gradient 10%-80% ACN in water + 0.1% TFA; 60 min run; injection 4mL (~10-15 mg/mL); temperature 25°C; DAD λ 214 nm and λ 254 nm) (28 mg, 13% yield). The desired product was isolated as TFA salt (yellow oil). 1H NMR (400 MHz, $CDCl_3$) δ 9.70 (s, 1H), 9.55 (s, 1H), 7.46 – 7.40 (m, 4H), 7.38 – 7.29 (m, 6H), 7.20 (t, $J = 8.3$ Hz, 1H), 6.92 – 6.82 (m, 2H), 6.77 (d, $J = 8.1$ Hz, 1H), 3.59 (s, 3H), 3.03 (s, 3H), 2.90 (m, 1H), 2.81 (m, 1H), 2.58 (s, 2H), 2.47 (d, $J = 8.2$ Hz, 2H), 2.29 (s, 3H), 1.51 (m, 1H), 1.27 (d, $J = 7.0$ Hz, 1H). ^{13}C NMR (101 MHz, $CDCl_3$) δ 175.77, 158.30, 139.39, 139.13, 129.22, 128.32, 128.00, 127.90, 127.82, 125.70, 120.41, 110.02, 94.90, 62.53, 54.96, 45.30, 41.84, 39.42, 37.71, 37.16, 17.26, 11.05. Analytical HPLC: Phenomenex Gemini C18 4.6 x 50 mm, 3 μ m; gradient 10%-80% ACN in water + 0.1% TFA; 60 min run; injection 20 μ L (1 mg/mL); temperature 40°C; t_R 20.656 min, purity >95%. HRMS-MS/MS $C_{28}H_{32}N_2O_2 + H^+$ calculated 429.25365, found 429.25310.

2,2-Diethyltetrahydro-4H-pyran-4-one (85)^{73,75} Conc. H_2SO_4 (11.4 g, 6.19 mL, 116 mmol) was added portion-wise to a solution of pentan-3-one (10.0 g, 116 mmol) and but-3-en-1-ol (8.37 g,

116 mmol) in DCM (20 mL) at -78°C . The mixture was warmed to RT and was stirred for additional 2 h. The reaction completion and formation of the alcohol intermediate was monitored by GC/MS (GC/MS 'R 5.555 min, m/z 157.2 ($-\text{H}^+$)). The solution was diluted with water, and the organic phase was washed with 2N aq. NaOH and brine. The organic layer was dried over Na_2SO_4 , filtered, and diluted with DCM. The solution was cooled to 0°C , and DMP (49.24 g, 116.1 mmol) was added portion-wise to the stirring solution. The mixture was allowed to warm to RT and stirred for additional 1 h. The reaction was quenched and washed with sat. aq. NaHCO_3 . The organic phase was dried over Na_2SO_4 , filtered, and evaporated under vacuum. The crude material was purified by flash chromatography, eluting with 30% EtOAc in hexanes to yield the desired product (7.38 g, 41% yield over 2 steps). GC/MS 'R 5.197 min, m/z 156.2.

6-Oxaspiro[4.5]decan-9-one (86) The compound was prepared following the same procedure described for **85**, starting from cyclopentanone (6.00 g, 71.3 mmol) and but-3-en-1-ol (10.3 g, 143 mmol). The desired product was isolated by flash chromatography, eluting with 30% EtOAc in hexane (5.00 g, 45% yield over 2 steps). GC/MS 'R 5.629 min, m/z 154.1. ^1H NMR (400 MHz, CDCl_3) δ 3.95 (d, $J = 5.8$ Hz, 2H), 2.45 (m, 4H), 1.96 – 1.37 (m, 8H).

4-(Pyridin-2-yl)tetrahydro-2H-pyran-4-ol (87) *n*-Butyllithium (18 mL, 2.5 M, 45 mmol) was added drop-wise to a solution of 2-bromopyridine (7.1 g, 45 mmol) in TBME (100 mL) at -78°C . The mixture was stirred for 1 h, followed by drop-wise addition of tetrahydro-4H-pyran-4-one (3.0 g, 30 mmol). The reaction was allowed to warm to RT and stirred overnight. The mixture was diluted with sat. aq. NH_4Cl and stirred for 30 min. The organic layer was separated, dried over Na_2SO_4 , filtered, and evaporated under vacuum. The desired product was isolated by flash

chromatography, eluting with 70% EtOAc in hexane (4.2 g, 78% yield). GC/MS t_R 7.438 min, m/z 179.1

2,2-Diethyl-4-(pyridin-2-yl)tetrahydro-2H-pyran-4-ol (88) The compound was prepared following the same procedure described for **87**, starting from **85** (3.00 g, 19.2 mmol). The desired product was isolated by flash chromatography, eluting with 40% EtOAc in hexanes (2.10 g, 46% yield). GC/MS t_R 9.059 min, m/z 235.2. 1H NMR (400 MHz, $CDCl_3$) δ 8.53 (d, $J = 4.7$ Hz, 1H), 7.74 (t, $J = 7.7$ Hz, 1H), 7.40 (d, $J = 7.9$ Hz, 1H), 7.25 – 7.17 (m, 1H), 4.22 – 4.07 (m, 2H), 2.45 – 2.33 (m, 1H), 2.09 (dd, $J = 12.5, 5.3$ Hz, 1H), 1.84 – 1.35 (m, 7H), 0.85 (q, $J = 7.6$ Hz, 6H).

9-(Pyridin-2-yl)-6-oxaspiro[4.5]decan-9-ol (89) The compound was prepared following the same procedure described for **87**, starting from **86** (2.5 g, 16.2 mmol). The desired product was isolated by flash chromatography, eluting with 50% EtOAc in hexanes (2.3 g, 58% yield). GC/MS t_R 9.595 min, m/z 233.1. 1H NMR (400 MHz, $CDCl_3$) δ 8.53 (d, $J = 4.6$ Hz, 1H), 7.73 (t, $J = 8.0$ Hz, 1H), 7.40 (d, $J = 8.4$ Hz, 1H), 7.22 (t, $J = 5.3$ Hz, 1H), 5.24 (s, 1H), 4.13 (t, $J = 12.0$ Hz, 1H), 3.79 (dd, $J = 11.8, 5.1$ Hz, 1H), 2.47 – 2.32 (m, 1H), 2.19 – 2.01 (m, 1H), 1.87 – 1.37 (m, 10H).

2-(4-(Allyloxy)tetrahydro-2H-pyran-4-yl)pyridine (90) Intermediate **87** (550 mg, 3.07 mmol) was dissolved in a mixture of TBME (40 mL) and THF (10 mL), then cooled to 0°C. Sodium hydride (737 mg, 30.7 mmol) was added portion-wise and the suspension was stirred at 0°C for 1 h and warmed to RT. DMF (5 mL) was added to facilitate solubility, followed by dropwise addition of allyl bromide (0.26 mL, 3.04 mmol). The mixture was refluxed for 2 h, then stirred at RT for 48 h. The suspension was washed with brine and the organic phase was dried over Na_2SO_4 , filtered,

and evaporated under vacuum. The desired product was isolated by flash chromatography, eluting with 30% EtOAc in hexane (470 mg, 70% yield). GC/MS t_R 8.196 min, m/z 218.1 ($-H^+$). 1H NMR (400 MHz, $CDCl_3$) δ 8.58 (d, $J = 3.4$ Hz, 1H), 7.71 (t, $J = 7.7$ Hz, 1H), 7.53 (d, $J = 8.0$ Hz, 1H), 7.24 – 7.08 (m, 1H), 5.98 – 5.79 (m, 1H), 5.29 (d, $J = 17.2$ Hz, 1H), 5.14 (d, $J = 10.4$ Hz, 1H), 3.98 – 3.74 (m, 4H), 3.71 – 3.58 (m, 2H), 2.35 – 2.18 (m, 2H), 1.98 (d, $J = 14.0$ Hz, 2H).

2-(4-(Allyloxy)-2,2-diethyltetrahydro-2H-pyran-4-yl)pyridine (91) Sodium hydride (1.29 g, 54.0 mmol) was added to a solution of **88** (4.20 g, 18.0 mmol) in DMF (20 mL) at 0°C. The mixture was stirred at RT for 15 min, followed by drop-wise addition of allyl bromide (4.40 g, 36.0 mmol). The solution was heated to 90°C and stirred overnight in a sealed flask. The reaction mixture was diluted with water and extracted with EtOAc. The organic layer was dried over Na_2SO_4 , filtered, and evaporated under vacuum. The desired product was isolated by flash chromatography, eluting with 30% EtOAc in hexanes (1.78 g, 36% yield). GC/MS t_R 9.450 min, m/z 275.1. 1H NMR (400 MHz, $CDCl_3$) δ 8.57 (d, $J = 5.2$ Hz, 1H), 7.69 (t, $J = 7.5$ Hz, 1H), 7.53 (d, $J = 8.2$ Hz, 1H), 7.21 – 7.13 (m, 1H), 5.91 – 5.82 (m, 1H), 5.28 (d, $J = 17.2$ Hz, 1H), 5.12 (d, $J = 10.5$ Hz, 1H), 3.99 (t, $J = 11.5$ Hz, 1H), 3.79 – 3.62 (m, 2H), 3.56 (dd, $J = 12.47, 4.9$ Hz, 1H), 2.42 – 2.28 (m, 1H), 2.21 (dq, $J = 15.1, 7.7$ Hz, 1H), 1.97 (t, $J = 11.9$ Hz, 2H), 1.86 (d, $J = 14.5$ Hz, 1H), 1.68 (dq, $J = 15.3, 7.6$ Hz, 1H), 1.48 (dq, $J = 14.3, 7.7$ Hz, 1H), 1.34 (dq, $J = 14.2, 7.3$ Hz, 1H), 0.83 (dt, $J = 25.7, 7.5$ Hz, 6H).

2-(9-(Allyloxy)-6-oxaspiro[4.5]decan-9-yl)pyridine (92) The compound was prepared following the same procedure described for **91**, starting from **89** (2.20 g, 9.42 mmol). The desired product was isolated by flash chromatography eluting with 20% EtOAc in hexanes (1.40 g, 56% yield).

GC/MS ¹R 10.069 min, m/z 273.1. ¹H NMR (400 MHz, CDCl₃) δ 8.58 (d, *J* = 4.8 Hz, 1H), 7.70 (t, *J* = 7.8 Hz, 1H), 7.52 (d, *J* = 7.9 Hz, 1H), 7.22 – 7.14 (m, 1H), 5.96 – 5.80 (m, 1H), 5.29 (d, *J* = 17.2 Hz, 1H), 5.12 (d, *J* = 10.5 Hz, 1H), 3.97 (t, *J* = 11.7 Hz, 1H), 3.76 (dt, *J* = 11.7, 3.6 Hz, 1H), 3.70 – 3.54 (m, 2H), 2.39 – 2.23 (m, 2H), 2.20 (d, *J* = 14.1 Hz, 1H), 2.06 – 1.92 (m, 2H), 1.84 – 1.37 (m, 7H).

3-((4-(Pyridin-2-yl)tetrahydro-2H-pyran-4-yl)oxy)propan-1-ol (93) Borane tetrahydrofuran complex (6.43 mL, 1 M in THF, 6.43 mmol) was added drop-wise to a solution of **90** (470 mg, 2.14 mmol) in THF (20 mL) at 0°C. The reaction was stirred at RT for 3 h. The solution was cooled to 0°C, then 2M aq. NaOH (10 mL, 20 mmol) and H₂O₂ (10 mL, 35% Wt) were added dropwise. The mixture was allowed to warm to RT and stirred overnight. The reaction was quenched with sat. aq. NH₄Cl and extracted with EtOAc. The organic phase was washed with brine and 2M aq. NaOH, then dried over Na₂SO₄, filtered, and evaporated under vacuum. The desired product was isolated by flash chromatography, eluting with 70% EtOAc in hexanes (100 mg, 20% yield). GC/MS ¹R 9.732 min, m/z 237.1. ¹H NMR (400 MHz, CDCl₃) δ 8.60 (d, *J* = 4.7 Hz, 1H), 7.74 (t, *J* = 8.3 Hz, 1H), 7.46 (d, *J* = 7.8 Hz, 1H), 7.25 – 7.16 (m, 1H), 3.93 – 3.83 (m, 4H), 3.78 (t, *J* = 5.5 Hz, 2H), 3.51 (s, 1H), 3.32 (t, *J* = 5.6 Hz, 2H), 2.30 – 2.11 (m, 2H), 2.00 (m, 2H), 1.87 – 1.72 (m, 2H).

3-((2,2-Diethyl-4-(pyridin-2-yl)tetrahydro-2H-pyran-4-yl)oxy)propan-1-ol (94) The compound was prepared following the same procedure described for **93**, starting from **91** (1.78 g, 6.45 mmol). The desired product was isolated by flash chromatography, eluting with 70% EtOAc in hexanes (0.30 g, 16% yield). ¹H NMR (400 MHz, CDCl₃) δ 8.59 (d, *J* = 4.3 Hz, 1H), 7.72 (t, *J*

= 7.8 Hz, 1H), 7.47 (d, $J = 8.0$ Hz, 1H), 7.24 – 7.16 (m, 1H), 3.97 (t, $J = 11.1$ Hz, 1H), 3.75 (d, $J = 11.6$ Hz, 3H), 3.41 – 3.31 (m, 1H), 3.29 (s, 1H), 3.21 – 3.10 (m, 1H), 2.32 – 2.12 (m, 2H), 2.00 (d, $J = 14.3$ Hz, 2H), 1.85 – 1.63 (m, 4H), 1.47 (dd, $J = 14.5, 7.6$ Hz, 1H), 1.38 – 1.22 (m, 1H), 0.83 (dt, $J = 30.0, 7.4$ Hz, 6H).

3-((9-(Pyridin-2-yl)-6-oxaspiro[4.5]decan-9-yl)oxy)propan-1-ol (95) The compound was prepared following the same procedure described for **93**, starting from **92** (1.2 g, 4.4 mmol). The desired product was isolated by flash chromatography, eluting with 70% EtOAc in hexanes (130 mg, 20% yield). GC/MS t_R 11.426 min, m/z 291.1 1H NMR (400 MHz, $CDCl_3$) δ 8.60 (d, $J = 5.3$ Hz, 1H), 7.73 (td, $J = 7.7, 1.7$ Hz, 1H), 7.46 (d, $J = 7.9$ Hz, 1H), 7.22 (dd, $J = 7.1, 4.8$ Hz, 1H), 3.95 (td, $J = 11.5, 2.0$ Hz, 1H), 3.86 – 3.70 (m, 3H), 3.40 – 3.31 (m, 1H), 3.24 – 3.15 (m, 1H), 2.35 – 2.18 (m, 2H), 2.13 – 1.96 (m, 3H), 1.86 – 1.36 (m, 10H).

3-((4-(Pyridin-2-yl)tetrahydro-2H-pyran-4-yl)oxy)propyl 4-methylbenzenesulfonate (96) DMAP (77.2 mg, 0.632 mmol) and *p*-TsCl (121 mg, 0.632 mmol) were added to a solution of **93** (100 mg, 0.421 mmol) in DCM (20 mL), at 0 °C. The mixture was stirred at RT overnight, then the solvent was evaporated under vacuum, and the residue was purified by flash chromatography, eluting with 50% EtOAc in hexanes, to yield the desired product (40 mg, 24% yield). 1H NMR (400 MHz, $CDCl_3$) δ 8.56 (s, 1H), 7.78 (d, $J = 7.9$ Hz, 2H), 7.70 (t, $J = 7.7$ Hz, 1H), 7.38 (m, 3H), 7.23 – 7.15 (m, 1H), 4.18 (t, $J = 6.2$ Hz, 2H), 3.83 – 3.61 (m, 4H), 3.11 (t, $J = 5.8$ Hz, 2H), 2.46 (s, 3H), 2.23 – 2.16 (m, 2H), 1.97 – 1.80 (m, 4H).

3-((2,2-Diethyl-4-(pyridin-2-yl)tetrahydro-2H-pyran-4-yl)oxy)propyl 4-

methylbenzenesulfonate (97) The compound was prepared following the same procedure described for **96**, starting from **94** (300 mg, 1.02 mmol). The crude was purified by flash chromatography, eluting with 60% EtOAc in hexanes, to yield the desired product (152 mg, 33% yield). ¹H NMR (400 MHz, CDCl₃) δ 8.56 (s, 1H), 7.78 (d, *J* = 9.2 Hz, 2H), 7.70 (br s, 1H), 7.43 (d, *J* = 7.4 Hz, 1H), 7.35 (d, *J* = 8.3 Hz, 2H), 7.19 (s, 1H), 4.15 (m, 2H), 3.91 – 3.78 (m, 1H), 3.71 (d, *J* = 15.1 Hz, 1H), 3.16 (m, 1H), 2.97 (m, 1H), 2.46 (s, 3H), 2.31 (m, 1H), 2.02 (m, 1H), 1.95 – 1.69 (m, 5H), 1.57 (m, 1H), 1.42 (m, 1H), 1.26 (m, 1H), 0.88 – 0.70 (m, 6H).

3-((9-(Pyridin-2-yl)-6-oxaspiro[4.5]decan-9-yl)oxy)propyl 4-methylbenzenesulfonate (98)

The compound was prepared following the same procedure described for **96**, starting from **95** (130 mg, 0.45 mmol). The crude was purified by flash chromatography, eluting with 70% EtOAc in hexanes, to yield the desired product (70 mg, 35% yield). ¹H NMR (400 MHz, CDCl₃) δ 8.56 (d, *J* = 4.0 Hz, 1H), 7.78 (d, *J* = 8.3 Hz, 2H), 7.70 (td, *J* = 7.7, 1.7 Hz, 1H), 7.42 (d, *J* = 8.0 Hz, 1H), 7.35 (d, *J* = 8.1 Hz, 2H), 7.19 (dd, *J* = 6.9, 5.3 Hz, 1H), 4.22 – 4.13 (m, 2H), 3.81 (td, *J* = 11.5, 2.1 Hz, 1H), 3.71 (dt, *J* = 11.7, 4.4 Hz, 1H), 3.15 (dt, *J* = 9.1, 6.1 Hz, 1H), 2.99 (dt, *J* = 9.2, 5.7 Hz, 1H), 2.46 (s, 3H), 2.35 – 2.21 (m, 1H), 2.15 – 2.02 (m, 1H), 1.98 – 1.79 (m, 4H), 1.77 – 1.21 (m, 8H).

1-(2,3-Dichlorophenyl)-4-(3-((4-(pyridin-2-yl)tetrahydro-2H-pyran-4-

yl)oxy)propyl)piperazine (99) A solution of 1-(2,3-dichlorophenyl)piperazine (39 mg, 0.17 mmol), **96** (60 mg, 0.15 mmol) and K₂CO₃ (210 mg, 1.5 mmol) in ACN (20 mL) was heated to reflux and stirred for 2 h. The solvent was evaporated under vacuum, and the residue was purified by flash chromatography, eluting with 5% DMA, to afford the desired product (20 mg, 29% yield).

¹H NMR (400 MHz, CDCl₃) δ 8.59 – 8.55 (m, 1H), 7.71 (td, *J* = 7.7, 1.8 Hz, 1H), 7.51 (d, *J* = 7.9 Hz, 1H), 7.23 – 7.09 (m, 3H), 6.95 (dd, *J* = 6.6, 3.0 Hz, 1H), 3.90 (dd, *J* = 11.2, 2.2 Hz, 1H), 3.87 – 3.78 (m, 3H), 3.16 (t, *J* = 6.3 Hz, 2H), 3.05 (br s, 4H), 2.63 (br s, 4H), 2.52 (t, *J* = 7.5 Hz, 2H), 2.24 (ddd, *J* = 15.2, 11.1, 5.0 Hz, 2H), 1.97 (dd, *J* = 14.3, 2.5 Hz, 2H), 1.79 (p, *J* = 6.6 Hz, 2H). ¹³C NMR (101 MHz, CDCl₃) δ 163.68, 151.25, 148.67, 136.51, 134.03, 127.43, 124.55, 122.21, 120.58, 118.57, 63.82, 60.21, 55.36, 53.26, 51.29, 34.64, 27.50. The free base was converted into the corresponding oxalate salt, obtained as a white solid (m.p. 191-195°C). HRMS-MS/MS C₂₃H₂₉Cl₂N₃O₂ + H⁺ calculated 450.17096, found 450.17045. Elemental analysis (C₂₃H₂₉Cl₂N₃O₂ + H₂C₂O₄ + 0.5H₂O) calculated C 54.65, H 5.87, N 7.65, found C 54.89, H 5.58, N 7.60

1-(3-((4-(Pyridin-2-yl)tetrahydro-2H-pyran-4-yl)oxy)propyl)-4-(6-(trifluoromethyl)pyridin-2-yl)piperazine (100) The compound was prepared following the same procedure described for **99** starting from 1-(6-(trifluoromethyl)pyridin-2-yl)piperazine (120 mg, 0.51 mmol) and **96** (40 mg, 0.10 mmol) in ACN (10 mL). The reaction was heated to reflux and stirred for 2 h. The solvent was evaporated under vacuum, and the residue was purified by flash chromatography, eluting with 10% DMA, to afford the desired product (10 mg, 22% yield, yellow oil). ¹H NMR (400 MHz, CDCl₃) δ 8.59 (s, 1H), 7.72 (t, *J* = 7.7 Hz, 1H), 7.61 (s, 1H), 7.48 (d, *J* = 7.7 Hz, 1H), 7.21 (s, 1H), 6.99 (d, *J* = 7.0 Hz, 1H), 6.79 (d, *J* = 9.2 Hz, 1H), 3.95 – 3.58 (m, 8H), 3.18 (br s, 2H), 2.71 (br s, 6H), 2.23 (br s, 2H), 1.98 (br s + d, *J* = 13.9 Hz, 4H). ¹³C NMR (101 MHz, CDCl₃) δ 148.80, 146.66, 146.32, 138.54, 136.65, 122.88, 122.42, 120.60, 109.64, 70.56, 63.82, 59.81, 55.55, 52.37, 34.58, 29.71, 22.70. Analytical HPLC: Chiralpak AD-H 4.6 x 250 mm, 5 μm; gradient 10%-30% 2-PrOH in n-hexane; 60 min run; injection 20 μL (1 mg/mL); temperature 40°C; *t*_R 10.553 min, purity >99%; Chiralcel OD-H 4.6 x 250 mm, 5 μm; gradient 10%-30% 2-PrOH in n-hexane; 60

min run; injection 20 μ L (1 mg/mL); temperature 40°C; t_R 9.529 min, purity >99%; HRMS-MS/MS $C_{23}H_{29}F_3N_4O_2 + H^+$ calculated 451.23154, found 451.23147

1-(2,3-Dichlorophenyl)-4-(3-((2,2-diethyl-4-(pyridin-2-yl)tetrahydro-2H-pyran-4-

yl)oxy)propyl)piperazine (101) The compound was prepared following the same procedure described for **99**, starting from 1-(2,3-dichlorophenyl)piperazine HCl (30 mg, 0.11 mmol) and **97** (50 mg, 0.11 mmol). The solvent was evaporated under vacuum, and the residue was purified by flash chromatography, eluting with 10% DMA, to afford the desired product (51 mg, 90% yield, yellow oil). 1H NMR (400 MHz, $CDCl_3$) δ 8.63 (s, 1H), 7.73 (t, $J = 8.0$ Hz, 1H), 7.50 (d, $J = 7.9$ Hz, 1H), 7.30 – 7.11 (m, 3H), 6.97 (d, $J = 7.4$ Hz, 1H), 3.95 (t, $J = 12.0$ Hz, 1H), 3.75 (d, $J = 11.0$ Hz, 1H), 3.33 – 2.65 (m, 12H), 2.39 – 2.25 (m, 1H), 2.20 (dd, $J = 14.3, 7.8$ Hz, 1H), 2.05 – 1.80 (m, 4H), 1.74 (s, 1H), 1.65 (dd, $J = 14.5, 7.4$ Hz, 1H), 1.58 – 1.39 (m, 1H), 1.39 – 1.20 (m, 1H), 0.87 (t, $J = 7.4$ Hz, 3H), 0.79 (t, $J = 7.5$ Hz, 3H). ^{13}C NMR (101 MHz, $CDCl_3$) δ 163.88, 148.85, 136.86, 134.13, 129.55, 127.56, 125.07, 122.46, 120.73, 118.73, 75.65, 60.62, 57.17, 55.73, 53.12, 50.48, 41.65, 31.80, 31.66, 25.16, 7.83, 7.56. Analytical HPLC: Phenomenex Gemini C18 4.6 x 50 mm, 3 μ m; gradient 10%-80% ACN in water + 0.1% TFA; 50 min run; injection 20 μ L (1 mg/mL); temperature 40°C; t_R 21.014 min, purity >99%. HRMS-MS/MS $C_{27}H_{37}Cl_2N_3O_2 + H^+$ calculated 506.23356, found 506.23279.

1-(3-((2,2-Diethyl-4-(pyridin-2-yl)tetrahydro-2H-pyran-4-yl)oxy)propyl)-4-(6-

(trifluoromethyl)pyridin-2-yl)piperazine (102) The compound was prepared following the same procedure described for **99**, starting from 1-(6-(trifluoromethyl)pyridin-2-yl)piperazine (83 mg, 0.36 mmol) and **97** (70 mg, 0.16 mmol). The solvent was evaporated under vacuum, and the residue was purified by flash chromatography, eluting with 5% DMA, to afford the desired product

(15 mg, 12% yield, brown oil). ^1H NMR (400 MHz, CDCl_3) δ 8.57 (d, $J = 4.5$ Hz, 1H), 7.69 (td, $J = 7.6, 1.7$ Hz, 1H), 7.61 – 7.48 (m, 2H), 7.21 – 7.15 (m, 1H), 6.94 (d, $J = 7.3$ Hz, 1H), 6.76 (d, $J = 8.7$ Hz, 1H), 3.96 (td, $J = 11.7, 1.9$ Hz, 1H), 3.78 – 3.70 (m, 1H), 3.60 (br s, 4H), 3.24 – 3.15 (m, 1H), 3.07 – 2.98 (m, 1H), 2.50 (m, 6H), 2.41 – 2.25 (m, 1H), 2.18 (dd, $J = 14.4, 7.3$ Hz, 1H), 1.96 (m, 2H), 1.82 – 1.55 (m, 4H), 1.46 (dq, $J = 15.0, 7.5$ Hz, 1H), 1.33 (dq, $J = 15.4, 7.9$ Hz, 1H), 0.87 (t, $J = 7.5$ Hz, 3H), 0.79 (t, $J = 7.5$ Hz, 3H). ^{13}C NMR (101 MHz, CDCl_3) δ 164.31, 158.78, 148.56, 146.91, 146.57, 146.24, 145.90, 138.24, 136.47, 122.10, 120.61, 109.38, 108.85, 77.91, 75.67, 60.40, 57.26, 55.37, 52.81, 44.71, 41.46, 31.75, 31.69, 27.42, 25.13, 7.87, 7.55. Analytical HPLC: Phenomenex Gemini C18 4.6 x 50 mm, 3 μm ; gradient 10%-80% ACN in water + 0.1% TFA; 60 min run; injection 20 μL (1 mg/mL); temperature 40°C; t_{R} 20.589 min, purity >99%. HRMS-MS/MS $\text{C}_{27}\text{H}_{37}\text{F}_3\text{N}_4\text{O}_2 + \text{H}^+$ calculated 507.29414, found 507.29353; $\text{C}_{27}\text{H}_{37}\text{F}_3\text{N}_4\text{O}_2 + \text{Na}^+$ calculated 529.27608, found 529.27577.

1-(3-((9-(Pyridin-2-yl)-6-oxaspiro[4.5]decan-9-yl)oxy)propyl)-4-(6-(trifluoromethyl)pyridin-2-yl)piperazine (103) The compound was prepared following the same procedure described for **99**, starting from **98** (70 mg, 0.16 mmol) and 1-(6-(trifluoromethyl)pyridin-2-yl)piperazine (54 mg, 0.24 mmol). The solvent was evaporated under vacuum, and the residue was purified by flash chromatography, eluting with 10% DMA, to afford the desired product (41 mg, 52% yield, colorless oil). ^1H NMR (400 MHz, CDCl_3) δ 8.58 (d, $J = 4.6$ Hz, 1H), 7.69 (t, $J = 6.9$ Hz, 1H), 7.57 (t, $J = 8.0$ Hz, 1H), 7.51 (d, $J = 8.1$ Hz, 1H), 7.22 – 7.14 (m, 1H), 6.94 (d, $J = 7.3$ Hz, 1H), 6.76 (d, $J = 8.6$ Hz, 1H), 3.94 (t, $J = 11.4$ Hz, 1H), 3.76 (d, $J = 12.1$ Hz, 1H), 3.59 (br s, 4H), 3.24 – 3.12 (m, 1H), 3.13 – 3.00 (m, 1H), 2.52 (br s, 6H), 2.37 – 2.19 (m, 2H), 2.12 (d, $J = 14.1$ Hz, 1H), 1.98 (d, $J = 14.0$ Hz, 2H), 1.85 – 1.48 (m, 8H), 1.43 (m, 1H). ^{13}C NMR (101 MHz, CDCl_3) δ 164.02, 158.82, 148.60, 146.92, 146.58, 146.24, 145.91, 138.21, 136.43, 122.13, 120.66, 109.35,

108.82, 108.79, 82.71, 77.76, 60.49, 58.37, 55.36, 52.83, 44.77, 43.55, 41.09, 34.93, 32.43, 27.49, 24.37, 22.54. Analytical HPLC: Phenomenex Gemini C18 4.6 x 50 mm, 3 μ m; gradient 10%-80% ACN in water + 0.1% TFA; 60 min run; injection 20 μ L (1 mg/mL); temperature 40°C; *t*_R 19.854 min, purity >99%. HRMS-MS/MS C₂₇H₃₅F₃N₄O₂ + H⁺ calculated 505.27849, found 505.27717; C₂₇H₃₅F₃N₄O₂ + Na⁺ calculated 527.26043, found 527.25933.

3-((2,2-Diethyl-4-(pyridin-2-yl)tetrahydro-2H-pyran-4-yl)oxy)-N-((6-

(trifluoromethyl)pyridin-2-yl)methyl)propan-1-amine (104) The compound was prepared following the same procedure described for **99**, starting from (6-(trifluoromethyl)pyridine-2-yl)methanamine HCl (28 mg, 0.13 mmol) and **97** (50 mg, 0.11 mmol). The solvent was evaporated under vacuum, and the residue was purified by flash chromatography, eluting with 10% DMA, to afford the desired product (8.4 mg, 17% yield, colorless oil). ¹H NMR (400 MHz, CDCl₃) δ 8.93 (d, *J* = 5.2 Hz, 1H), 8.17 (d, *J* = 8.0 Hz, 1H), 7.98 (t, *J* = 7.9 Hz, 1H), 7.81 (t, *J* = 8.0 Hz, 1H), 7.65 (d, *J* = 8.0 Hz, 1H), 7.35 (d, *J* = 8.2 Hz, 2H), 4.74 – 4.64 (m, 1H), 4.49 (d, *J* = 14.0 Hz, 1H), 4.00 – 3.87 (m, 1H), 3.74 (d, *J* = 11.2 Hz, 1H), 3.56 (s, 1H), 3.40 – 3.25 (m, 3H), 2.41 – 2.25 (m, 2H), 2.06 (d, *J* = 7.2 Hz, 2H), 1.95 (d, *J* = 13.4 Hz, 1H), 1.82 (d, *J* = 14.6 Hz, 1H), 1.70 – 1.40 (m, 3H), 1.26 (s, 2H), 0.80 (t, *J* = 7.3 Hz, 3H), 0.68 (t, *J* = 7.6 Hz, 3H). ¹³C NMR (101 MHz, CDCl₃) δ 162.36, 149.08, 139.05, 138.51, 127.69, 123.26, 120.93, 120.64, 75.61, 62.76, 56.52, 47.46, 42.09, 32.34, 31.95, 24.28, 7.57, 7.31. Analytical HPLC: Phenomenex Gemini C18 4.6 x 50 mm, 3 μ m; gradient 10%-80% ACN in water + 0.1% TFA; 30 min run; injection 20 μ L (1 mg/mL); temperature 40°C; *t*_R 18.238 min, purity >99%. HRMS-MS/MS C₂₄H₃₂F₃N₃O₂ + H⁺ calculated 452.25194, found 452.25140; C₂₄H₃₂F₃N₃O₂ + Na⁺ calculated 474.23388, found 474.23318

***N*-(2,3-Dichlorobenzyl)-3-((2,2-diethyl-4-(pyridin-2-yl)tetrahydro-2*H*-pyran-4-**

yl)oxy)propan-1-amine (105) The compound was prepared following the same procedure described for **99**, starting from (2,3-dichlorophenyl)methanamine (19 mg, 0.11 mmol) and **97** (40 mg, 0.89 mmol). The solvent was evaporated under vacuum, and the residue was purified by flash chromatography, eluting with 10% DMA, followed by C18 preparative HPLC (Phenomenex Gemini NX-C18 110 Å, AXIA Packed, 150 x 30 mm, 5 µm; gradient 10%-80% ACN in water + 0.1% TFA; 60 min run; injection 4mL (~10-15 mg/mL); temperature 25°C; DAD λ214 nm and λ254 nm) to afford the desired product (9.5 mg, 24% yield, pink oil) as TFA salt. ¹H NMR (400 MHz, CD₃OD) δ 8.55 (s, 1H), 8.01 (t, *J* = 7.5 Hz, 1H), 7.66 (t, *J* = 8.7 Hz, 2H), 7.58 (d, *J* = 7.6 Hz, 1H), 7.52 – 7.38 (m, 2H), 4.57 (s, 2H), 4.00 – 3.90 (m, 1H), 3.72 (d, *J* = 12.7 Hz, 1H), 3.48 (s, 1H), 3.27 (s, 1H), 3.14 (s, 1H), 2.38 – 1.86 (m, 6H), 1.64 (d, *J* = 14.7 Hz, 1H), 1.58 – 1.43 (m, 2H), 1.39 – 1.24 (m, 2H), 0.83 (t, *J* = 7.4 Hz, 3H), 0.74 (t, *J* = 7.7 Hz, 3H). ¹³C NMR (101 MHz, CDCl₃) δ 161.85, 148.24, 139.30, 133.94, 132.32, 131.76, 131.26, 128.44, 128.31, 123.74, 121.22, 78.22, 75.76, 61.16, 56.41, 47.15, 45.57, 42.82, 32.30, 31.51, 24.24, 24.17, 7.43, 7.40. Analytical HPLC: Phenomenex Gemini C18 4.6 x 50 mm, 3 µm; gradient 10%-80% ACN in water + 0.1% TFA; 30 min run; injection 20 µL (1 mg/mL); temperature 40°C; *t*_R 18.972 min, purity >99%. HRMS-MS/MS C₂₄H₃₂Cl₂N₂O₂ + H⁺ calculated 451.19136, found 451.19108; C₂₄H₃₂Cl₂N₂O₂ + Na⁺ calculated 473.17330, found 473.17291.

Ethyl 4-(pyridin-2-yl)tetrahydro-2*H*-pyran-4-carboxylate⁸³ (107) Starting material **106** (5.00 g, 4.61 mL, 30.3 mmol), 1-bromo-2-(2-bromoethoxy)ethane (8.42 g, 4.57 mL, 36.3 mmol), and NaH (3.63 g, 90.8 mmol) were dissolved in DMF (20 mL) and heated to 40°C. The reaction was stirred for 2 h, then diluted with brine. The organic layer was extracted with DCM, dried over NaSO₄, filtered, and evaporated under vacuum. The crude material was purified by flash

chromatography, eluting with 50% EtOAc in hexanes, to yield the desired product (3.2 g, 45% yield). GC/MS t_R 8.733 min, m/z 235.1. 1H NMR (400 MHz, $CDCl_3$) δ 8.58 (d, $J = 4.6$ Hz, 1H), 7.67 (t, $J = 7.5$ Hz, 1H), 7.34 (d, $J = 8.6$ Hz, 1H), 7.17 (t, $J = 6.2$ Hz, 1H), 4.25 – 4.10 (m, 2H), 3.91 – 3.88 (m, 2H), 3.64 (t, $J = 11.2$ Hz, 2H), 2.48 (d, $J = 13.8$ Hz, 2H), 2.17 (t, $J = 12.2$ Hz, 2H), 1.20 (t, $J = 7.1$ Hz, 3H).

(4-(Pyridin-2-yl)tetrahydro-2H-pyran-4-yl)methanol (108) THF (40 mL) was added drop-wise to LAH (1.0 g, 27 mmol), under argon atmosphere at 0°C. A solution of **107** (3.2 g, 14 mmol) in THF (10 mL) was added dropwise to the stirring suspension. The reaction was allowed to warm to RT and stirred for additional 3 h. The mixture was quenched with 2M aq. NaOH (1 mL) and MeOH (1mL). The solution was filtered and diluted with DCM. The organic phase was washed with 2M aq. NaOH, dried over Na_2SO_4 , filtered, and evaporated under vacuum. The crude product was used without further purification (1.7 g, 65% yield).

4-(Pyridin-2-yl)tetrahydro-2H-pyran-4-carbaldehyde (109) Intermediate **108** (1.7 g, 8.8 mmol) was dissolved in DCM (50 mL). DMP (3.7 g, 8.8 mmol) was added portion-wise at 0°C, and the reaction was stirred for 1 h. The mixture was washed with sat. aq. $NaHCO_3$. The organic phase was dried over Na_2SO_4 , filtered, and evaporated under vacuum. The desired product was isolated by flash chromatography, eluting with 5% MeOH in DCM (750 mg, 45% yield). GC/MS t_R 7.922 min, m/z 191.0. 1H NMR (400 MHz, $CDCl_3$) δ 9.65 (s, 1H), 8.64 (d, $J = 4.1$ Hz, 1H), 7.72 (t, $J = 8.6$ Hz, 1H), 7.27 (s, 1H), 7.24 – 7.18 (m, 1H), 3.91 – 3.78 (m, 2H), 3.73 – 3.60 (m, 2H), 2.40 (d, $J = 13.9$ Hz, 2H), 2.32 – 2.16 (m, 2H).

2-(4-(2-Methoxyvinyl)tetrahydro-2H-pyran-4-yl)pyridine (110) *t*-BuOK (1.06 g, 9.42 mmol) was added to a solution of (methoxymethyl)triphenylphosphonium chloride (2.42 g, 7.07 mmol) in THF (15 mL) at 0°C. The mixture was stirred for 15 min, followed by drop-wise addition of **109** (0.750 g, 3.92 mmol) in THF (15 mL) at 0°C. The mixture was allowed to reach RT and stirred for additional 3 h. The reaction was quenched with sat. aq. NH₄Cl and was extracted with EtOAc. The organic phase was dried over Na₂SO₄, filtered, and evaporated under vacuum. The crude material was purified by flash chromatography, eluting with 50% EtOAc in hexanes, to yield the desired product as E and Z isomers (300 mg, 35% yield). GC/MS ^rR 8.827 min (2 peaks E+Z), m/z 219.1. ¹H NMR (400 MHz, CDCl₃) (mixture of E+Z isomers) δ 8.68 – 8.51 (m, 1H), 7.64 (q, *J* = 9.0, 8.5 Hz, 1H), 7.41 (d, *J* = 7.8 Hz, 1H), 7.11 (d, *J* = 6.6 Hz, 1H), 6.15 and 5.92 (2 x d, *J* = 13.2 Hz, *J* = 6.7 Hz, 1H; E/Z isomers), 4.89 and 4.45 (2 x d, *J* = 14.8 Hz, *J* = 6.5 Hz, 1H; E/Z isomers), 3.91 – 3.53 (m, 4H), 3.48 (2 x s, 3H; E/Z isomers), 2.43 – 2.31 (m, 1H), 2.26 – 2.08 (m, 2H), 2.00 (m, *J* = 7.4 Hz, 1H).

2-(4-(Pyridin-2-yl)tetrahydro-2H-pyran-4-yl)acetaldehyde (111) Conc. HCl in water (37%; 1.5 mL) was added to a stirring solution of **110** (250 mg, 1.14 mmol) in DCM (5 mL). The mixture was stirred for 1 h, then basified with 2M aq. NaOH and extracted with DCM. The organic phase was dried over Na₂SO₄, filtered, and evaporated under vacuum. The crude product was used without further purification (210 mg, 90% yield). GC/MS ^rR 8.617 min, m/z 204.1

rel-trans-2-(4-Chlorophenyl)-N-(2-(4-(pyridin-2-yl)tetrahydro-2H-pyran-4-yl)ethyl)cyclopropan-1-amine (112) A solution of **111** (100 mg, 0.487 mmol), *rel-trans*-2-(4-chlorophenyl)cyclopropan-1-amine (123 mg, 0.731 mmol) and cat. AcOH, in DCE (10 mL), was stirred for 1 h at RT. STAB (155 mg, 0.731 mmol) was added, then the mixture was stirred at RT

for 1 h. The solution was diluted with 1% NH₄OH in MeOH, then evaporated under vacuum and purified by flash chromatography, eluting with 10% DMA, to yield the desired product (20 mg, 12% yield, yellow oil). ¹H NMR (400 MHz, CDCl₃) δ 8.58 (s, 1H), 7.64 (t, *J* = 8.1 Hz, 1H), 7.36 – 7.07 (m, 5H), 6.87 (d, *J* = 8.1 Hz, 1H), 3.80 (d, *J* = 11.7 Hz, 2H), 3.48 (s, 2H), 2.49 – 2.18 (m, 4H), 2.11 (s, 1H), 1.99 – 1.57 (m, 6H), 1.01 – 0.90 (m, 1H), 0.84 (d, *J* = 6.5 Hz, 1H). ¹³C NMR (101 MHz, CDCl₃) δ 171.19, 164.45, 149.05, 140.79, 136.22, 131.02, 128.60, 128.23, 127.10, 126.95, 121.17, 121.02, 64.62, 64.47, 64.44, 44.21, 42.95, 41.58, 41.26, 35.96, 35.84, 35.76, 35.70, 24.52, 17.04. Analytical HPLC: Phenomenex Gemini C18 4.6 x 50 mm, 3 μm; gradient 10%-80% ACN in water + 0.1% TFA; 45 min run; injection 20 μL (1 mg/mL); temperature 40°C; *t*_R 14.729 min, purity 92%. HRMS-MS/MS C₂₁H₂₅ClN₂O + H⁺ calculated 357.17282, found 357.17372.

4-(4-(2,3-Dichlorophenyl)piperazin-1-yl)-N-(2-(4-(pyridin-2-yl)tetrahydro-2H-pyran-4-yl)ethyl)butan-1-amine (113) The compound was prepared following the same procedure described for **112**, starting from **111** (87 mg, 0.42 mmol) and **42**⁸² (150 mg, 0.50 mmol). The crude material was purified by flash chromatography, eluting with 10% DMA, to yield the desired product (30 mg, 14% yield, hygroscopic solid/yellow oil). ¹H NMR (400 MHz, CD₃OD) δ 8.58 (d, *J* = 3.9 Hz, 1H), 7.82 (t, *J* = 8.7 Hz, 1H), 7.51 (d, *J* = 8.1 Hz, 1H), 7.31 – 7.21 (m, 3H), 7.12 (d, *J* = 9.4 Hz, 1H), 3.82 (d, *J* = 12.1 Hz, 2H), 3.46 (t, *J* = 9.5 Hz, 2H), 3.15 (br s, 4H), 2.92 (br s, 5H), 2.70 (m, 4H), 2.40 (d, *J* = 14.0 Hz, 2H), 2.13 (d, *J* = 17.2 Hz, 2H), 1.93 (m, 3H), 1.70 (br s, 4H). ¹³C NMR (101 MHz, CD₃OD) δ 162.57, 150.18, 148.94, 137.09, 133.58, 127.77, 127.07, 125.04, 121.69, 121.60, 118.99, 63.97, 56.46, 52.42, 49.38, 43.21, 40.70, 37.74, 34.97, 23.60, 21.93. Analytical HPLC: Phenomenex Gemini C18 4.6 x 50 mm, 3 μm; gradient 10%-80% ACN in water + 0.1% TFA; 30 min run; injection 20 μL (1 mg/mL); temperature 40°C; *t*_R 14.687 min, purity >95%. HRMS-MS/MS C₂₆H₃₆Cl₂N₄O + H⁺ calculated 491.23389, found 491.23363.

1-(2,3-Dichlorophenyl)-4-(2-(4-(pyridin-2-yl)tetrahydro-2H-pyran-4-yl)ethyl)piperazine

(114) The compound was prepared following the same procedure described for **112**, starting from **111** (100 mg, 0.487 mmol) and 1-(2,3-dichlorophenyl)piperazine (169 mg, 0.731 mmol). The crude material was purified by flash chromatography, eluting with 10% DMA, to yield the desired product (77 mg, 38% yield, off-white solid m.p. 108-111°C). ¹H NMR (400 MHz, CDCl₃) δ 8.61 (d, *J* = 4.4 Hz, 1H), 7.66 (t, *J* = 7.7 Hz, 1H), 7.29 (d, *J* = 8.2 Hz, 1H), 7.20 – 7.06 (m, 3H), 6.91 (d, *J* = 6.9 Hz, 1H), 3.82 (d, *J* = 11.7 Hz, 2H), 3.50 (t, *J* = 10.5 Hz, 2H), 2.98 (br s, 4H), 2.58 – 2.30 (m, 6H), 2.15 – 2.04 (m, 2H), 1.98 – 1.80 (m, 4H). ¹³C NMR (101 MHz, CDCl₃) δ 164.14, 151.00, 148.79, 135.90, 133.72, 127.15, 124.25, 120.94, 120.71, 118.26, 110.89, 64.43, 53.11, 52.90, 51.01, 40.95, 39.26, 35.63. Analytical HPLC: Phenomenex Gemini C18 4.6 x 50 mm, 3 μm; gradient 10%-80% ACN in water + 0.1% TFA; 30 min run; injection 20 μL (1 mg/mL); temperature 40°C; *R*_t 16.479 min, purity >99%. HRMS-MS/MS C₂₂H₂₇Cl₂N₃O + H⁺ calculated 420.16039, found 357.16085.

1-(2-(4-(Pyridin-2-yl)tetrahydro-2H-pyran-4-yl)ethyl)-4-(6-(trifluoromethyl)pyridin-2-yl)piperazine (115)

The compound was prepared following the same procedure described for **112**, starting from **111** (93 mg, 0.456 mmol) and 1-(6-(trifluoromethyl)pyridin-2-yl)piperazine (105 mg, 0.456 mmol). The crude material was purified by flash chromatography, eluting with 10% DMA, to yield the desired product (55 mg, 29% yield). ¹H NMR (400 MHz, CDCl₃) δ 8.60 (d, *J* = 4.8 Hz, 1H), 7.65 (t, *J* = 7.7 Hz, 1H), 7.53 (t, *J* = 7.9 Hz, 1H), 7.28 (d, *J* = 9.1 Hz, 1H), 7.16 – 7.09 (m, 1H), 6.90 (d, *J* = 7.2 Hz, 1H), 6.70 (d, *J* = 8.6 Hz, 1H), 3.82 (d, *J* = 11.6 Hz, 2H), 3.59 – 3.43 (m, 6H), 2.44 – 2.30 (m, 6H), 2.10 – 2.02 (m, 2H), 1.98 – 1.82 (m, 4H). The free base was converted to the oxalate salt, obtained as a white solid (m.p. 167-169°C). ¹³C NMR (101 MHz, d₆-DMSO) δ 163.20, 163.08, 157.86, 148.74, 144.58, 139.19, 136.60, 121.31, 121.19, 111.02, 109.32,

63.48, 51.69, 50.89, 42.43, 40.51, 36.00, 34.89. HRMS-MS/MS $C_{22}H_{27}F_3N_4O + H^+$ calculated 421.22097, found 421.22061. Elemental analysis ($C_{22}H_{27}F_3N_4O + H_2C_2O_4 + 0.5H_2O$) calculated C 55.49, H 5.82, N 10.78, found C 55.63, H 5.69, N 10.61

Methyl-2-cyano-2-(6-oxaspiro[4.5]decan-9-ylidene)acetate³⁶ (116) A solution of **86** (4.0 g, 26 mmol), methyl 2-cyanoacetate (3.1 g, 31 mmol), AcOH (0.30 mL, 5.2 mmol) and AcONH₄ (0.50 g, 6.5 mmol) in toluene (35 mL), was stirred at reflux, in presence of molecular sieves (3Å), under argon atmosphere, overnight. The reaction was cooled to RT, the mixture was filtered, diluted with EtOAc and washed with water. The organic phase was dried over Na₂SO₄, filtered, and evaporated under vacuum. The residue was purified by flash chromatography, eluting with 30% EtOAc in hexanes, to yield the desired product (2.8 g, 46% yield). ¹H NMR (400 MHz, CDCl₃) δ 3.92 – 3.75 (s + m, 3H + 2H), 3.19 – 3.10 (m, 2H), 2.81 – 2.70 (m, 2H), 1.91 – 1.49 (m, 8H).

Methyl 2-cyano-2-(9-(pyridin-2-yl)-6-oxaspiro[4.5]decan-9-yl)acetate (117) 2-Bromopyridine (2.90 g, 18.4 mmol) was dissolved in anhydrous THF (30 mL) and cooled to 0°C. Isopropyl magnesium chloride (9.18 mL, 2M in THF, 18.4 mmol) was added drop-wise and stirred for 2.5 h. CuI (1.40 g, 7.34 mmol) was added and stirred at RT for 30 min. A solution of **116** (1.44 g, 6.12 mmol) in THF (20 mL) was added dropwise, and the mixture was stirred at RT for 16 h. The reaction was quenched with sat. aq. NH₄Cl. The aqueous layer was extracted with EtOAc. The combined organic layer was dried over NaSO₄, filtered, and evaporated under vacuum. The crude material was purified by flash chromatography, eluting with 50% EtOAc in hexanes, to yield the desired product (0.66 g, 34% yield). GC/MS ^tR 11.668 min, m/z 313.1 (-H⁺). ¹H NMR (400 MHz, CDCl₃) δ 8.61 (s, 1H), 7.72 (d, *J* = 8.6 Hz, 1H), 7.43 (dd, *J* = 45.3, 8.4 Hz, 1H; isomers), 7.23 (d, *J* = 7.6 Hz, 1H), 3.94 – 3.67 (m, 3H), 3.64 and 3.52 (2 x s, 3H; isomers), 2.71 (d, *J* = 14.2 Hz, 1H),

2.66 – 2.55 (m, 1H), 2.28 (d, $J = 14.0$ Hz, 1H), 2.11 (d, $J = 13.1$ Hz, 1H), 1.88 – 1.35 (m, 7H), 0.64 (2 x m, 1H; isomers).

2-(9-(Pyridin-2-yl)-6-oxaspiro[4.5]decan-9-yl)acetonitrile (118) A solution of **117** (650 mg, 2.07 mmol) and KOH (232 mg, 4.13 mmol) in ethylene glycol (5 mL) was stirred at 120°C for 24 h. The reaction was diluted with water, and the aqueous layer was extracted with EtOAc. The combined organic layer was dried with NaSO₄, filtered, and evaporated under vacuum. The crude material was purified by flash chromatography, eluting with 20% EtOAc in hexanes, to yield the desired product (480 mg, 90% yield). GC/MS R_t 10.648 min, m/z 255.1 ($-H^+$). ¹H NMR (400 MHz, CDCl₃) δ 8.61 (d, $J = 4.7$ Hz, 1H), 7.72 (td, $J = 7.8, 1.8$ Hz, 1H), 7.40 (d, $J = 8.0$ Hz, 1H), 7.23 – 7.16 (m, 1H), 4.23 – 4.20 (m, 2H), 2.80 (d, $J = 16.5$ Hz, 1H), 2.61 (d, $J = 16.5$ Hz, 1H), 2.50 (t, $J = 15.3$ Hz, 2H), 1.86 – 1.38 (m, 9H), 0.83 – 0.75 (m, 1H).

2-(9-(Pyridin-2-yl)-6-oxaspiro[4.5]decan-9-yl)ethan-1-ol (120) Nitrile **118** (250 mg, 0.98 mmol) was dissolved in ethylene glycol (4 mL), followed by addition of KOH (821 mg, 14.6 mmol). The mixture was heated to 110°C and stirred for 48 h. The reaction mixture was diluted with 2N HCl until the pH was ~6-7, extracted with DCM:2-PrOH (3:1), dried over NaSO₄, filtered, and the organic layer was evaporated under vacuum. The carboxylic acid intermediate **119** was dissolved in THF (10 mL), and BH₃-methyl sulfide complex (277 μ L, 2.93 mmol) was added dropwise to the stirring solution at 0°C. After reaching RT, the reaction was stirred overnight. The reaction was quenched with 2N aq. HCl (1 mL) and stirred for 1 h. 2N aq. NaOH was added until basic pH (~8-9). The desired product was extracted from the mixture with EtOAc and partially

purified by flash chromatography, eluting with 10% MeOH in DCM (36 mg, 14% yield). The crude was used in the following step without further purification.

rel-*trans*-2-(4-Chlorophenyl)-N-(2-(9-(pyridin-2-yl)-6-oxaspiro[4.5]decan-9-yl)ethyl)cyclopropan-1-amine (121) Alcohol **120** (20 mg, 0.077 mmol) was dissolved in DCM (10 mL), followed by portion-wise addition of DMP (32 mg, 0.077 mmol) at 0°C. The reaction was allowed to warm to RT and stirred for additional 1 h. The mixture was washed with sat. aq. NaHCO₃. The organic phase was dried over Na₂SO₄, filtered, and evaporated under vacuum to yield the crude aldehyde intermediate, which was immediately dissolved in DCE (10 mL), in presence of cat. AcOH (2 drops) and rel-*trans*-2-(4-chlorophenyl)cyclopropan-1-amine (13 mg, 0.077 mmol). The mixture was stirred for 1 h, then STAB (24 mg, 0.11 mmol) was added portion-wise. The reaction was stirred overnight at RT. The solvent was evaporated under vacuum, and the desired product was isolated by C18 preparative HPLC as TFA salt (Phenomenex Gemini NX-C18 110 Å, AXIA Packed, 150 x 30 mm, 5 µm; gradient 10%-80% ACN in water + 0.1% TFA; 60 min run; injection 4mL (~10-15 mg/mL); temperature 25°C; DAD λ₂₁₄ nm and λ₂₅₄ nm) (9.2 mg, 29% yield over 2 steps, hygroscopic solid/off-white oil). Analytical HPLC: Phenomenex Gemini C18 4.6 x 50 mm, 3 µm; gradient 10%-80% ACN in water + 0.1% TFA; 35 min run; injection 20 µL (1 mg/mL); temperature 40°C; ^tR 17.279 min, purity >95%. HRMS-MS/MS C₂₅H₃₁ClN₂O + H⁺ calculated 411.21977, found 411.21931.

Alternatively, adapted from the patent literature,^{73, 75} **118** (375 mg, 1.46 mmol) was dissolved in toluene (10 mL), at -78°C, followed by dropwise addition of DIBAL-H (1.76 mL, 1M in toluene, 1.76 mmol). The mixture was allowed to reach RT, and it was stirred for 1.5 h. The reaction was quenched with addition of MeOH (1 mL) and sat. aq. Na₂SO₄ (1 mL). The suspension was filtered,

the filtrate was concentrated under vacuum, the residue was suspended with sat. aq. NH_4Cl and extracted with DCM. The organic phase was dried over Na_2SO_4 , filtered, and evaporated under vacuum to yield the crude aldehyde intermediate which was immediately dissolved in DCE (12 mL), and reacted with *rel-trans*-2-(4-chlorophenyl)cyclopropan-1-amine as described above. The crude material was purified by flash chromatography (10% DMA), followed by C-18 preparative HPLC, using the method reported above, to obtain the desired product as TFA salt (46 mg, 8% yield over 2 steps, hygroscopic solid/off-white oil). Analytical HPLC: Phenomenex Gemini C18 4.6 x 50 mm, 3 μm ; gradient 10%-80% ACN in water + 0.1% TFA; 35 min run; injection 20 μL (1 mg/mL); temperature 40°C; t_R 17.244 min, purity >99%. The diastereomeric ratio (%dr) was determined by chiral HPLC (Chiralpak AD-H 4.6 x 250 mm, 5 μm ; 10% 2-PrOH in n-hexane; 60 min run; injection 20 μL (1 mg/mL); temperature 40°C; t_R 8.342, 8.780, 10.365, 13.550 min, purity >99%; dr 1:1:1:1). HRMS-MS/MS $\text{C}_{25}\text{H}_{31}\text{ClN}_2\text{O} + \text{H}^+$ calculated 411.21977, found 411.21920; ^1H NMR (400 MHz, CDCl_3) δ 8.68 (br s, 1H), 8.33 (br s, 1H), 7.80 (m, 2H), 7.23 (br s, 2H), 6.95 (m, 2H), 3.78 (m, 2H), 3.16 (br s, 1H), 2.69 – 2.21 (m, 7H), 2.08 (br s, 1H), 1.87 (m, 2H), 1.56 (m, 6H), 1.21 (m, 2H), 0.83 (m, 1H). ^{13}C NMR (101 MHz, CDCl_3) δ 160.53, 160.48, 144.71, 144.25, 136.16, 136.13, 132.94, 132.93, 128.83, 127.79, 127.73, 124.99, 124.75, 82.36, 57.76, 44.65, 44.37, 43.73, 41.20, 39.09, 39.00, 37.96, 37.92, 37.28, 35.91, 35.81, 32.35, 32.14, 23.54, 23.51, 22.84, 20.75, 20.69, 13.08, 12.99.

1-(2-(9-(Pyridin-2-yl)-6-oxaspiro[4.5]decan-9-yl)ethyl)-4-(6-(trifluoromethyl)pyridin-2-yl)piperazine (122) Adapted from the patent literature,^{73, 75} DIBAL-H (1.17 mL, 1M in toluene, 1.17 mmol) was added dropwise to a stirring solution of **118** (250 mg, 0.975 mmol) in toluene (10 mL), at -78°C. The mixture was allowed to reach RT, and it was stirred for additional 1.5 h. The reaction was quenched with addition of MeOH (1 mL) and sat. aq. Na_2SO_4 (1 mL). The suspension

was filtered, the filtrate was concentrated under vacuum, the residue was suspended with sat. aq. NH_4Cl and extracted with DCM. The organic phase was dried over Na_2SO_4 , filtered, and evaporated under vacuum to yield the crude aldehyde intermediate which was immediately dissolved in DCE (12 mL), in presence of cat. AcOH (2 drops) and 1-(6-(trifluoromethyl)pyridin-2-yl)piperazine (271 mg, 1.17 mmol). The mixture was stirred for 1 h, then STAB (248 mg, 1.17 mmol) was added portion-wise. The reaction was stirred overnight at RT. The reaction was diluted with 1% NH_4OH in MeOH, the solvent was evaporated under vacuum, and the desired product was isolated by flash chromatography eluting with 10% MeOH in DCM (130 mg, 28% yield, colorless oil). ^1H NMR (400 MHz, CDCl_3) δ 8.59 (d, $J = 4.6$ Hz, 1H), 7.64 (t, $J = 7.8$ Hz, 1H), 7.54 (t, $J = 8.1$ Hz, 1H), 7.31 (d, $J = 8.0$ Hz, 1H), 7.18 – 7.09 (m, 1H), 6.92 (d, $J = 7.3$ Hz, 1H), 6.71 (d, $J = 8.8$ Hz, 1H), 3.78 (d, $J = 7.5$ Hz, 2H), 3.55 (br s, 4H), 2.53 – 2.26 (m, 7H), 2.04 (s, 1H), 1.94 (d, $J = 13.8$ Hz, 1H), 1.65 – 1.33 (m, 9H), 1.12 (s, 1H), 0.70 (m, 1H). ^{13}C NMR (101 MHz, CDCl_3) δ 174.67, 164.51, 158.65, 148.84, 146.93, 146.59, 146.25, 138.25, 136.03, 122.95, 121.24, 121.02, 120.22, 109.37, 108.95, 108.92, 83.02, 59.36, 53.41, 53.01, 52.48, 45.79, 44.26, 41.31, 40.84, 34.22, 33.31, 24.02, 22.53, 21.05. Analytical HPLC: Phenomenex Gemini C18 4.6 x 50 mm, 3 μm ; gradient 10%-80% ACN in water + 0.1% TFA; 35 min run; injection 20 μL (1 mg/mL); temperature 40°C; t_R 17.402 min, purity >99%. HRMS-MS/MS $\text{C}_{26}\text{H}_{33}\text{F}_3\text{N}_4\text{O} + \text{H}^+$ calculated 475.26792, found 475.26716

Radioligand Binding Studies

hD₂R and hD₃R. Radioligand binding assays were conducted similarly as previously described.⁴⁷ HEK293 cells stably expressing human D₂L_R or D₃R were grown in a 50:50 mix of DMEM and Ham's F12 culture media, supplemented with 20 mM HEPES, 2 mM L-glutamine, 0.1 mM non-

essential amino acids, 1X antibiotic/antimycotic, 10% heat-inactivated fetal bovine serum, and 200 µg/mL hygromycin (Life Technologies, Grand Island, NY) and kept in an incubator at 37°C and 5% CO₂. Upon reaching 80–90% confluence, cells were harvested using premixed Earle's balanced salt solution with 5 mM EDTA (Life Technologies) and centrifuged at 3000 rpm for 10 min at 21°C. The supernatant was removed, and the pellet was resuspended in 10 mL hypotonic lysis buffer (5 mM MgCl₂, 5 mM Tris, pH 7.4 at 4°C) and centrifuged at 14 500 rpm (~25000g) for 30 min at 4°C. The pellet was then resuspended in binding buffer. Bradford protein assay (Bio-Rad, Hercules, CA) was used to determine the protein concentration. For [³H]-*N*-methylspiperone binding studies membranes were diluted to 500 µg/mL, in fresh EBSS binding buffer made from 8.7 g/L Earle's Balanced Salts without phenol red (US Biological, Salem, MA), 2.2 g/L sodium bicarbonate, pH to 7.4, and stored in a -80 °C freezer for later use. On the test day, each test compound was diluted into half-log serial dilutions using the 30% dimethyl sulfoxide (DMSO) vehicle. When it was necessary to assist solubilization of the drugs at the highest tested final concentration of 100 µM or 10 µM, 0.1% or 0.01% AcOH (final concentration v/v) was added alongside the vehicle, respectively. Membranes were diluted in fresh binding buffer. Radioligand competition experiments were conducted in 96-well plates containing 300 µL fresh binding buffer, 50 µL of the diluted test compound, 100 µL of membranes (for [³H]-*N*-methylspiperone assays: 10–20 µg/well total protein for both hD_{2L}R and hD₃R), and 50 µL of radioligand diluted in binding buffer ([³H]-*N*-methylspiperone: 0.4 nM final concentration for all the hD₂-like receptor subtypes; Novandi Chemistry AB). Aliquots of radioligands solution were also quantified accurately in each experiment replicate, to determine how much radioactivity was added, taking in account the experimentally determined counter efficiency. Nonspecific binding was determined using 10 µM (+)-butaclamol (Sigma-Aldrich, St. Louis, MO), and total binding was determined with the 30%

DMSO vehicle (3% final concentration). All compound dilutions were tested in triplicate, and the reaction incubated for 60 min at RT. The reaction was terminated by filtration through PerkinElmer Uni-Filter-96 GF/C, presoaked for the incubation time in 0.5% polyethylenimine, using a Brandel 96-Well Plates Harvester Manifold (Brandel Instruments, Gaithersburg, MD). The filters were washed thrice with 3 mL (3 times ~1 mL/well) of ice-cold binding buffer. PerkinElmer MicroScint 20 Scintillation Cocktail (65 μ L) was added to each well, and filters were counted using a PerkinElmer MicroBeta Microplate Counter. IC₅₀ values for each compound were determined from dose–response curves, and K_i values were calculated using the Cheng–Prusoff equation. K_d values were determined via separate homologous competitive binding experiments. When a complete inhibition could not be achieved at the highest tested concentrations, K_i values have been extrapolated by constraining the bottom of the dose–response curves (=0% residual specific binding) in the nonlinear regression analysis. These analyses were performed using GraphPad Prism version 9 for Macintosh (GraphPad Software, San Diego, CA). All results were rounded to the third significant figure. K_i values were determined from at least three independent experiments and are reported as the mean \pm standard error of the mean (SEM).

hMOR. Radioligand binding experiments were conducted, and the results analyzed, as described above, and similarly as previously reported.^{47, 84} HEK293 cells stably expressing hMOR were grown in a DMEM medium, supplemented with 10% FBS, 2 mM L-glutamine, 1% penicillin-streptomycin (or antibiotic/antimycotic) and hygromycin B (50 μ g/mL). Upon reaching confluence the cells were harvested and the membranes prepared as detailed before. The binding buffer was made of 50 mM Tris and 5 mM MgCl₂ at pH 7.4. The experiments were performed in presence of [³H]-DAMGO (final concentration 3 nM; Novandi Chemistry AB) and ~30 μ g/well of membranes (final concentration). The reactions were incubated for 60 min at RT and terminated by rapid

filtration through Perkin Elmer Uni-Filter-96 GF/C, presoaked for 60 min in 0.5% polyethylenimine. The non-specific binding was determined using 10 μ M Naloxone. The radioligand K_d was measured via radioligand saturation experiments.

Bioluminescence Resonance Energy Transfer (BRET) Studies

Unless otherwise stated, reagents were purchased from Sigma Aldrich-Merck. Experiments were performed in human embryonic kidney 293 T (HEK 293T) cells, transiently transfected with a range of BRET sensors as described previously.^{85, 86} Briefly, cells were cultured at 37 °C, 5 % CO₂ in Dulbecco's modified eagle medium (DMEM) supplemented with 10 % (v/v) fetal bovine serum (FBS). Cells were seeded in 10 cm Petri dishes (3 x 10⁶ cells per dish) and allowed to grow overnight in full media at 37 °C, 5 % CO₂. Cells were transiently transfected the next day, in media supplemented with antibiotics (100 U/mL penicillin and 100 μ g/mL streptomycin, Gibco) using a 1:6 total DNA to PEI (PolySciences Inc) ratio. BRET constructs were as follows: 4 μ g of Nb33-Venus and 1 μ g of mMOR-Rluc8 for Nb33 recruitment, 4 μ g of arrestin-3-Venus, 2 μ g of WT-GRK2 and 1 μ g of mMOR-Rluc8 for arrestin-3 recruitment and 2 μ g of WT-G α (i2 or oA), 1 μ g of G β 1-Venus(156-239), 1 μ g of G γ 2-Venus(1-155), 1 μ g of masGRK3ct-Rluc8 and 1 μ g of receptor (SNAP-mMOR or hD₃R) for GPA⁸⁷ assays. The following day, cells were plated in Greiner poly-D-lysine-coated, white bottom 96-well plates (SLS) in full media. On the day of the assay (48h post-transfection), cells were washed once with D-PBS (Lonza, SLS) and incubated in D-PBS for 30 min at 37 °C. The Rluc substrate coelenterazine h (NanoLight) was added to each well (final concentration of 5 μ M) and ligands (final concentration from 10 μ M to 0.01 nM in D-PBS) were added to the wells before reading the plate at 37 °C in a PHERAstar FSX microplate reader (Venus and Rluc emission signals at 535 and 475 nm, respectively, BMG Labtech) every

minute for 10 min, with an additional 30 min read at the end of the assay. For the D₃R antagonist-mode of the GPA assay, a final concentration of 3 nM of quinpirole was added to the wells just after compound addition, to induce a 50 % response that can then be inhibited by D₃R antagonists or weak partial agonists. The ratio between Venus fluorescence and Rluc luminescence was used to quantify the BRET signal in each well. Data were normalized to maximal and minimal response of DAMGO or quinpirole for MOR or D₃R, respectively. All data points represent the mean of at least three independent experiments performed in duplicate. Error bars represent the standard error of the mean (SEM) and data points were fitted using the built-in log(agonist) vs. response (three parameters) model in Prism 9.0 (GraphPad software Inc., San Diego, CA). For the antagonist-mode assays, data points were fitted using the built-in log(antagonist) vs. response (three parameters) model.

Molecular Docking and Computer Aided Drug Design

The inactive-state cryoEM structure of dopamine D₃ (PDBID: 3PBL) were obtained from RCSB representing an antagonist-bound state. All objects except the receptor protein subunit and the crystallized ligand were deleted. The protein was prepared by adding and optimizing hydrogen atoms and the side-chain residues.

The active-state X-ray structure of MOR (PDBID: 5C1M) was accessed from RCSB representing an agonist-bound state. All objects except three crystallographic water molecules (wa* 8, 25, and 46) were deleted. The protein was prepared by adding and optimizing hydrogen atoms and the side-chain residues.

Before performing molecular docking, ligands were conceptualized with chiral definitions, given formal charges, and their energies were optimized. All-atom docking was carried out using the

energy-minimized structures for all ligands with an effort value of 10, and the ligand docking box for possible grid docking was selected to encompass the extracellular half of the protein.

A variety of rigid-protein docking combinations were used while docking into the inactive-state D₃R and active-state MOR receptors. In addition, side chain flexible combinations including D149^{3,32} residue in MOR have been tested. The top-scoring docking solutions from these docking experiments were further improved using successive rounds of minimization and Monte Carlo sampling of the ligand conformation, which included sidechain residues close to the ligand (within 5 Å) in the D₃R and MOR orthosteric sites. All the above-mentioned molecular modeling operations were performed in the ICM-Pro v3.9-2b molecular modeling and drug discovery suite (Molsoft LLC).

ASSOCIATED CONTENT

Supporting Information

The supporting information is available free of charge [on the ACS Publications website](#): Molecular formula strings (CSV), PDB files of the docking studies, physicochemical parameters and CNS-MPO scores, analytical data summary (combustion elemental analyses), HPLC chromatograms, HRMS-MS/MS reports, and ¹H-¹³C NMR spectra.

Author Contributions

A.B. and A.H.N. designed the project; A.B., E.S. and A.H.N. wrote the manuscript with input of all the authors; A.B., E.S., J.S., A.L.N., V.K., M.C., J.R.L and A.H.N., designed experiments and data analysis; A.B., E.S., J.S., A.L.N., S.A.Z. and K.J. performed experiments.

Corresponding Authors Information:

Amy Hauck Newman: anewman@intra.nida.nih.gov

Alessandro Bonifazi: alessandro.bonifazi2@nih.gov

Formatted: Font: Bold

Formatted: Underline

Formatted: Underline

Notes

The authors declare no competing financial interest. Original TOC graphic has been created by the authors adapting templates from BioRender.com, under a premium license.

ACKNOWLEDGMENTS

This project was supported by the National Institute on Drug Abuse – Intramural Research Program (ZIADA000609; ZIADA000424), as well as grant funding for V.K., M.C. and J.R.L (BB/T013966/1 and AMSPR\1013). The Royal Society International Exchanges award (IES\R3\203125) supported a short-term visit at NIDA-IRP for JS. The authors thank Jian-Jing Cao (NIDA-IRP Medicinal Chemistry Section) for the CNS-MPO score calculations, Dr. Shelley Jackson (NIDA-IRP Translational Analytical Core (TAC)) for high-resolution mass spectrometry (HRMS-MS/MS) analyses, Dr. Ning Sheng Cai (NIDA-IRP Integrative Neurobiology Section) for assistance with cell lines and tissue culture protocols, and Dr. Caleb Vogt (NIDA-IRP Medicinal Chemistry Section) for constructive edits to the paper.

ABBREVIATIONS

ACN, acetonitrile; AcOH, acetic acid; β arr, β -arrestin; BBB, blood-brain barrier; BRET, bioluminescence resonance energy transfer; CADD, computer-aided drug design; CNS-MPO, central nervous system-multi-parameter optimization; DA, dopamine; D₂-likeR, dopamine D₂-like receptors; DIBAL-H, diisobutylaluminium hydride; DIPEA, *N,N*-diisopropylethylamine; -DMA, dichloromethane, methanol, and ammonium hydroxide; DMP, Dess–Martin periodinane; EDC, 1-ethyl-3-(3-dimethylaminopropyl)carbodiimide; GPA, G-protein activation; HEK293 cells, human embryonic kidney 293 cells; HOBt, hydroxybenzotriazole; HPLC, high performance liquid chromatography; HRMS, high-resolution mass spectrometry; LAH, lithium aluminum hydride; MOR, μ -opioid receptor; OIH, opioid induced hyperalgesia, OUD, opioid use disorders; ~~CADD, computer-aided drug design; BRET, bioluminescence resonance energy transfer; BBB, blood-brain barrier; CNS MPO, central nervous system multi parameter optimization; OIH, opioid induced hyperalgesia, HEK293 cells, human embryonic kidney 293 cells; HPLC, high performance liquid chromatography; HRMS, high resolution mass spectrometry; DMA, dichloromethane, methanol, and ammonium hydroxide; EDC, 1-ethyl-3-(3-dimethylaminopropyl)carbodiimide; HOBt, hydroxybenzotriazole; DIPEA, *N,N*-diisopropylethylamine; STAB, sodium triacetoxyborohydride; TBAF, tetra-*n*-butylammonium fluoride; TBDMSCl, *tert*-butylchlorodimethylsilane; DMP, Dess–Martin periodinane; ACN, acetonitrile; LAH, lithium aluminum hydride; DIBAL-H, diisobutylaluminium hydride; TFA, trifluoroacetic acid; AcOH, acetic acid; TBAF, tetra-*n*-butylammonium fluoride; TBDMSCl, *tert*-butylchlorodimethylsilane; THP, tetrahydropyran; PDB, protein data bank; β arr, β -arrestin; GPA, G-protein activation.~~

Formatted: Font: Italic

Formatted: Font: Italic

REFERENCES

- (1) *Wide-ranging online data for epidemiologic research (WONDER)*; CDC, National Center for Health Statistics, 2020.
- (2) Mattson, C. L.; Tanz, L. J.; Quinn, K.; Kariisa, M.; Patel, P.; Davis, N. L. Trends and Geographic Patterns in Drug and Synthetic Opioid Overdose Deaths - United States, 2013-2019. *MMWR Morb Mortal Wkly Rep* **2021**, 70 (6), 202-207.
- (3) *2017 National Survey on Drug Use and Health: Detailed Tables*; Center for Behavioral Health Statistics and Quality (CBHSQ), 2018.
- (4) Muhuri, P. K.; Gfroerer, J. C.; Davies, M. C. *Associations of Nonmedical Pain Reliever Use and Initiation of Heroin Use in the United States*; CBHSQ Data Rev., 2013.

- (5) Cicero, T. J.; Ellis, M. S.; Surratt, H. L.; Kurtz, S. P. The changing face of heroin use in the United States: a retrospective analysis of the past 50 years. *JAMA Psychiatry* **2014**, *71* (7), 821-826.
- (6) Carlson, R. G.; Nahhas, R. W.; Martins, S. S.; Daniulaityte, R. Predictors of transition to heroin use among initially non-opioid dependent illicit pharmaceutical opioid users: A natural history study. *Drug Alcohol Depend* **2016**, *160*, 127-134.
- (7) Shafi, A.; Berry, A. J.; Sumnall, H.; Wood, D. M.; Tracy, D. K. Synthetic opioids: a review and clinical update. *Ther Adv Psychopharmacol* **2022**, *12*, 20451253221139616.
- (8) Rasmussen, K.; White, D. A.; Acri, J. B. NIDA's medication development priorities in response to the Opioid Crisis: ten most wanted. *Neuropsychopharmacology* **2019**, *44* (4), 657-659.
- (9) Galaj, E.; Newman, A. H.; Xi, Z. X. Dopamine D3 receptor-based medication development for the treatment of opioid use disorder: Rationale, progress, and challenges. *Neurosci Biobehav Rev* **2020**, *114*, 38-52.
- (10) Newman, A. H.; Ku, T.; Jordan, C. J.; Bonifazi, A.; Xi, Z. X. New Drugs, Old Targets: Tweaking the Dopamine System to Treat Psychostimulant Use Disorders. *Annu Rev Pharmacol Toxicol* **2021**, *61*, 609-628.
- (11) Jordan, C. J.; Humburg, B.; Rice, M.; Bi, G. H.; You, Z. B.; Shaik, A. B.; Cao, J.; Bonifazi, A.; Gadiano, A.; Rais, R.; et al. The highly selective dopamine D(3)R antagonist, R-VK4-40 attenuates oxycodone reward and augments analgesia in rodents. *Neuropharmacology* **2019**, *158*, 107597.
- (12) Jordan, C. J.; Humburg, B. A.; Thorndike, E. B.; Shaik, A. B.; Xi, Z. X.; Baumann, M. H.; Newman, A. H.; Schindler, C. W. Newly Developed Dopamine D(3) Receptor Antagonists, R-

VK4-40 and R-VK4-116, Do Not Potentiate Cardiovascular Effects of Cocaine or Oxycodone in Rats. *J Pharmacol Exp Ther* **2019**, *371* (3), 602-614.

(13) Newman, A. H.; Xi, Z. X.; Heidbreder, C. Current Perspectives on Selective Dopamine D(3) Receptor Antagonists/Partial Agonists as Pharmacotherapeutics for Opioid and Psychostimulant Use Disorders. *Curr Top Behav Neurosci* **2023**, *60*, 157-201.

(14) You, Z. B.; Bi, G. H.; Galaj, E.; Kumar, V.; Cao, J.; Gadiano, A.; Rais, R.; Slusher, B. S.; Gardner, E. L.; Xi, Z. X.; et al. Dopamine D(3)R antagonist VK4-116 attenuates oxycodone self-administration and reinstatement without compromising its antinociceptive effects. *Neuropsychopharmacology* **2019**, *44* (8), 1415-1424.

(15) de Guglielmo, G.; Kallupi, M.; Sedighim, S.; Newman, A. H.; George, O. Dopamine D(3) Receptor Antagonism Reverses the Escalation of Oxycodone Self-administration and Decreases Withdrawal-Induced Hyperalgesia and Irritability-Like Behavior in Oxycodone-Dependent Heterogeneous Stock Rats. *Front Behav Neurosci* **2019**, *13*, 292.

(16) Botz-Zapp, C. A.; Foster, S. L.; Pulley, D. M.; Hempel, B.; Bi, G. H.; Xi, Z. X.; Newman, A. H.; Weinshenker, D.; Manvich, D. F. Effects of the selective dopamine D(3) receptor antagonist PG01037 on morphine-induced hyperactivity and antinociception in mice. *Behav Brain Res* **2021**, *415*, 113506.

(17) Miyamoto, S.; Miyake, N.; Jarskog, L. F.; Fleischacker, W. W.; Lieberman, J. A. Pharmacological treatment of schizophrenia: a critical review of the pharmacology and clinical effects of current and future therapeutic agents. *Mol Psychiatry* **2012**, *17* (12), 1206-1227.

(18) Ballon, J. S.; Pajvani, U.; Freyberg, Z.; Leibel, R. L.; Lieberman, J. A. Molecular pathophysiology of metabolic effects of antipsychotic medications. *Trends Endocrinol Metab* **2014**, *25* (11), 593-600.

- (19) Farino, Z. J.; Morgenstern, T. J.; Maffei, A.; Quick, M.; De Solis, A. J.; Wiriyasermkul, P.; Freyberg, R. J.; Aslanoglou, D.; Sorisio, D.; Inbar, B. P.; et al. New roles for dopamine D(2) and D(3) receptors in pancreatic beta cell insulin secretion. *Mol Psychiatry* **2020**, *25* (9), 2070-2085.
- (20) Meltzer, H. Y. Update on typical and atypical antipsychotic drugs. *Annu Rev Med* **2013**, *64*, 393-406.
- (21) Ehrlich, A. T.; Kieffer, B. L.; Darcq, E. Current strategies toward safer mu opioid receptor drugs for pain management. *Expert Opin Ther Targets* **2019**, *23* (4), 315-326.
- (22) Raehal, K. M.; Walker, J. K.; Bohn, L. M. Morphine side effects in beta-arrestin 2 knockout mice. *J Pharmacol Exp Ther* **2005**, *314* (3), 1195-1201.
- (23) Kliewer, A.; Schmiedel, F.; Sianati, S.; Bailey, A.; Bateman, J. T.; Levitt, E. S.; Williams, J. T.; Christie, M. J.; Schulz, S. Phosphorylation-deficient G-protein-biased mu-opioid receptors improve analgesia and diminish tolerance but worsen opioid side effects. *Nat Commun* **2019**, *10* (1), 367.
- (24) Azevedo Neto, J.; Costanzini, A.; De Giorgio, R.; Lambert, D. G.; Ruzza, C.; Calo, G. Biased versus Partial Agonism in the Search for Safer Opioid Analgesics. *Molecules* **2020**, *25* (17).
- (25) Kliewer, A.; Gillis, A.; Hill, R.; Schmiedel, F.; Bailey, C.; Kelly, E.; Henderson, G.; Christie, M. J.; Schulz, S. Morphine-induced respiratory depression is independent of beta-arrestin2 signalling. *Br J Pharmacol* **2020**, *177* (13), 2923-2931.
- (26) Bachmutsky, I.; Wei, X. P.; Durand, A.; Yackle, K. ss-arrestin 2 germline knockout does not attenuate opioid respiratory depression. *Elife* **2021**, *10*.
- (27) He, L.; Gooding, S. W.; Lewis, E.; Felth, L. C.; Gaur, A.; Whistler, J. L. Pharmacological and genetic manipulations at the micro-opioid receptor reveal arrestin-3 engagement limits analgesic

tolerance and does not exacerbate respiratory depression in mice. *Neuropsychopharmacology* **2021**, *46* (13), 2241-2249.

(28) Brzezinski, M.; Hammer, G. B.; Candiotti, K. A.; Bergese, S. D.; Pan, P. H.; Bourne, M. H.; Michalsky, C.; Wase, L.; Demitrack, M. A.; Habib, A. S. Low Incidence of Opioid-Induced Respiratory Depression Observed with Oliceridine Regardless of Age or Body Mass Index: Exploratory Analysis from a Phase 3 Open-Label Trial in Postsurgical Pain. *Pain Ther* **2021**, *10* (1), 457-473.

(29) Conibear, A. E.; Kelly, E. A Biased View of mu-Opioid Receptors? *Mol Pharmacol* **2019**, *96* (5), 542-549.

(30) Gillis, A.; Gondin, A. B.; Kliewer, A.; Sanchez, J.; Lim, H. D.; Alamein, C.; Manandhar, P.; Santiago, M.; Fritzwanker, S.; Schmiedel, F.; et al. Low intrinsic efficacy for G protein activation can explain the improved side effect profiles of new opioid agonists. *Sci Signal* **2020**, *13* (625).

(31) Gillis, A.; Kliewer, A.; Kelly, E.; Henderson, G.; Christie, M. J.; Schulz, S.; Canals, M. Critical Assessment of G Protein-Biased Agonism at the mu-Opioid Receptor. *Trends Pharmacol Sci* **2020**, *41* (12), 947-959.

(32) Benredjem, B.; Gallion, J.; Pelletier, D.; Dallaire, P.; Charbonneau, J.; Cawkill, D.; Nagi, K.; Gosink, M.; Lukashova, V.; Jenkinson, S.; et al. Exploring use of unsupervised clustering to associate signaling profiles of GPCR ligands to clinical response. *Nat Commun* **2019**, *10* (1), 4075.

(33) Pineyro, G.; Nagi, K. Signaling diversity of mu- and delta- opioid receptor ligands: Re-evaluating the benefits of beta-arrestin/G protein signaling bias. *Cell Signal* **2021**, *80*, 109906.

(34) DeWire, S. M.; Yamashita, D. S.; Rominger, D. H.; Liu, G.; Cowan, C. L.; Graczyk, T. M.; Chen, X. T.; Pitis, P. M.; Gotchev, D.; Yuan, C.; et al. A G protein-biased ligand at the mu-opioid

receptor is potently analgesic with reduced gastrointestinal and respiratory dysfunction compared with morphine. *J Pharmacol Exp Ther* **2013**, *344* (3), 708-717.

(35) Fossler, M. J.; Sadler, B. M.; Farrell, C.; Burt, D. A.; Pitsiu, M.; Skobieranda, F.; Soergel, D. G. Oliceridine (TRV130), a Novel G Protein-Biased Ligand at the mu-Opioid Receptor, Demonstrates a Predictable Relationship Between Plasma Concentrations and Pain Relief. I: Development of a Pharmacokinetic/Pharmacodynamic Model. *J Clin Pharmacol* **2018**, *58* (6), 750-761.

(36) Chen, X. T.; Pitis, P.; Liu, G.; Yuan, C.; Gotchev, D.; Cowan, C. L.; Rominger, D. H.; Koblisch, M.; Dewire, S. M.; Crombie, A. L.; et al. Structure-activity relationships and discovery of a G protein biased mu opioid receptor ligand, [(3-methoxythiophen-2-yl)methyl](2-[(9R)-9-(pyridin-2-yl)-6-oxaspiro[4.5]decan-9-yl]ethyl)amine (TRV130), for the treatment of acute severe pain. *J Med Chem* **2013**, *56* (20), 8019-8031.

(37) Manglik, A.; Lin, H.; Aryal, D. K.; McCorvy, J. D.; Dengler, D.; Corder, G.; Levit, A.; Kling, R. C.; Bernat, V.; Hubner, H.; et al. Structure-based discovery of opioid analgesics with reduced side effects. *Nature* **2016**, *537* (7619), 185-190.

(38) Hill, R.; Disney, A.; Conibear, A.; Sutcliffe, K.; Dewey, W.; Husbands, S.; Bailey, C.; Kelly, E.; Henderson, G. The novel mu-opioid receptor agonist PZM21 depresses respiration and induces tolerance to antinociception. *Br J Pharmacol* **2018**, *175* (13), 2653-2661.

(39) James, I. E.; Skobieranda, F.; Soergel, D. G.; Ramos, K. A.; Ruff, D.; Fossler, M. J. A First-in-Human Clinical Study With TRV734, an Orally Bioavailable G-Protein-Biased Ligand at the mu-Opioid Receptor. *Clin Pharmacol Drug Dev* **2020**, *9* (2), 256-266.

(40) Ramos, K. A.; James, I. E.; Skobieranda, F.; Soergel, D. G.; Ruff, D.; Fossler, M. J. Two-Part Phase 1 Multiple-Ascending-Dose Study to Evaluate the Safety, Tolerability, Pharmacodynamics,

and Pharmacokinetics of TRV734 in Healthy Adults. *Clin Pharmacol Drug Dev* **2022**, *11* (1), 51-62.

(41) Mercadante, S.; Arcuri, E.; Santoni, A. Opioid-Induced Tolerance and Hyperalgesia. *CNS Drugs* **2019**, *33* (10), 943-955.

(42) Araldi, D.; Ferrari, L. F.; Levine, J. D. Mu-opioid Receptor (MOR) Biased Agonists Induce Biphasic Dose-dependent Hyperalgesia and Analgesia, and Hyperalgesic Priming in the Rat. *Neuroscience* **2018**, *394*, 60-71.

(43) Stein, C.; Clark, J. D.; Oh, U.; Vasko, M. R.; Wilcox, G. L.; Overland, A. C.; Vanderah, T. W.; Spencer, R. H. Peripheral mechanisms of pain and analgesia. *Brain Res Rev* **2009**, *60* (1), 90-113.

(44) Bruce, D. J.; Peterson, C. D.; Kitto, K. F.; Akgun, E.; Lazzaroni, S.; Portoghese, P. S.; Fairbanks, C. A.; Wilcox, G. L. Combination of a delta-opioid Receptor Agonist and Loperamide Produces Peripherally-mediated Analgesic Synergy in Mice. *Anesthesiology* **2019**, *131* (3), 649-663.

(45) DeHaven-Hudkins, D. L.; Cowan, A.; Cortes Burgos, L.; Daubert, J. D.; Cassel, J. A.; DeHaven, R. N.; Kehner, G. B.; Kumar, V. Antipruritic and antihyperalgesic actions of loperamide and analogs. *Life Sci* **2002**, *71* (23), 2787-2796.

(46) Spahn, V.; Del Vecchio, G.; Labuz, D.; Rodriguez-Gaztelumendi, A.; Massaly, N.; Temp, J.; Durmaz, V.; Sabri, P.; Reidelbach, M.; Machelska, H.; et al. A nontoxic pain killer designed by modeling of pathological receptor conformations. *Science* **2017**, *355* (6328), 966-969.

(47) Bonifazi, A.; Battiti, F. O.; Sanchez, J.; Zaidi, S. A.; Bow, E.; Makarova, M.; Cao, J.; Shaik, A. B.; Sulima, A.; Rice, K. C.; et al. Novel Dual-Target mu-Opioid Receptor and Dopamine D(3)

Receptor Ligands as Potential Nonaddictive Pharmacotherapeutics for Pain Management. *J Med Chem* **2021**, *64* (11), 7778-7808.

(48) Jordan, C. J.; He, Y.; Bi, G. H.; You, Z. B.; Cao, J.; Xi, Z. X.; Newman, A. H. (+/-)VK4-40, a novel dopamine D(3) receptor partial agonist, attenuates cocaine reward and relapse in rodents. *Br J Pharmacol* **2020**, *177* (20), 4796-4807.

(49) Newman, A. H.; Battiti, F. O.; Bonifazi, A. 2016 Philip S. Portoghese Medicinal Chemistry Lectureship: Designing Bivalent or Bitopic Molecules for G-Protein Coupled Receptors. The Whole Is Greater Than the Sum of Its Parts. *J Med Chem* **2020**, *63* (5), 1779-1797.

(50) Bonifazi, A.; Newman, A. H.; Keck, T. M.; Gervasoni, S.; Vistoli, G.; Del Bello, F.; Giorgioni, G.; Pavletic, P.; Quaglia, W.; Piergentili, A. Scaffold Hybridization Strategy Leads to the Discovery of Dopamine D(3) Receptor-Selective or Multitarget Bitopic Ligands Potentially Useful for Central Nervous System Disorders. *ACS Chem Neurosci* **2021**, *12* (19), 3638-3649.

(51) Wager, T. T.; Hou, X.; Verhoest, P. R.; Villalobos, A. Moving beyond rules: the development of a central nervous system multiparameter optimization (CNS MPO) approach to enable alignment of druglike properties. *ACS Chem Neurosci* **2010**, *1* (6), 435-449.

(52) Wager, T. T.; Chappie, T.; Horton, D.; Chandrasekaran, R. Y.; Samas, B.; Dunn-Sims, E. R.; Hsu, C.; Nawreen, N.; Vanase-Frawley, M. A.; O'Connor, R. E.; et al. Dopamine D3/D2 Receptor Antagonist PF-4363467 Attenuates Opioid Drug-Seeking Behavior without Concomitant D2 Side Effects. *ACS Chem Neurosci* **2017**, *8* (1), 165-177.

(53) Mugnaini, M.; Iavarone, L.; Cavallini, P.; Griffante, C.; Oliosi, B.; Savoia, C.; Beaver, J.; Rabiner, E. A.; Micheli, F.; Heidbreder, C.; et al. Occupancy of brain dopamine D3 receptors and drug craving: a translational approach. *Neuropsychopharmacology* **2013**, *38* (2), 302-312.

- (54) Takai, N.; Miyajima, N.; Tonomura, M.; Abe, K. Relationship between receptor occupancy and the antinociceptive effect of mu opioid receptor agonists in male rats. *Brain Res* **2018**, *1680*, 105-109.
- (55) Henriksen, G.; Willoch, F. Imaging of opioid receptors in the central nervous system. *Brain* **2008**, *131* (Pt 5), 1171-1196.
- (56) Kumar, V.; Banala, A. K.; Garcia, E. G.; Cao, J.; Keck, T. M.; Bonifazi, A.; Deschamps, J. R.; Newman, A. H. Chiral Resolution and Serendipitous Fluorination Reaction for the Selective Dopamine D3 Receptor Antagonist BAK2-66. *ACS Med Chem Lett* **2014**, *5* (6), 647-651.
- (57) Kumar, V.; Bonifazi, A.; Ellenberger, M. P.; Keck, T. M.; Pommier, E.; Rais, R.; Slusher, B. S.; Gardner, E.; You, Z. B.; Xi, Z. X.; et al. Highly Selective Dopamine D3 Receptor (D3R) Antagonists and Partial Agonists Based on Eticlopride and the D3R Crystal Structure: New Leads for Opioid Dependence Treatment. *J Med Chem* **2016**, *59* (16), 7634-7650.
- (58) de Paulis, T. Perospirone (Sumitomo Pharmaceuticals). *Curr Opin Investig Drugs* **2002**, *3* (1), 121-129.
- (59) Onrust, S. V.; McClellan, K. Perospirone. *CNS Drugs* **2001**, *15* (4), 329-337; discussion 338.
- (60) Yasui-Furukori, N.; Furukori, H.; Nakagami, T.; Saito, M.; Inoue, Y.; Kaneko, S.; Tateishi, T. Steady-state pharmacokinetics of a new antipsychotic agent perospirone and its active metabolite, and its relationship with prolactin response. *Ther Drug Monit* **2004**, *26* (4), 361-365.
- (61) Chen, J.; Levant, B.; Jiang, C.; Keck, T. M.; Newman, A. H.; Wang, S. Tranylcypromine substituted cis-hydroxycyclobutyl-naphthamides as potent and selective dopamine D(3) receptor antagonists. *J Med Chem* **2014**, *57* (11), 4962-4968.
- (62) Shaik, A. B.; Kumar, V.; Bonifazi, A.; Guerrero, A. M.; Cemaj, S. L.; Gadiano, A.; Lam, J.; Xi, Z. X.; Rais, R.; Slusher, B. S.; et al. Investigation of Novel Primary and Secondary

Pharmacophores and 3-Substitution in the Linking Chain of a Series of Highly Selective and Bitopic Dopamine D(3) Receptor Antagonists and Partial Agonists. *J Med Chem* **2019**, *62* (20), 9061-9077.

(63) Shaik, A. B.; Boateng, C. A.; Battiti, F. O.; Bonifazi, A.; Cao, J.; Chen, L.; Chitsazi, R.; Ravi, S.; Lee, K. H.; Shi, L.; et al. Structure Activity Relationships for a Series of Eticlopride-Based Dopamine D(2)/D(3) Receptor Bitopic Ligands. *J Med Chem* **2021**, *64* (20), 15313-15333.

(64) Battiti, F. O.; Zaidi, S. A.; Katritch, V.; Newman, A. H.; Bonifazi, A. Chiral Cyclic Aliphatic Linkers as Building Blocks for Selective Dopamine D(2) or D(3) Receptor Agonists. *J Med Chem* **2021**, *64* (21), 16088-16105.

(65) Desai, P. V.; Raub, T. J.; Blanco, M. J. How hydrogen bonds impact P-glycoprotein transport and permeability. *Bioorg Med Chem Lett* **2012**, *22* (21), 6540-6548.

(66) Wager, T. T.; Hou, X.; Verhoest, P. R.; Villalobos, A. Central Nervous System Multiparameter Optimization Desirability: Application in Drug Discovery. *ACS Chem Neurosci* **2016**, *7* (6), 767-775.

(67) Ghose, A. K.; Ott, G. R.; Hudkins, R. L. Technically Extended MultiParameter Optimization (TEMPO): An Advanced Robust Scoring Scheme To Calculate Central Nervous System Druggability and Monitor Lead Optimization. *ACS Chem Neurosci* **2017**, *8* (1), 147-154.

(68) Urbina, F.; Zorn, K. M.; Brunner, D.; Ekins, S. Comparing the Pfizer Central Nervous System Multiparameter Optimization Calculator and a BBB Machine Learning Model. *ACS Chem Neurosci* **2021**, *12* (12), 2247-2253.

(69) Newman, A. H.; Beuming, T.; Banala, A. K.; Donthamsetti, P.; Pongetti, K.; LaBounty, A.; Levy, B.; Cao, J.; Michino, M.; Luedtke, R. R.; et al. Molecular determinants of selectivity and efficacy at the dopamine D3 receptor. *J Med Chem* **2012**, *55* (15), 6689-6699.

- (70) Tan, L.; Zhou, Q.; Yan, W.; Sun, J.; Kozikowski, A. P.; Zhao, S.; Huang, X. P.; Cheng, J. Design and Synthesis of Bitopic 2-Phenylcyclopropylmethylamine (PCPMA) Derivatives as Selective Dopamine D3 Receptor Ligands. *J Med Chem* **2020**, *63* (9), 4579-4602.
- (71) Yan, W.; Fan, L.; Yu, J.; Liu, R.; Wang, H.; Tan, L.; Wang, S.; Cheng, J. 2-Phenylcyclopropylmethylamine Derivatives as Dopamine D(2) Receptor Partial Agonists: Design, Synthesis, and Biological Evaluation. *J Med Chem* **2021**, *64* (23), 17239-17258.
- (72) Wang, L.; Wang, L. Opioid Receptor (MOR) Agonist Salt, Fumarate Salt Crystal Form I Thereof And Preparation Method Thereof. US11,014,914B2, 2021.
- (73) Huang, C.; Cheng, C. Deuterated compounds for treating pain. WO 2018/006077 A1, 2018.
- (74) Li, X.; Feng, B.; Chen, Y.; Liu, T.; He, F.; He, M.; Tao, W.; Sun, P. Oxa Spiro Derivative, Preparation Method Therefor, And Applications Thereof In Medicines. US 2018/0297988 A1, 2018.
- (75) Huang, C.; Cheng, C. Deuterated Compounds For Treating Pain And Related Diseases And Conditions, And Compositions And Methods Thereof. US 2020/0330444 A1, 2020.
- (76) Pajouhesh, H.; Lenz, G. R. Medicinal chemical properties of successful central nervous system drugs. *NeuroRx* **2005**, *2* (4), 541-553.
- (77) Cheng, Y.; Prusoff, W. H. Relationship between the inhibition constant (K₁) and the concentration of inhibitor which causes 50 per cent inhibition (I₅₀) of an enzymatic reaction. *Biochem Pharmacol* **1973**, *22* (23), 3099-3108.
- (78) Chien, E. Y.; Liu, W.; Zhao, Q.; Katritch, V.; Han, G. W.; Hanson, M. A.; Shi, L.; Newman, A. H.; Javitch, J. A.; Cherezov, V.; et al. Structure of the human dopamine D3 receptor in complex with a D2/D3 selective antagonist. *Science* **2010**, *330* (6007), 1091-1095.

- (79) Huang, W.; Manglik, A.; Venkatakrishnan, A. J.; Laeremans, T.; Feinberg, E. N.; Sanborn, A. L.; Kato, H. E.; Livingston, K. E.; Thorsen, T. S.; Kling, R. C.; et al. Structural insights into micro-opioid receptor activation. *Nature* **2015**, *524* (7565), 315-321.
- (80) Totrov, M.; Abagyan, R. Flexible protein-ligand docking by global energy optimization in internal coordinates. *Proteins* **1997**, *Suppl 1*, 215-220.
- (81) Uprety, R.; Che, T.; Zaidi, S. A.; Grinnell, S. G.; Varga, B. R.; Faouzi, A.; Slocum, S. T.; Allaoa, A.; Varadi, A.; Nelson, M.; et al. Controlling opioid receptor functional selectivity by targeting distinct subpockets of the orthosteric site. *Elife* **2021**, *10*.
- (82) Newman, A. H.; Cao, J.; Bennett, C. J.; Robarge, M. J.; Freeman, R. A.; Luedtke, R. R. N-(4-[4-(2,3-dichlorophenyl)piperazin-1-yl]butyl, butenyl and butynyl)arylcarboxamides as novel dopamine D(3) receptor antagonists. *Bioorg Med Chem Lett* **2003**, *13* (13), 2179-2183.
- (83) Quddus, A.; Novak, A.; Cousin, D.; Blackham, E.; Jones, G.; Wrigglesworth, J.; Duffy, L.; Birch, L.; George, P.; Ahmed, S. Aminopyrimidine Derivatives As CTPS1 Inhibitors. WO 2019/180244 A1, 2019.
- (84) Cai, N. S.; Quiroz, C.; Bonaventura, J.; Bonifazi, A.; Cole, T. O.; Purks, J.; Billing, A. S.; Massey, E.; Wagner, M.; Wish, E. D.; et al. Opioid-galanin receptor heteromers mediate the dopaminergic effects of opioids. *J Clin Invest* **2019**, *129* (7), 2730-2744.
- (85) Klein Herenbrink, C.; Sykes, D. A.; Donthamsetti, P.; Canals, M.; Coudrat, T.; Shonberg, J.; Scammells, P. J.; Capuano, B.; Sexton, P. M.; Charlton, S. J.; et al. The role of kinetic context in apparent biased agonism at GPCRs. *Nat Commun* **2016**, *7*, 10842.
- (86) Sanchez, J.; Z, E. H.; Lane, J. R.; Liu, X.; Bridgford, J. L.; Payne, R. J.; Canals, M.; Stone, M. J. Evaluation and extension of the two-site, two-step model for binding and activation of the chemokine receptor CCR1. *J Biol Chem* **2019**, *294* (10), 3464-3475.

(87) Hollins, B.; Kuravi, S.; Digby, G. J.; Lambert, N. A. The c-terminus of GRK3 indicates rapid dissociation of G protein heterotrimers. *Cell Signal* **2009**, *21* (6), 1015-1021.

Table of Contents (TOC)

